CYCLODEXTRINS FOR SENSING:
SOLUTION, SURFACE, AND SINGLE MOLECULE CHEMISTRY

PROEFSCHRIFT

ter verkrijging van
de graad van doctor aan de Universiteit Twente
op gezag van de rector magnificus,
prof. dr. F.A. van Vught,
volgens besluit van het College voor Promoties
in het openbaar te verdedigen
op woensdag 26 september 2001 te 15.00 uur.

door

Menno Rutger de Jong

geboren op 20 april 1973
te Ede

Dit proefschrift is goedgekeurd door:

Promotor	Prof. dr. ir. D. N. Reinhoudt
Assistent-promotor	Dr. ir. J. Huskens

Verantwoording omslag.
Het omslag geeft twee voorbeelden van inclusie in macrocycli van natuurlijk voorkomende materialen.

Contents

Chapter 1

General Introduction

The sensing of chemical species depends on the molecular recognition of these species by receptor molecules. The area of chemistry that is concerned with the study of recognition phenomena is called Supramolecular Chemistry.[1] Originating with the study of metal ion complexation by crown ethers, it has led to the development of highly selective and sensitive sensors for various metal ions.[2] Due to the weaker interactions involved, the area of receptors for organic compounds is less developed, especially in competitive solvents.

Cyclodextrins, cyclic oligosaccharides obtained from the degradation of starch by *Bacillus macerans*, were first isolated in the late nineteenth century.[3] Their ability to form inclusion complexes with suitable organic molecules was discovered soon thereafter.[4] With the development of the field of Supramolecular Chemistry, their complexation properties have been extensively studied.[5] Applications for cyclodextrins and their derivatives are sought in various areas of chemistry, including the sensing of organic molecules.[6]

Since the first report on self-assembled monolayers of dialkyldisulfides on gold,[7] they have received much attention. The incorporation of receptor moieties into these monolayers leads to extremely thin sensing layers with all hosts exposed to the medium. This enables instantaneous sensor response and has therefore prompted considerable research efforts.[8] Many new techniques have been developed to characterize these thin films, *e.g.* STM and AFM.[9] The sensitivity of these tools allows the detection of even single receptor-ligand interactions.[10]

This thesis describes possible roles of cyclodextrin derivatives in the development of sensors for organic molecules. The utility of cooperative binding by multiple cyclodextrin cavities in solution or in self-assembled monolayers is explored. Chapter 2 introduces the development of receptors and sensors for organic molecules and the available techniques to probe the interactions between receptors and ligands. Particular attention is paid to the role of cyclodextrin derivatives.

Chapter 3 describes the design of cyclodextrin dimers with and without an appended fluorophore for use in optical detection schemes. Using a docking procedure, a commonly used tool in medicinal chemistry, several guests for these dimers are identified.

In Chapter 4, the complexation properties of the dimers with one of the classes of guests identified, are investigated in detail. The influence of the second cavity is elucidated by comparison to monomeric analogues of the dimers.

The possibility to use cyclodextrin dimers in radiopharmaceutical applications is discussed in Chapter 5. Native cyclodextrin and cyclodextrin dimers are employed to enhance the water solubility of lipophilic metal complexes and to enable their synthesis under aqueous conditions. Finally, a new method for radiolabeling of biomolecules based on the strong inclusion of suitable guests into cyclodextrin dimers is introduced.

In Chapter 6, self-assembled monolayers on gold are introduced as a method to immobilize cyclodextrin-based receptors. Monolayers are obtained from cyclodextrins functionalized with seven thioether chains or a single thiol chain. The binding properties of cyclodextrin monolayers are monitored by surface plasmon resonance spectroscopy. The selectivity of the monolayers is governed by their architecture. If the cyclodextrin is attached to the surface through a single connection, the increased flexibility of the headgroup allows for the cooperative binding of suitable guests.

Surface immobilization of both the host and the guest allows for the study of the interaction between single ligand-receptor pairs. Chapter 7 describes the probing of cyclodextrin monolayers with guest-modified AFM tips. Histograms of the pull-off events showed quantized forces, corresponding to single decomplexation events. A model to relate the magnitude of these forces for complexes with various guests to the thermodynamic stability is proposed.

References

[1]   Pedersen, C.J. *Angew. Chem. Int. Ed. Engl.* **1988**, *27*, 1021-1027. Cram, D.J. *Angew. Chem. Int. Ed. Engl.* **1988**, *27*, 1009-1020. Lehn, J.-M. *Angew. Chem. Int. Ed. Engl.* **1988**, *27*, 89-112.

[2]   *Comprehensive Supramolecular Chemistry, Vol. 1,10*, (Eds.: J. L. Atwood, J. E. D. Davies, D. D. MacNicol, F. Vögtle, J.- M. Lehn), Pergamon, Oxford, **1996**.

[3]   Villiers, A. *Compt. Rend.* **1891**, *112*, 536-539.

[4]   (a) Schardinger, F. *Zentralbl. Bakteriol. Abt. II* **1911**, *29*, 188-197; (b) Freudenberg, K.; Schaaf, E.; Dumpert, G.; Ploetz, T. *Naturwissenschaften* **1937**, *27*, 850-853.

2

5 (a) Wenz, G. *Angew. Chem. Int. Ed. Engl.* **1994**, *33*, 803-822; (b) *Chem. Rev.* **1998**, *98*, Issue 5; (c) *Comprehensive Supramolecular Chemistry, Vol. 3*, (Eds.: J. L. Atwood, J. E. D. Davies, D. D. MacNicol, F. Vögtle, J.- M. Lehn), Pergamon, Oxford, **1996**.

6 Ueno, A. *Supramol. Sci.* **1996**, *3*, 31-36.

7 Nuzzo, R.G.; Allara, D.L. *J. Am. Chem. Soc.* **1983**, *105*, 4481-4483.

8 (a) Rubinstein, L; Steinberg, S.; Tor, Y.; Shanzer, A.; Sagiv, J. *Nature* **1988**, *332*, 426-429; (b) Schierbaum, K.-D.; Weiss, T.; Thoden van Velzen, E. U.; Engbersen, J. F. J.; Reinhoudt, D. N.; Göpel, W. *Science* **1994**, *265*, 1413-1415; (c) Motesharei, K.; Myles, D. C. *J. Am. Chem. Soc.*, **1994**, *116*, 7413-7414.

9 (a) Binnig, G.; Rohrer, H.; Gerber, Ch.; Weibel, E. *Appl. Phys. Lett.* **1982**, *40*, 178-180; (b) Binnig, G.; Quate, C. F.; Gerber, C. *Phys. Rev. Lett.* **1986**, *56*, 930-933.

10 (a) Florin, E.-L.; Moy, V. T.; Gaub, H. E. *Science* **1994**, *264*, 415-417; (b) Lee, G. U.; Kidwell, D. A.; Colton, R. J. *Langmuir* **1994**, *10*, 354-357.

Organic Molecule Sensing

2.1   Introduction

A sensor molecule or system transforms a selective complexation event into an analytical signal. Such sensors depend on molecular recognition, an area of chemistry that is studied by supramolecular chemistry.[1] This field of chemistry began with the study of the selective complexation of metal cations. The construction of chemosensors[2] for organic substances is much less developed than that of metal ion sensors, because the interactions involved are much weaker. This renders selectivity towards a particular analyte of interest hard to achieve. Most attempts so far are based on recognition by an array of hydrogen bonds in molecular clefts or tweezers or on solvophobic binding in a macrocycle. Alternatively, the selectivity of biomolecules can be used in so-called biosensors for *e.g.* glucose. The drawbacks of biosensors are the sometimes limited stability of biomolecules and the lack of receptors for abiotic molecules.

Most chemosensors are conjugate, *i.e.* consisting of two separate building blocks: a receptor with selectivity for the analyte of interest and a transducer responsible for the generation of measurable signals upon binding of the analyte to the receptor. If receptor and transducer are integrated, the chemosensor is called an intrinsic sensor. The final step towards practical use of a sensing mechanism is the immobilization of the chemosensor to allow incorporation into a device.

This review on the sensing of organic molecules starts with a brief overview of the mechanisms available for the transduction of a binding event into a sensor signal. Following this, examples of chemosensors for organic molecules are discussed, with the emphasis on cyclodextrin-based sensing molecules. After a description of the immobilization of receptors, this Chapter ends with a discussion on the detection of binding events between single molecules.

2.2   Sensing principles

Several means of communicating a binding event are known. They all depend on the change of some measurable physical property of the chemosensor upon complexation. The

sensing mechanism may either originate from the sensing molecules themselves, or from a change in the material that the sensing molecules are part of.

Most optical detection methods are based on molecular mechanisms. They have a number of advantages over other techniques, including the high information capacity of light and the availability of several miniaturized devices due to impulses from the telecommmunications industry. Complexation events can result in changes in UV absorption and fluorescence emission, which both have been used extensively. Of these two techniques, fluorescence is potentially more sensitive, because the Stoke's shift causes the emission spectrum to have a zero or near zero background.[2]

Both steady state fluorescence spectroscopy, measuring the fluorescence intensity, or dynamic fluorescence spectroscopy, measuring the fluorescence lifetime are used. A multitude of mechanisms effecting the photophysical phenomena exists. Perhaps the simplest mechanism is the sensitivity of fluorescence to a change in the polarity of the microenvironment. When the polarity of the microenvironment changes, fluorescence can be shifted to a longer or shorter wavelength or a change in quantum yield may occur. Frequently used polarity probes include ANS, TNS, and the dansyl group. If complexation of a guest induces or prohibits the proximity of two fluorophores, changes in excimer[3] fluorescence are observed.

More elaborate transduction mechanisms use the sensitivity of fluorescence to the presence of a donor atom near the fluorophore, which quenches the fluorescence through photoinduced electron transfer (PET).[2,4] An interaction of a guest with the donor atom may inhibit PET, causing an increase in fluorescence.[5,6] Related to PET are chelation enhanced fluorescence (CHEF) and chelation enhanced quenching (CHEQ).[7] These phenomena occur when a donor atom that is part of the structure of the fluorophore is involved in a chelation event, thereby influencing fluorescence intensity. Finally, binding events can cause a shift in the ratio of normal planar (NP) excited state to a twisted intramolecular charge transfer (TICT) state, thus allowing detection.[8]

Surface plasmon resonance is an optical technique that depends on the evanescent field originating from oscillations of conducting electrons (plasmons) at a metal surface.[9] Light reflecting from the surface is coupled to the oscillations. At a certain angle of incidence, resonance occurs, which is apparent from a minimum in the reflected light. The angle at which resonance occurs is proportional to changes in the refractive index near the surface and thus to the amount of material bound to the surface. Several optical configurations exploiting this for sensing applications have been reported.[10] The technique is frequently used in immunosensing.[11]

Electrochemical detection methods can be roughly divided into potentiometric and voltammetric methods. Potentiometric chemical sensors were the first to be developed. The complexation of a charged species in a receptor immobilized in a membrane leads to a change in the membrane potential, and this can be transformed into an electrical signal. Voltammetric methods detect electrical currents that result from an applied voltage. Cyclic

voltammetry measures changes in the redox properties of the host or guest upon complexation. Impedance spectroscopy records changes in the resistance of a thin film as a result of the complexation of a guest.

The most obvious physical property of a material that changes when an analyte is incorporated into a layer of sensor molecules, is the mass of this layer. As the mass changes involved in this process are very small, a sensitive device for measuring the mass of a layer is needed. These devices include quartz microbalances (QMBs) and surface acoustic wave resonators (SAWs). Both devices use the mass-dependent resonance frequency of piezoelectric crystals,[12] but a QMB operates in the bulk shear mode, whereas an SAW uses surface waves resonance. This enables an SAW to operate at higher resonance frequencies, which results in greater sensitivity. [13,14,15] A disadvantage of SAW devices is that they cannot be used in solution, because resonance is disturbed. The use of other wave types, *e. g.* Love waves avoids this problem.

2.3   Sensing molecules

2.3.1 Cyclodextrins

A class of host molecules that has often been used in sensor applications is that of the cyclodextrins,[16] cyclic oligosaccharides that consist of six (α-cyclodextrin), seven (β-cyclodextrin, Figure 2.1), or eight (γ-cyclodextrin) glucose moieties. Cyclodextrins are naturally occurring products of the degradation of starch by the enzyme glycosyl transferase from *Bacillus macerans*.[17] The remaining free hydroxyl groups of the glucose moieties are located on the rims of the torus-shaped molecules, rendering them water-soluble. The secondary hydroxyl groups, located at C-2 and C-3 of the glucose units are all situated at the broader, secondary rim of the molecule, where they form a network of intramolecular hydrogen bonds, providing rigidity to the structure. The most striking feature of cyclodextrins is the presence of a central cavity, shaped by the carbon atoms of the glucose units, rendering it relatively apolar. This feature enables the inclusion of a variety of organic molecules in aqueous solution.
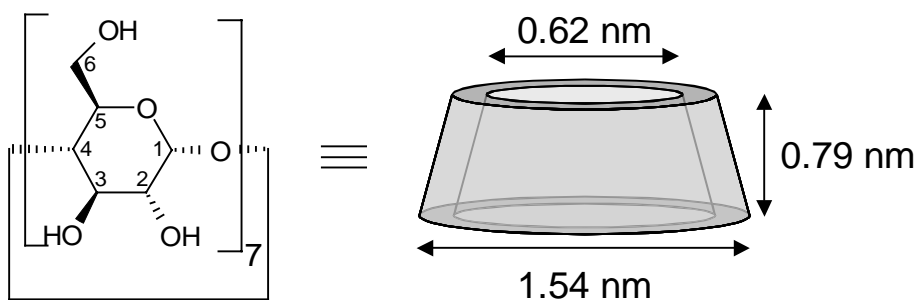

Figure 2.1. *The structure of β-cyclodextrin.*

The driving force for the inclusion of guests into the cavity has been extensively studied.[18] Rather than being a classical hydrophobic effect, complexation by cyclodextrins is governed by several factors, the most important of which are van der Waals and hydrophobic interactions, hydrogen bonding interactions, release of the water molecules initially included in the cavity to the bulk, and conformational changes or strain release of the cyclodextrin molecule upon complexation.

The method of choice to gain structural information about complexes between cyclodextrins and guests is NMR spectroscopy.[19] In view of the use of cyclodextrins and derivatives in sensing applications, the effect that complexation in the cyclodextrin cavity has on optical and electrochemical properties of the guests is of greater interest here. Although the cyclodextrins are spectroscopically almost transparent, the transition of a guest from bulk water to the hydrophobic cavity may have a large influence on the spectroscopic properties of polarity probes (*vide supra*). UV and fluorescence spectroscopy have therefore since long been used to study complexation by cyclodextrins.[20] Co-inclusion of two fluorophores in a γ-cyclodextrin cavity leads to increased excimer formation.[21] Because the cyclodextrin cavity is chiral, it induces circular dichroism upon complexation of non-chiral guests. Apart from proving the inclusion of a guest, this induced circular dichroism signal (ICD) can give information about the orientation of a guest in a cavity.[22]

Another useful effect of inclusion in a cyclodextrin cavity, is the effect on the redox properties of an encapsulated redox center.[23] The hydrophobic cavity stabilizes the uncharged state of a redox couple. This is reflected in increased binding constants for the uncharged state as compared to the charged state. Inclusion of ferrocene carboxylate by β-cyclodextrin induces a shift in the half-wave potential for the oxidation to more positive values, consistent with the stabilization of the reduced form of the redox couple.[24] Besides, the currents associated with the oxidation wave decrease, due to the decreased diffusion of the complex compared to free ferrocene. This phenomenon is explained by a two-step oxidation process, where the complex has to dissociate before the oxidation can take place. The same type of oxidation behavior was observed for cobaltocene[25] and organic guests such as viologens[26] and quinones. The effect of oxidation and reduction on the inclusion properties of metallocenes has been used by Kaifer and coworkers for the electrochemically reversible breakup and formation of large supramolecular asemblies from ferrocene[27] or cobaltocene[28] terminated dendrimers and β-cyclodextrin.

2.3.2 Cyclodextrin-based sensor molecules

Most studies on cyclodextrin-based sensing molecules have focused on optical detection methods. The spectroscopic transparency of cyclodextrins can be overcome by covalently attaching one of the spectroscopically active guests discussed in the previous section as a

detector moiety. The various changes in the self-inclusion behavior of this type of molecule that are possible upon the inclusion of an external guest enable the optical detection of spectroscopically inactive guests. Several sensing schemes can be envisioned (Figure 2.2), most of which have been employed first by Ueno and coworkers.[29]
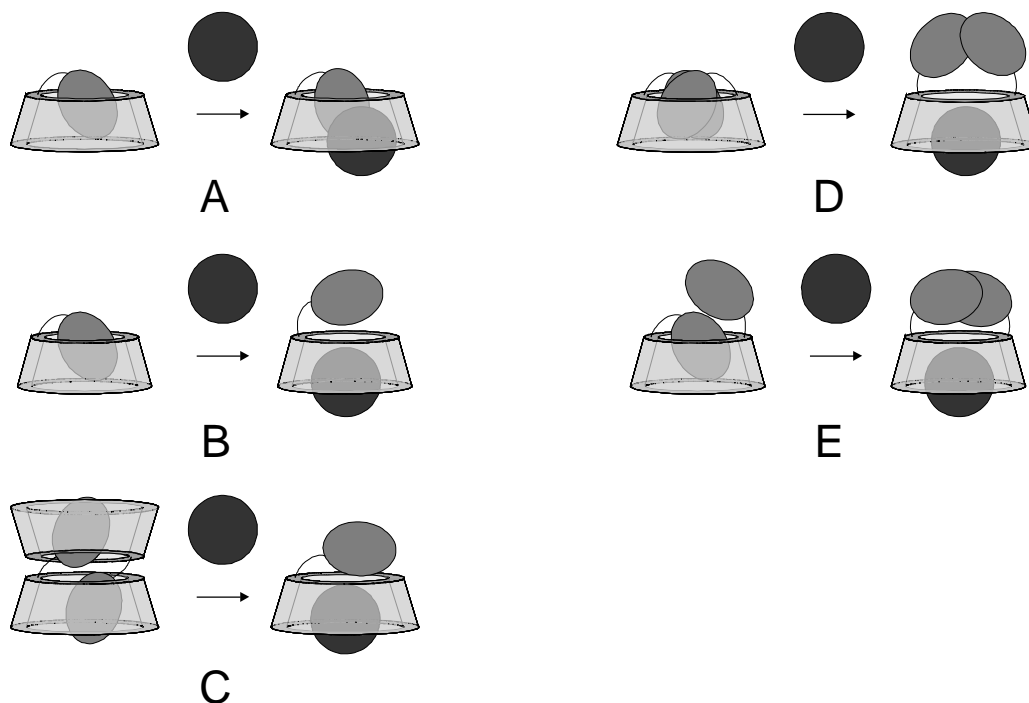
Figure 2.2. *Sensing mechanisms for chromophore- or fluorophore-appended cyclodextrins.*

Chemosensors that use guest-induced changes in absorption offer the possibility of constructing color-change indicators. Because of this very convenient way of communicating detection, several attempts have been made to create such sensors. Ueno and coworkers synthesized Methyl Red- and p-Methyl Red-modified β-cyclodextrin **1**.[30,31] These molecules were used as type B (Figure 2.2) color-change indicators for 1-adamantanol and 1-adamantanecarboxylic acid. The use of these sensors was restricted to acidic media, because at neutral pH strong self-inclusion of the dye moiety prevented the binding of guests. Later, phenolphthalein-[32] and *p*-nitrophenol-modified[33] sensors that recognized guests in alkaline and neutral media, respectively, were prepared.

1
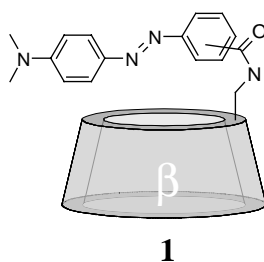
Changes in fluorescence can often be more sensitively detected than changes in UV/Vis absorption. As a first approach to fluorescent cyclodextrin sensors, pyrene-appended γ-cyclodextrin derivatives were synthesized. Compound **2**, modified at the primary side, proved to be more effective than the derivatives that had pyrene appended at the secondary side. Molecule **2** exists as a dimer in aqueous solution, giving rise to a strong excimer fluorescence band. Upon complexation of *l*-borneol the dimer dissociates, resulting in a shift from excimer to monomer fluorescence, thus enabling detection (Figure 2.2, type C).[34]
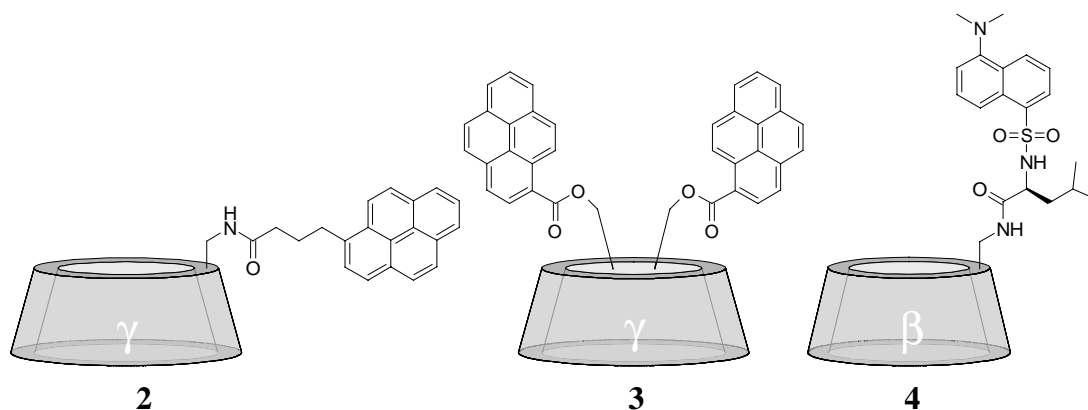
Although sensor signals could be obtained from **2**, its sensing behavior is far from ideal. The necessity for the dissociation of the dimer of **2** to generate the signal, entails that the signaling behavior is dependent on the concentration of **2**. This was solved by preparing cyclodextrin derivatives with two appended fluorophores, that show intramolecular changes in the ratio of excimer to monomer fluorescence.[35,36] All four regioisomers of bispyrene-modified γ-cyclodextrin derivatives **3** were prepared and shown to have concentration-independent excimer fluorescence. They were capable of detection of a variety of guests.[35]

Cyclodextrin derivatives such as **3** enable the detection of a variety of organic compounds, but the lack of methods for the selective bisfunctionalization of cyclodextrins causes the synthesis of this type of compound to require tedious purification procedures, resulting in low yields. Therefore, research attention changed to the dansyl moiety, a fluorophore whose fluorescence quantum yield and emission maximum are highly sensitive to the polarity of its microenvironment.[37] A variety of sensor molecules, with the dansyl group attached to the primary or secondary side of β- or γ-cyclodextrin via *L*-leucyl, *D*-leucyl, or glycyl spacers was prepared.[38,39,40] Usually, complexation of guests was found to cause a fluorescence decrease due to expulsion of the dansyl moiety from the cyclodextrin cavity. In a few cases, co-complexation of a very small external guest and the dansyl moiety in the cavity of γ-cyclodextrin gave rise to an increase in the fluorescence intensity.[41] The most sensitive host proved to be **4**, which allowed the detection of micromolar concentrations of steroids.[41] Work from the group of Nolte later showed that the decreased sensitivity of β-

cyclodextrin derivatives with the dansyl moiety applied at the secondary side is probably due to strong self-inclusion of the dansyl moiety.[42]

In recent years, the focus in this type of sensor work is shifting to ways of changing the cyclodextrin cavity, thus altering the selectivity of these sensor molecules. In a series of papers, Valeur and coworkers studied multichromophoric β-cyclodextrin derivatives as model systems for photosynthetic processes. They noticed that the naphthyl modified compound **5** showed increased binding constants with elongated dyes compared to native cyclodextrin.[43] Continuing on this finding, they used this anionic cyclodextrin derivative for the detection of cationic surfactants in micromolar concentrations.[44]

5
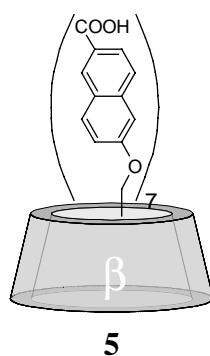
Several groups are aiming to modify the selectivity of cyclodextrin sensors by combining fluorophore-appended cyclodextrins with other receptor motifs. Ueno and coworkers appended monensin, a naturally occurring ionophore for sodium, to a dansyl-modified β-cyclodextrin derivative.[45] The hydrophobic monensin cap of **6** markedly increased the binding affinity for acyclic guests, whereas a smaller improvement was observed for cyclic compounds. Further increases of the binding affinities for organic guests were observed upon the addition of sodium, as the monensin complexes the sodium by folding around it, thus generating a more effective hydrophobic cap. Addition of avidin to biotin-appended cyclodextrin sensors was also shown to enhance binding affinities for organic guests.[46] In our own group a calix[4]arene was used as a hydrophobic cap.[47] The fluorophore-appended β-cyclodextrin-calixarene couple **7** showed increased binding properties for large guests compared to the parent β-cyclodextrin.[48] The sensor properties of this type of host molecules were shown to depend more on their aggregation behavior than on expulsion of a self-included moiety.[49]

6   **7**
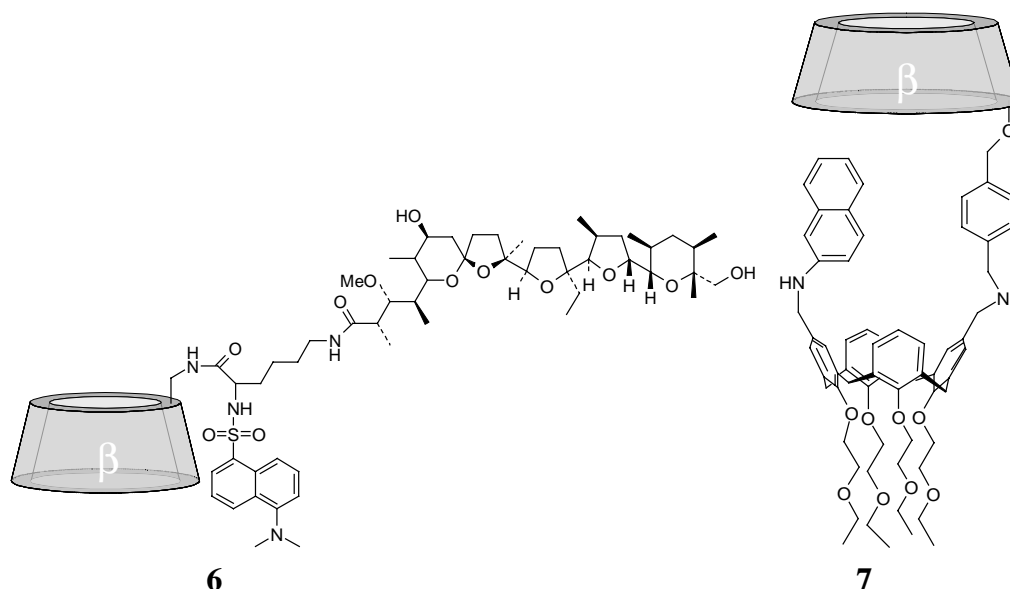
Although the driving forces for the formation of several structural motifs of proteins, *e.g.* α-helices, are well understood, mimicking the hydrophobic pockets found in proteins is much more difficult, as these are often formed by amino acid residues that are far apart in the primary structure of the protein. In peptide-cyclodextrin hybrids, cyclodextrins may be a convenient way to create a hydrophobic pocket in a protein-like environment. Additional interactions are provided by carefully chosen amino acid residues. Several examples exist of cyclodextrin-modified peptides.[50] Recently, α-helical peptides appended with both a dansyl and a cyclodextrin moiety[51] or with a pyrene, a nitrobenzene, and a cyclodextrin moiety[52] were shown to have sensing properties for organic guests.

Cyclodextrin-based sensor molecules with off-on signaling were prepared by Nocera and coworkers.[53,54] In the absence of aromatic guests, the Tb-complex of DTPA-capped cyclodextrin **8** shows very weak luminescence owing to the low absorbance of the Tb^{3+}-ion. Aromatic hydrocarbons that are included in the cavity sensitize the emission of the lanthanide, resulting in strongly enhanced luminescence. As the DTPA moiety also functions as a hydrophobic cap over the cyclodextrin, the binding constants for guests such as naphthalene are markedly enhanced compared to native β-cyclodextrin.

8   **9**
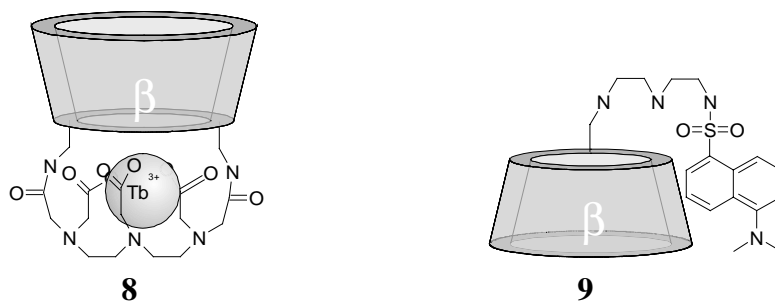
Switch-on luminescence was also observed in the ternary system developed by Corradini and coworkers.[55] The fluorescence of **9** is quenched by the addition of Cu^{2+}, owing to the

coordination of the copper to the nitrogen of the sulfonamide group. Fluorescence can only be restored by the addition of guests for cyclodextrin that also contain a bidentate ligand for copper.

An effective way to modify the binding affinity of cyclodextrin based receptors is by covalently combining two or more cyclodextrin moieties in one molecule. Strong cooperative binding has been observed for cyclodextrin dimers.[56,57] Nolte and coworkers monitored the strong interaction of cyclodextrin dimers with elongated fluorescent guests by following the changes in the fluorescence.[58] Following up on these findings, the rutheniumcomplex **10** was prepared.[59] Although the addition of steroids to this complex caused no change in the Ru[II] luminescence intensity, the luminescence was quenched by the binding of viologens. The subsequent displacement of the viologens from the cavities by stronger binding steroids reconstituted the luminescence, enabling the fluoresent detection of the latter guests.

10
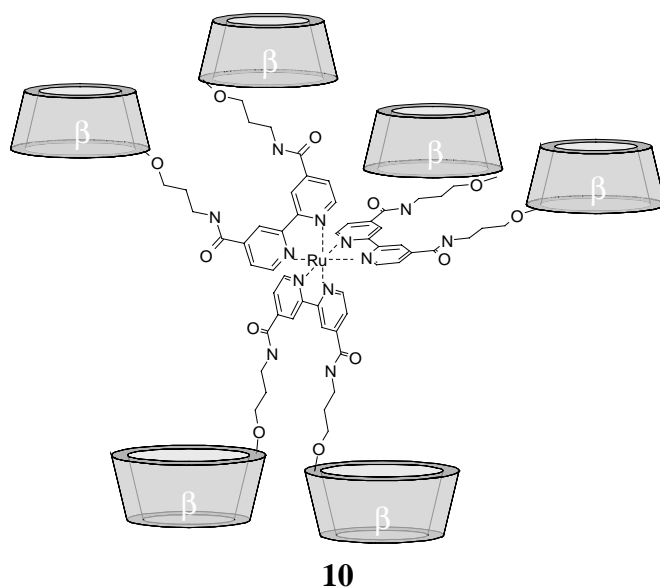
Multiple cyclodextrin moieties can be covalently combined in a polymer. β-Cyclodextrin-appended poly(allylamine) polymers were shown to detect pyrene more sensitively than native β-cyclodextrin, owing to cooperative binding of pyrene by two cyclodextrins.[60] The affinity of the polymer for pyrene increases with a higher degree of substitution with cyclodextrins, indicating that mainly neighboring cyclodextrin units cooperate in the binding. Komiyama showed that molecularly imprinted polymers of β-cyclodextrins, crosslinked with diisocyanates in the presence of cholesterol, are selective receptors for these steroids, whereas β-cyclodextrin polymers crosslinked in the absence of cholesterol show considerably less interaction.[61] This seems a promising approach for the preparation of cyclodextrin-based sensor molecules with varying selectivities.[62]

2.3.3 Other sensing molecules

Many other receptors than cyclodextrins have been applied in organic molecule sensing systems. Depending on the kind of species to be detected several types of interaction can be employed, including bonding in molecular clefts, hydrogen bond donor/acceptor arrays, π-π-stacking, solvophobic interaction, and charge transfer donor/acceptors. As these types of interaction are usually much weaker than the electrostatic interaction in ion recognition, competition by solvent molecules for the binding sites is hard to overcome in competitive solvents. Most systems developed sofar can therefore only be used in rather apolar solvents. An example is the fluorescent sensor for barbiturates (**11**) developed by Shinkai *et al.*[63] based on a synthetic receptor for barbiturates developed by Hamilton and coworkers.[64] The system is based on the complexation of barbiturate derivatives in a molecular cleft by hydrogen bonding and functions best in hexane.
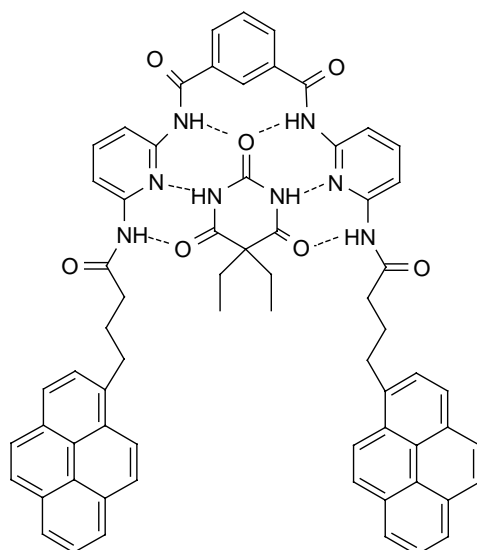
11

Noteworthy exceptions to the rule that organic molecule sensors work best in apolar solution are the boronic acid-based sugar sensors. Some debate exists if these are really sensor molecules, depending on whether the bonds to the boron that are being formed and broken are seen as reversible covalent bonds or as coordination bonds. Regardless, these molecules are capable of selective recognition of sugars in aqueous solutions. The scheme shown in Figure 2.3 summarizes the principle of saccharide detection using boronic acid derivatives.[65] Detection is based on the difference in fluorescence between the ionized and non-ionized species. At pH values between the pK_a of the free acid and that of the polyol complex, the strongly fluorescent boronic acid is transformed into the weakly fluorescent ionized polyol complex upon binding a sugar molecule.
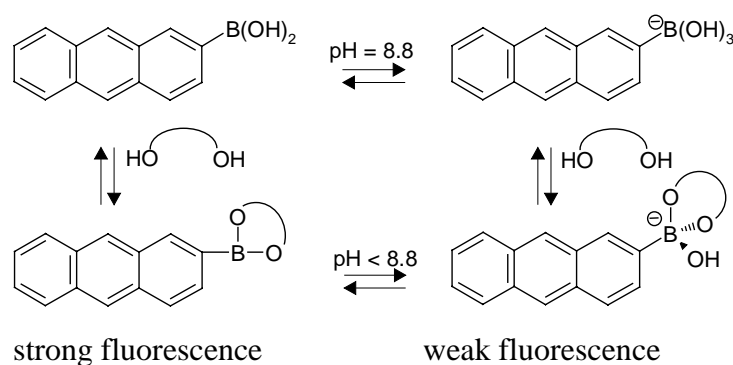
Figure 2.3. *Sugar sensing using phenylboronic acid fluorescence.*

Several sensors based on changes in boronic acid pK_a on polyol binding have been reported. James and coworkers constructed sensor **12**.[66] At pH 7.7 the anthracene fluorescence of this molecule is quenched due to the PET effect of the tertiary amine. Binding of a polyol increased the acidity of the boronic acid, resulting in a stronger boron-nitrogen bond. This reduced the PET effect and enhanced fluorescence. Because there are two boronic acid groups in this molecule, it is able to bind guests with two diols cooperatively. Cooperative binding was most effective in the case of glucose. Continuing on this theme, chiral sensor **13** capable of discriminating between the enantiomers of several sugars was constructed.[67] Several other variations on this theme have been reported since.

12　　　　　　　　**13**
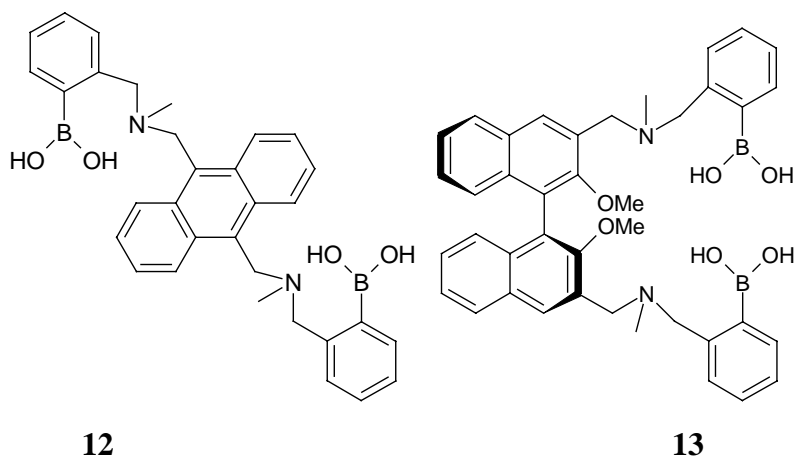
Most of the research on the development of organic molecule sensors focuses on charged species and utilizes modifications of the receptors employed in metal ion sensing and inorganic anion sensing. Thus, crown ethers[68] and aza crowns[69] are used to detect ammonium ions and nucleosides, respectively. Calixarenes are used as cation, anion or neutral molecule sensors, depending on their functionalization.[70] Many more examples can be found in a recent review.[71] Other promising approaches for the selective recognition of organic analytes, which have also been reviewed recently, are the use of conjugated polymers[72] and molecularly imprinted polymers.[73]

2.4   Sensing systems

2.4.1 Introduction

As mentioned before, immobilization of receptor sites is vital for the creation of sensor devices. Incorporation of receptor molecules into polymeric matrices or sol gels has been studied extensively, and these techniques are being used in commercially available sensors. An increasing interest exists in the development of rapid-responding sensors for on-line sensing applications. This has stimulated research into the use of monolayers for sensing applications.

2.4.2 Monolayer-based sensing systems

Since the first report[74] on self-assembled monolayers (SAMs) of dialkyldisulfides on gold, these systems have been extensively studied.[75,76] The strong S-Au interaction allows the easy preparation of highly stable self-assembled monolayers of thiols, disulfides, and thioethers. Research initially focused on a fundamental understanding of the structure and properties of SAMs, but it soon shifted to potential applications, *e.g.* sensing.

The use of monolayers of receptor molecules is a very attractive way to achieve the immobilization of the receptors that is necessary to make a sensor device, because of their ease of preparation and high stability. An additional benefit of using monolayers is the very small quantity of material required to prepare a monolayer. Finally, as the monolayers are only a single layer of molecules thick, no diffusion into the film is necessary to obtain an interaction between the receptor and its analyte, offering the possibility of very short response times. Monolayers can be prepared on various surfaces, self-assembled monolayers of sulfur compounds on gold or silver and of alkyltrichlorosilanes on glass are most often used in sensing applications.

The first examples of molecular recognition at a self-assembled monolayer on gold were published by Rubinstein and coworkers.[77] They used voltammetric techniques to study metal ion binding at monolayers of sulfide-based tetradentate ligands. Another early example of molecular recognition at a monolayer was the recognition of streptavidin by a biotin-functionalized monolayer.[78]

Whitesides *et al.*[79] used surface plasmon resonance to measure the interaction of detergents with self-assembled monolayers of hexadecanethiolate. The association constants obtained by fitting titration curves to a Langmuir isotherm, correlated with the critical micelle concentration of the detergent.

In contrast to the previous example, most SAM-based organic molecule sensing systems rely on the incorporation of receptor molecules into the monolayers. Motesharei and Myles

prepared mixed monolayers containing a fluorescent isophthalic acid derivative and studied the interaction with barbiturates (Figure 2.4).[80] The binding of barbiturate ligands from solutions in acetonitrile or dichloromethane was detected by an up to 15 nm shift of the emission maximum of the receptor.
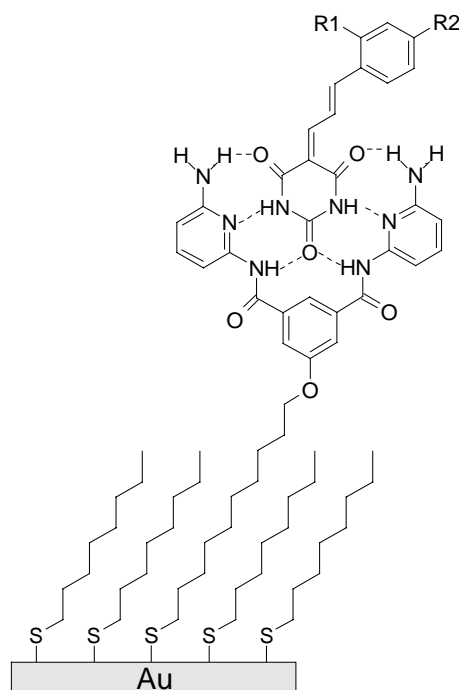
Figure 2.4. *Interaction of barbiturate guests with a receptor monolayer.*

Substantial research efforts are directed to sequence-selective detection of DNA, *e.g.* for gene analyses and forensic applications. Several assays for the detection of DNA based on the immobilization of oligonucleotides on gold have been published in recent years. Interaction of the immobilized oligonucleotide with the target DNA has been transduced in several ways. Maeda and coworkers used ferrocene-appended oligonucleotides as the reporter oligonucleotide and monitored the binding of the target by differential pulse voltammetry (Figure 2.5).[81] A mismatch of one of the seven basepairs formed between the immobilized oligonucleotide and the target led to a tenfold drop of the signal, proving the selectivity of the system. A similar approach was followed by Willner *et al.*[82] They monitored the binding of the target by impedance spectroscopy, and used a biotin-appended oligonucleotide as the reporter. This enabled amplification of the signal through interaction of the biotin with avidin. Recently, Mirkin and coworkers used oligonucleotides immobilized on gold colloids as probes for the detection of target DNA.[83] The sharp melting profiles of colloid-immobilized oligonucleotides and the use of silver enhancement[84] allowed detection of oligonucleotides with a sensitivity that exceeds that of existing fluorophore systems by two orders of magnitude. A different approach, reported

recently by Gimzewski, involves the use of cantilever arrays[85] for the detection of oligonucleotides.[86]
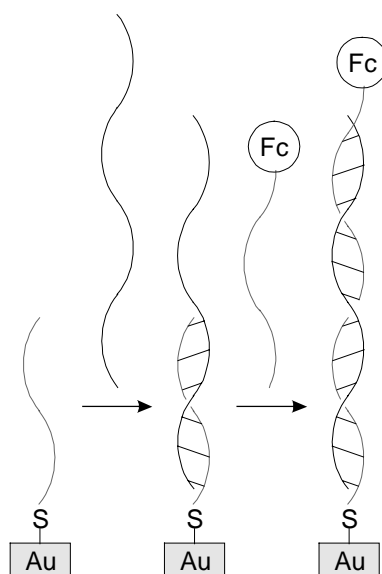
Figure 2.5. *Voltammetric detection of DNA at a SAM of immobilized oligonucleotides.*

Our group has reported the self-assembly of various receptor molecules, including resorcin[4]arenes[87] on gold. Interactions of resorcin[4]arene monolayers with organic vapors were monitored by quartz crystal microbalance (QCM).[88] The highest affinity was found for perchloroethylene. Reference monolayers of didecanesulfide and octadecanethiolate hardly showed a response to the vapors. Surface plasmon resonance (SPR) enabled the detection of the interaction of monolayers of cavitands **14**-**17** with organic guests both in the gas phase[89] and in aqueous solution.[90] Although these receptor monolayers show a certain degree of selectivity, the formation of multilayers did not allow the determination of association constants. When the cavity of the cavitand receptor was enlarged by the attachment of two calix[4]arene moieties, complexation of larger, biologically relevant molecules is possible. We used SAMs of receptor **18** for the selective complexation of a variety of steroids.[91] More groups have studied interactions at monolayers of calixarenes. Recently, Crooks *et al.* monitored the interaction of monolayers of calix[4]arenes and calix[6]arenes with guests by QCM.[92]

14 R = H

15 R = OMe

16 R = OC(O)Me

17 R = OCH₂C(O)N(Et)₂
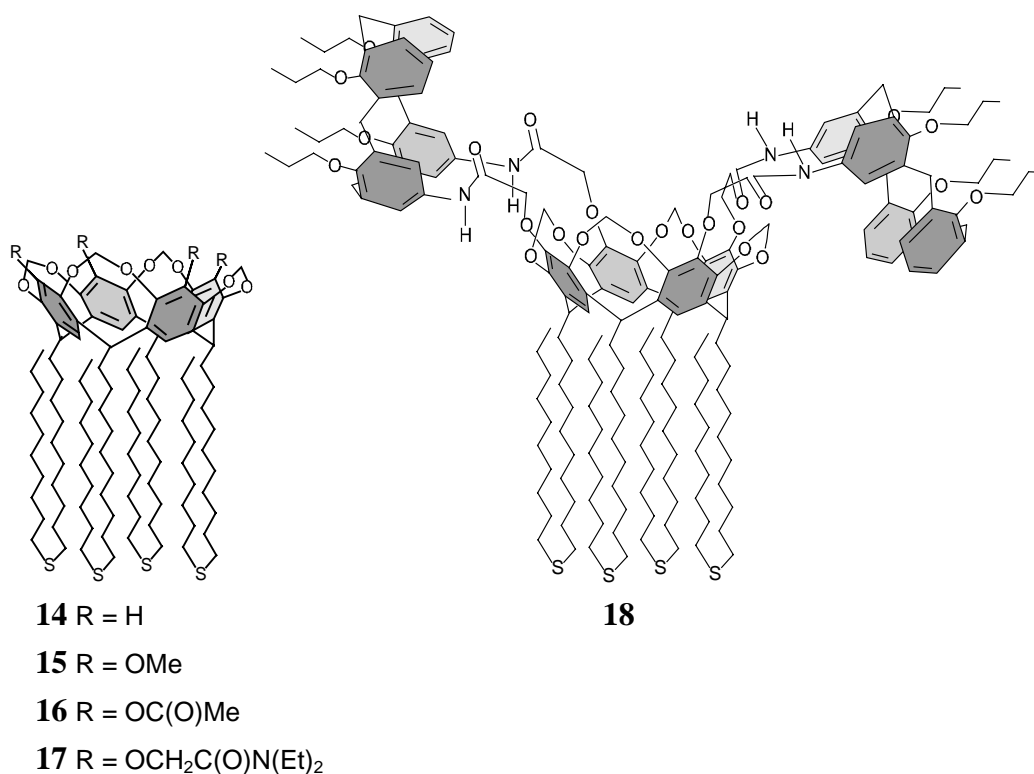
Sulfur-modified β-cyclodextrin derivatives have been used by several groups for the preparation of SAMs on gold.[93] Kaifer *et al.* used per-6-deoxy-(per-6-thio)-β-cyclodextrin **19** which has seven thiol moieties for binding to the gold surface.[94] After sealing the monolayers with pentanethiol in the presence of an external guest, they were capable of detecting ferrocene in solution by cyclic voltammetry. The linear dependence of the redox current on the scan rate proves the complexation of ferrocene by the cyclodextrin cavities.[94] The use of this cyclodextrin derivative to stabilize gold colloids, yielded particles capable of recognizing guests.[95] Wenz and coworkers found that mono- and multithiolated cyclodextrins all form monolayers on gold in which they expose their cavities to the solution.[96] The monothiolated cyclodextrins formed more homogeneous surfaces than the multithiolated derivative. SPR studies at these monolayers were ambiguous about the binding being specific or aspecific.[97] Galla *et al.* synthesized cyclodextrins with one thiol moiety as attachment point (**20**), which were shown to form densely packed monolayers.[98] The binding properties for positively and negatively charged guests were studied by impedance spectroscopy with a negatively charged reporter redox couple.[99] A two-stage adsorption process was observed, possibly due to the disorder in the monolayer. In our own group, β-cyclodextrin derivatives persubstituted at their primary sides with thiol or thioether moieties were prepared.[100] Heptapodant thioether receptor adsorbates were shown to use their attachment points more effectively than thiol adsorbates. The β-cyclodextrin adsorbates with free hydroxyl groups at the 2- and 3-positions complexed guests from aqueous solution.[101]

19   **20**
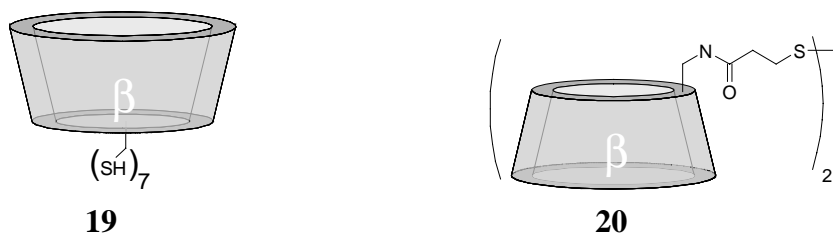
Kitano and coworkers studied the complexation of phenylalanine derivatives and phenylethylamine derivatives in monolayers of thiolated α-cyclodextrin.[102] The complexation was stereo- and regioselective. Recent studies on the inclusion of phthalate esters by these monolayers indicate the complexation of the same guests to be enthalpy-driven in solution and entropy-driven at the monolayers.[103]

Interactions between hosts and guests at interfaces can also be studied with guests immobilized at the surface and hosts in solution. Hussey *et al.* used this approach to study the complexation of cyclodextrins at monolayers of a cationic ferrocene derivative coassembled with nonanethiol by cyclic voltammetry.[104]

2.5   Single molecule detection

Ultimately, all sensing events depend on how single molecules interact with each other. The methods discussed sofar for studying the interactions between molecules, *e.g.* NMR, calorimetry, fluorescence spectroscopy, and cyclic voltammetry, can provide very precise values for thermodynamic parameters such as the Gibbs free energy and the enthalpy of binding. These are, however, average values for large ensembles of molecules. In recent years, considerable research efforts have been directed to the detection of single molecules and the interactions between single pairs of molecules. The study of single molecules depends on the measuring of interactions between interfaces with high precision, a task for which various tools exist nowadays.

The first device for the direct measurement of intermolecular forces to become available was the surface force apparatus.[105] Drawbacks of this method were the limitation to atomically flat transparent surfaces and a lack of lateral resolution. Other techniques capable of measuring intermolecular forces are laser tweezers and the micropipette technique.

A very versatile class of tools became available in the mid 1980s with the development of scanning probe microscopy techniques such as scanning tunneling microscopy (STM),[106] near-field scanning optical microscopy (NSOM),[107] and atomic force microscope (AFM, Figure 2.6).[108]   STM and AFM can both be used for imaging with (sub)nanometer resolution. STM allows imaging of conducting surfaces through the distance-dependent

tunneling current flowing between an atomically sharp tip and the surface. AFM detects forces between a tip and a surface down to the piconewton range. Topography, elastic moduli, friction coefficients, chemical residues, surface charges, and energy loss during the oscillation of the cantilever can all be imaged with high resolution. NSOM uses a tip containing an optical fiber, enabling simultaneous imaging of forces and optical properties. The optical resolution is approximately $\lambda/50$, sufficient for the optical imaging of sub-monolayers of fluorescent dyes.[109]
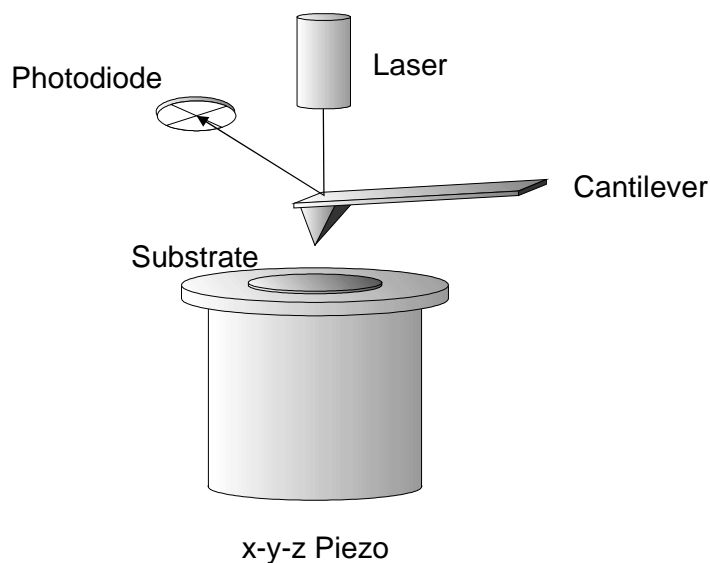
Figure 2.6. *Schematic drawing of a force microscope.*

Scanning probe techniques are now extensively used in the imaging of surfaces. More interesting in view of sensing is the development of force spectroscopy, the study of the forces resulting from the interactions between surfaces. A special case of this is chemical force microscopy (CFM),[110] which studies the interactions between chemically modified surfaces. Functionalization is most often achieved through covering tip and surface with gold and subsequently chemisorbing thiolated molecules of interest. Alternatively, silane chemistry can be used for the functionalization of silicon oxide surfaces with the interacting molecules of interest. Using these techniques, the adhesion forces between amine and carboxylate terminated layers were found to be in accordance with their binding strength: $COOH/NH_2 > COOH/COOH > NH_2/NH_2$.[111] McKendry *et al.* found different adhesion forces for different combinations of enantiomers of acetylphenylglycine on the tip and patterned surfaces of mandelic acid (Figure 2.7).[112]
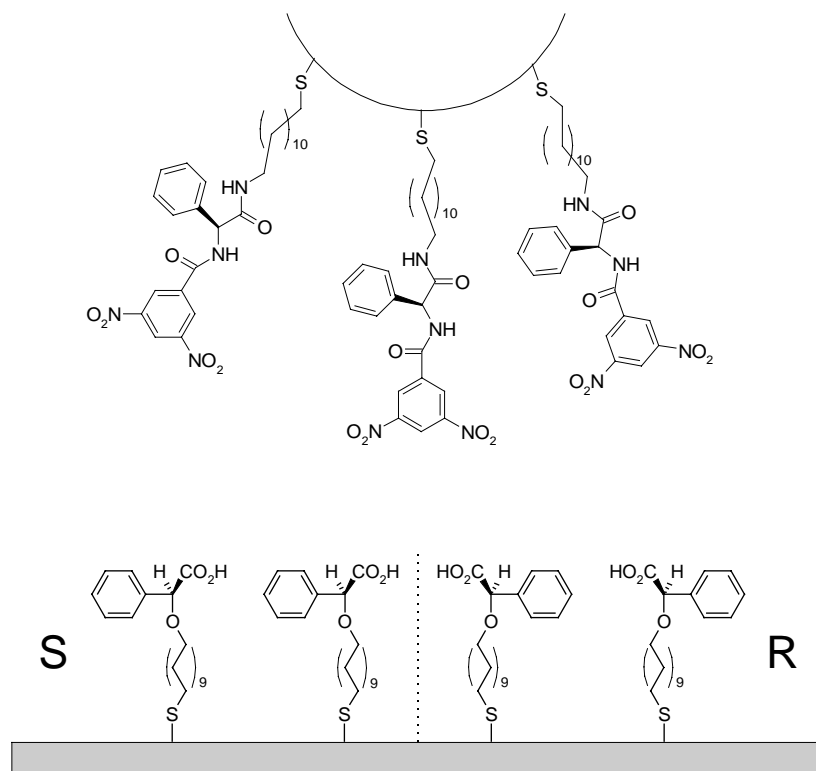
Figure 2.7. *Schematic drawing of chiral discrimination in an AFM experiment.*

Genuine single molecular interactions have been mostly studied for biological systems, as the large size of these systems compared to most synthetic systems facilitates the study of single interactions. In 1994, the groups of Gaub[113] and Colton[114] simultaneously reported AFM studies on the biotin-avidin (Figure 2.8) and biotin-streptavidin interactions, respectively. A histogram of the measured unbinding forces for biotin-avidin showed maxima at integer multiples of an elementary force quantum of 160 pN, which was attributed to single and multiple unbinding events.[113]
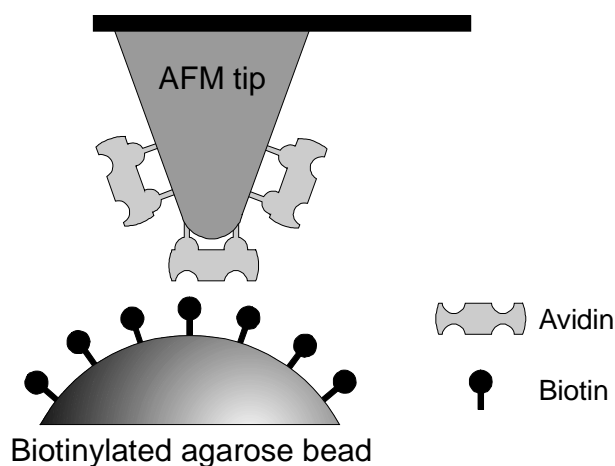
Figure 2.8. *Schematical representation of the setup used by Gaub et al. to measure biotin-avidin interactions.*

Other protein-ligand systems studied by AFM are antibody-antigen interactions[115,116,117] and the selectin-glycoprotein couple[118] involved in the inflammatory response of mammals. Protein studies are now also evolving in the direction of the unfolding of protein domains.[119]

From the very beginning, efforts to relate the rupture forces of receptor ligand pairs to macroscopic thermodynamic properties have been undertaken.[113] The unbinding processes for biological systems are very slow, and as a consequence, the rupture forces measured vary with the loading rate. Evans and Ritchie[120] used Monte Carlo simulations to connect experimental data with the results from modeling studies.[121] Three different regimes for the dependence of the unbinding force on the loading rate were predicted. If the loading rate is much slower than the rate of spontaneous dissociation, no force should be observed. Above this critical loading rate, strength increases first as a weak power and then as the logarithm of the loading rate. At very high loading rates, only frictional drag retards unbinding. Recently, they used a biomembrane force probe (BFP) to verify their theory for the avidin/streptavidin-biotin interaction.[122] Their results are indicative of the presence of more than one energy barrier along the dissociation path.

The best known molecular recognition event in nature, the base pairing in DNA, is also extensively studied by AFM. Colton and coworkers were the first to determine the binding strength of a DNA duplex.[123] Employing oligonucleotides with the sequence $(ACTG)_5$ on the tip and $(CAGT)_5$ on the sample they found quantized rupture forces of 1.52, 1.11 and 0.83 nN, which they ascribed to the breakage of 20, 16, and 12 base pairs, respectively. Lieber and coworkers studied the stretching and breaking of duplex DNA.[124] Struntz and coworkers found the force of unbinding DNA duplexes to depend exponentially on the number of base pairs and logarithmically on the loading rate.[125] Interestingly, the forces needed to pull apart hairpins in single-stranded λ-phage DNA[126] and poly(dG-dC) or poly(dA-dT) DNA[127] are independent of the number of base pairs and loading rate.

Recently, supramolecular interactions are beginning to be studied in synthetic systems. Samorì and coworkers studied the formation and rupture of the coordination bond between nickel(II), chelated by nitrilotriacetate (nta), and several consecutive histidine residues at the terminus of a protein.[128] They observed two different complexes with rupture forces of 350 pN and 500 pN. If more consecutive his-residues were present, the stronger binding was observed more frequently. Changing the metal ion to iron(III) led to the observation of larger rupture forces (750 pN).

In our own group, we studied the interaction between monolayers of cyclodextirn heptathioethers[100] and AFM tips coated with ferrocene.[129] A quantized rupture force of 56 pN was observed. Interestingly, the rupture force of this low molecular weight supramolecular system with very fast unbinding kinetics was loading rate independent.

2.6   Concluding remarks

Very few effective chemosensors for organic molecules exist. The relatively weak interactions responsible for recognition of organic molecules compared to the electrostatic interactions used for the detection of *e.g.* metal ions, hinder sensitivity, especially in competitive solvents. Cyclodextrins are a readily available class of receptors, capable of strong interactions with organic molecules in water. This thesis describes the modification of cyclodextrins to alter their selectivity (Chapters 3 and 4), potential applications of (modified) cyclodextrins in radiopharmaceuticals (Chapter 5), and the sensor properties of cyclodextrin derivatives incorporated into monolayers (Chapters 6 and 7). The control over the selectivity possible through modification off cyclodextrins is promising for future applications in sensor arrays.[130]

2.7   References

1   *Comprehensive Supramolecular Chemistry, Vol. 1,2,3,10*, Lehn, J.M., Ed.; Elsevier Science Ltd, Oxford, 1996.

2   *Fluorescent Chemosensors for Ion and Molecule Recognition*, Czarnik, A.W., Ed.; American Chemical Society, Washington DC, 1993

3   *Spectroscopy, Vol. 3*, Straughan, B.P.; Walker, S., Ed.; Chapman and Hall Ltd, London, 1976

4   Bissell, R.A.; De Silva, A.P.; Gunaratne, H.Q.N., Lynch, P.L.M.; Maguire, G.E.M.; McCoy, C.P.; Sandanayake, K.R.A.S. *Top. Curr. Chem.*, **1993**, 168, 223-264.

5   Huston, M.E.; Akkaya, E.U.; Czarnik, A.W. *J. Am. Chem. Soc.*, **1989**, 111, 8735-8737.

6   de Silva, A.P; Sandanayake, K.R.A.S. *Angew. Chem. Int. Ed. Engl.*, **1990**, 29, 1173-1175.

7   Sousa, L.R.; Larson, J.M. *J. Am. Chem. Soc.*, **1977**, 99, 307-310.

8   Rettig, W. *Angew. Chem. Int. Ed. Engl.* **1986**, *25*, 971-990.

9   Raether, H. in *Physics of Thin Films*, Hass, G.; Francombe, M.; Hoffman, R.; Eds., Academic Press: New York, 1977, vol. 9, pp. 145-261.

10   Matsubara, K.; Kawata, S.; Minami, S. *Appl. Opt.* **1988**, *27*, 1160-1163.

11   Liedberg, B.; Nylander, C.; Lundström, I. *Sens. Actuators* **1983**, *4*, 299-304.

12   Sauerbrey, G. Z. *Z. Physik* **1959**, *155*, 206.

13   Dickert, F.L.; Haunschildt, A. *Adv. Mater.*, **1993**, 5, 887-895.

14   Lucklum, R.; Henning, B.; Hauptmann, P.; Schierbaum, K.D.; Vaihinger, S.; Göpel, W. *Sens. Act. A*, **1991**, 25, 705-710.

15   Dickert, F.L.; Bauer, P.A. *Adv. Mater.* **1991**, 3, 436-438.

16   (a) Wenz, G. *Angew. Chem. Int. Ed. Engl.* **1994**, *33*, 803-822. (b) *Chem. Rev.* **1998**, *98*, Issue 5. (c) J. Szejtli, T. Osa, *Comprehensive Supramolecular Chemistry, Vol.*

3, (Eds.: J. L. Atwood, J. E. D. Davies, D. D. MacNicol, F. Vögtle, J.- M. Lehn), Pergamon, Oxford, **1996**.

[17] French, D. *Adv. Carbohydr. Chem.* **1957**, *12*, 189.

[18] Rekharsky, M. V.; Inoue, Y. *Chem. Rev.* **1998**, *98*, 1875-1917.

[19] Scneider, H.-J.; Hacket, F.; Rüdiger, V.; Ikeda, H. *Chem. Rev.* **1998**, *98*, 1755-1786.

[20] Bender, M. L.; Komiyama, M. *Cyclodextrin Chemistry*; Springer-Verlag: Berlin, 1978.

[21] Ueno, A.; Takahashi, K.; Osa, T. *Chem. Commun.* **1980**, 921-922.

[22] (a) Kodaka, M. *J. Am. Chem. Soc.* **1993**, *115*, 3702-3705; (b) Kodaka, M. *J. Phys. Chem. A* **1998**, *102*, 8101-8103.

[23] Cardona, C. M.; Mendoza, S.; Kaifer, A. E. *Chem. Soc. Rev.* **2000**, *29*, 37-42.

[24] Matsue, T.; Evans, D. H.; Osa, T.; Kobayashi, N. *J. Am. Chem. Soc.* **1985**, *107*, 3411-3417.

[25] Wang, Y.; Mendoza, S.; Kaifer, A. E. *Inorg. Chem.* **1998**, *37*, 317-320

[26] Mirzoian, A.; Kaifer, A. E. *Chem. Eur. J.* **1997**, *3*, 1052-1058.

[27] Castro, R.; Cuadrado, I.; Alonso, B.; Casado, C. M.; Morán, M.; Kaifer, A. E. *J. Am. Chem. Soc.* **1997**, *119*, 5760-5761.

[28] González, B.; Casado, C. M.; Alonso, B.; Cuadrado, I.; Morán, M.; Wang, Y.; Kaifer, A. E. *Chem. Commun.* **1998**, 2569-2570

[29] Ueno, A. *Supramol. Sci.* **1996**, *3*, 31-36.

[30] Ueno, A.; Kuwabara, T.; Nakamura, A.; Toda, F. *Nature* **1992**, *356*, 136-137.

[31] Kuwabara, T.; Nakamura, A.; Ueno, A.; Toda, F. *J. Phys. Chem.* **1994**, *98*, 6297-6303.

[32] Kuwabara, T.; Takamura, M.; Matsushita, A.; Ikeda, H.; Nakamura, A.; Ueno, A.; Toda, F. *J. Org. Chem.* **1998**, *63*, 8729-8735.

[33] Matsushita, A.; Kuwabara, T.; Nakamura, A.; Ikeda, H.; Ueno, A. *J. Chem. Soc., Perkin Trans. 2* **1997**, 1705-1710.

[34] Ueno, A.; Suzuki, I.; Osa, T. *J. Am. Chem. Soc.* **1989**, *111*, 6391-6397.

[35] Suzuki, I.; Ohkubo, M.; Ueno, A.; Osa, T. *Chem. Lett.* **1992**, 269-272.

[36] Ueno, A.; Minato, S.; Osa, T. *Anal. Chem.* **1992**, 64, 1154-1157.

[37] Li, Y.-H.; Chan, L.-M.; Tyer, L.; Moody, R. T.; Himel, C. M.; Hercules, D. M. *J. Am. Chem. Soc.* **1975**, *97*, 3118-3126.

[38] Ueno, A.; Minato, S.; Suzuki, I.; Fukushima, M.; Ohkubo, M.; Osa, T.; Hamada, F.; Murai, K. *Chem. Lett.* **1990**, 605-608.

[39] Wang, Y.; Ikeda, T.; Ueno, A.; Toda, F. *Chem. Lett.* **1992**, 863-866.

[40] Hamada,F.; Kondo, Y.; Ito, R.; Suzuki, I.; Osa, T.; Ueno, A. *J. Incl. Phenom.* **1993**, 15, 273-279.

[41] Ikeda, H.; Nakamura, M.; Ise, N.; Oguma, N.; Nakamura, A.; Ikeda, T.; Toda, F.; Ueno, A. *J. Am. Chem. Soc.* **1996**, *118*, 10980-10988.

[42] Nelissen, H. F. M.; Venema, F.; Uittenbogaard, R. M.; Feiters, M. C.; Nolte, R. J. M. *J. Chem. Soc., Perkin Trans. 2* **1997**, 2045-2053.

[43] Jullien, L.; Canceill, J.; Valeur, B.; Bardez, E.; Lefevre, J. P.; Lehn, J. M.; MarchiArtzner, V.; Pansu, R. *J. Am. Chem. Soc.* **1996**, *118*, 5432-5442.

[44] Choppinet, P.; Jullien, L.; Valeur, B. *J. Chem. Soc., Perkin Trans. 2* **1999**, 249-255.

[45] Nakamura, M.; Ikeda, A.; Ise, N.; Ikeda, T.; Ikeda, H.; Toda, F.; Ueno, A. *J. Chem. Soc., Chem. Commun.* **1995**, 725-726.

[46] Ikunaga, T.; Ikeda, H.; Ueno, A. *Chem. Eur. J.* **1999**, *5*, 2698-2704.

[47] Van Dienst, E.; Snellink, B. H. M.; Von Piekartz, I.; Engbersen, J. F. J.; Reinhoudt, D. N. *J. Chem. Soc., Chem. Commun.* **1995**, 1151-1152.

[48] Bügler, J.; Engbersen, J. F. J.; Reinhoudt, D. N. *J. Org. Chem.* **1998**, *63*, 5339-5344.

[49] Bügler, J. H.; Sommerdijk, N. A. J. M.; Visser, A. J. W. G.; van Hoek, A.; Nolte, R. J. M.; Engbersen, J. F. J.; Reinhoudt, D. N.; *J. Am. Chem. Soc.* **1999**, *121*, 28-33.

[50] (a) Djedaïni-Pilard, F.; Désalos, J.; Perly, B. *Tetrahedron Lett.* **1993**, *34*, 2457-2460. (b) Hristova-Kazermieski, M. K.; Horan, P.; Davis, P.; Yamamura, H. I.; Kramer, T.; Horvath, R.; Kazermieski, W. M.; Porreca, F.; Hruby, V. J. *Biorg. Med. Chem. Lett.* **1993**, *3*, 831-834. (c) Schaske, N.; Fiori, S.; Weyher, E.; Escrieut, C.; Fourmy, D.; Muller, G.; Moroder, L. *J. Am. Chem. Soc.* **1998**, *120*, 7030-7038. (d) Schaske, N.; Assfalg-Machleidt, I.; Machleidt, W.; Lassleben, T.; Sommerhoff, C. P.; Moroder, L. *Biorg. Med. Chem. Lett.* **2000**, *10*, 677-680. (e) Péan, C.; Créminon, C.; Wijkhuisen, A.; Grassi, J.; Guenot, P.; Jéhan, P.; Dalbiez, J.-P.; Perly, B.; Djedaïni-Pilard F., *J. Chem. Soc., Perkin Trans. 2* **2000**, 853-863.

[51] Matsumura, S.; Sakamoto, Ueno, A.; Mihara, H. *Chem. Eur. J.* **2000**, *6*, 1781-1788.

[52] Hossain, M. A.; Hamasaki, K.; Takahashi, K.; Mihara, H.; Ueno, A. *J. Am. Chem. Soc.* **2001**, *123*, 7435-7436.

[53] Mortellaro, M. A.; Nocera, D. G. *J. Am. Chem. Soc.* **1996**, *118*, 7414-7415.

[54] Rudzinski, C. M.; Engebretson, D. S.; Hartmann, W. K.; Nocera, D. G. *J. Phys. Chem. A* **1998**, *102*, 7442-7446.

[55] Corradini, R.; Dossena, A.; Galaverna, G.; Marchelli, R.; Panagia, A.; Sartor, G. *J. Org. Chem.* **1997**, *62*, 6283-6289.

[56] Breslow, R.; Chung, S. *J. Am. Chem. Soc.* **1990**, *112*, 9659-9660.

[57] Breslow, R. ; Zhang, B. *J. Am. Chem. Soc.* **1996**, *118*, 8495-8496.

[58] Venema, F.; Nelissen, H. F. M.; Berthault, P.; Birlirakis, N.; Rowan, A. E.; Feiters, M. C.; Nolte, R. J. M. *Chem. Eur. J.* **1998**, *4*, 2237-2250.

[59] Nelissen, H. F. M.; Schut, A. F. J.; Venema, F.; Feiters, M. C.; Nolte, R. J. M. *Chem. Commun.* **2000**, 577-578.

[60] Hollas, M.; Chung, M.-A.; Adams, J. *J. Phys. Chem. B* **1998**, *102*, 2947-2953.

[61]   (a) Asanuma, H.; Kakazu, M.; Shibata, M.; Hishiya, T.; Komiyama, M. *Chem. Commun.* **1997**, 1971-1972; (b) Hishiya, T.; Shibata, M.; Kakazu, M.; Asanuma, H.; Komiyama, M. *Macromolecules* **1999,** *32,* 2265-2269

[62]   Asanuma, H.; Hishiya, T.; Komiyama, M. *Adv. Mater.* **2000**, *12*, 1019-1030.

[63]   Aoki, I.; Kawahara, Y.; Sakaki, T.; Shinkai, S. *Bull. Chem. Soc. Jpn.* **1993**, 66, 927-933.

[64]   Chang, S.K.; Van Engen, D.; Fan, E.; Hamilton, A.D. *J. Am. Chem. Soc.*, **1991**, 113, 7640-7645.

[65]   Yoon, J.; Czarnik, A.W. *J. Am. Chem. Soc.*, **1992**, 114, 5874-5875.

[66]   James, T.D.; Sandanayake, K.R.A.S.; Shinkai, S. *Angew. Chem. Int. Ed. Engl.*, **1994**, 33, 2207-2209.

[67]   James, T.D.; Sandanayake, K.R.A.S.; Shinkai, S. *Nature*, **1995**, 374, 345-347.

[68]   Hossain, M.A.; Schneider, H.J. *J. Am. Chem. Soc.* **1998**, *120*, 11208-11209.

[69]   Fenniri, H.; Hosseini, M.W.; Lehn, J.-M. *Helv. Chim. Acta* **1997**, *80*, 786-803.

[70]   Diamond, D.; McKervey, M.A. *Chem. Soc. Rev.* **1996**, 15-24.

[71]   Hartley, J.H.; James, T.D.; Ward, C.J. *J. Chem. Soc. Perkin Trans. 1* **2000**, 3155-3184.

[72]   McQuade, D.T.; Pullen, A.E.; Swager, T.M. *Chem. Rev.* **2000**, *100*, 2537-2574.

[73]   Haupt, K.; Mosbach, K. *Chem. Rev.* **2000**, *100*, 2495-2504.

[74]   Nuzzo, R. G.; Allara, D.L. *J. Am. Chem. Soc.* **1983**, *105*, 4481-4483.

[75]   Ulman, A. *An Introduction to Ultrathin Organic Films*; Academic Press: San Diego, CA, **1991.**

[76]   Ulman, A. *Chem. Rev.* **1996**, *96*, 1533-1554.

[77]   Rubinstein, L; Steinberg, S.; Tor, Y.; Shanzer, A.; Sagiv, J. *Nature* **1988**, *332*, 426-429.

[78]   Häussling, L; Michel, B; Ringsdorf, H.; Rohrer, H. *Angew. Chem. Int. Ed.* **1991**, *30*, 569-572.

[79]   Sigal, G. B.; Mrksich, M.; Whitesides, G. M. *Langmuir* **1997**, *13*, 2749-2755.

[80]   (a) Motesharei, K.; Myles, D. C. *J. Am. Chem. Soc.*, **1994**, *116*, 7413-7414; (b) Motesharei, K.; Myles, D. C. *J. Am. Chem. Soc.*, **1998**, *120*, 7328-7336.

[81]   Ihara, T.; Nakayama, M.; Murata, M.; Nakano, K.; Maeda, M. *Chem. Commun.* **1997**, 1609-1610.

[82]   Bardea, A.; Patolsky, F.; Dagan, A.; Willner, I. *Chem. Commun.* **1999**, 21-22.

[83]   Taton, T. A.;Mirkin, C. A.; Letsinger, R. L. *Science*, **2000**, *289*, 1757-1760.

[84]   (a) Hacker, G. W., in *Colloidal Gold: Principles, Methods, and Applications*, M. A. Hayat, Ed. (Academic Press, San Diego, CA, 1989), vol. 1, chap. 10. (b) Zehbe, I.; Hacker, G. W.; Su, H.C.; HauserKronberger, C.; Hainfeld, J. F.; Tubbs, R. *Am. J. Pathol.* **1997**, *150,* 1553-1561.

[85] Baller, M.K.; Lang, H.P.; Fritz, J.; Gerber, C.; Gimzewski, J.K.; Drechsler, U.; Rothuizen, H.; Despont, M.; Vettiger, P.; Battiston, F.M.; Ramseyer, J.P.; Fornaro, P.; Meyer, E.; Guntherodt, H.J. *Ultramicroscopy* **2000**, *82*, 1-9.

[86] Fritz, J.; Baller, M.K.; Lang, H.P.; Rothuizen, H.; Vettiger, P.; Meyer, E.; Guntherodt, H.J.; Gerber, C.; Gimzewski, J.K. *Science* **2000**, *288*, 316-318.

[87] (a) Thoden van Velzen, E. U.; Engbersen, J. F. J.; Reinhoudt, D. N. *J. Am. Chem. Soc.* **1994**, *116*, 3597-3598; (b) Thoden van Velzen, E. U.; Engbersen, J. F. J.; Reinhoudt, D. N. *Synthesis* **1995**, *8*, 989-1008; (c) Thoden van Velzen, E. U.; Engbersen, J. F. J.; De Lange, P. J.; Mahy, J. W.; Reinhoudt, D. N. *J. Am. Chem. Soc.* **1995**, *117*, 6853-6862.

[88] Schierbaum, K.-D.; Weiss, T.; Thoden van Velzen, E. U.; Engbersen, J. F. J.; Reinhoudt, D. N.; Göpel, W. *Science* **1994**, *265*, 1413-1415.

[89] Huisman, B.-H.; Kooyman, R. P. H.; Van Veggel, F. C. J. M.; Reinhoudt, D. N. *Adv. Mater.* **1996**, *8*, 561-564.

[90] Friggeri, A.; Van Veggel, F. C. J. M.; Reinhoudt, D. N.; Kooyman, R. P. H. *Langmuir* **1998**, *14*, 5457-5463.

[91] Friggeri, A.; Van Veggel, F. C. J. M.; Reinhoudt, D. N. *Chem. Eur. J.* **1999**, *5*, 3595-3602.

[92] (a) Dermody, D. L. ; Crooks, R. M.; Kim, T. *J. Am. Chem. Soc.* **1996**, *118*, 11912-11917; (b) Dermody, D. L.; Lee, Y.; Kim, T.; Crooks, R. M. *Langmuir* **1999**, *15*, 8435-8440.

[93] (a) He, P.; Ye, J.; Fang, Y.; Suzuki, L.; Osa, T. *Anal. Chim. Acta* **1997**, *337*, 217-233; (b) Lahav, M.; Ranjit, K. T.; Katz, E.; Willner, I. *Chem. Commun.* **1997**, 259-260; (c) D'Souza, F.; Hsieh, Y.-Y.; Wickman, H.; Kutner, W. *Chem. Commun.* **1997**, 1191-1192; (d) Lee, J.-Y.; Park, S.-M. *J. Phys. Chem. B* **2000**, *102*, 9940-9945.

[94] Rojas, .M. T.; Köninger, R.; Stoddart, J. F.; Kaifer, A. E. *J. Am. Chem. Soc.* **1995**, *117*, 336-343.

[95] (a) Liu, J.; Mendoza, S.; Roman, E.; Lynn, M. J.; Xu, R. L. Kaifer, A. E. *J. Am. Chem. Soc.* **1999**, *121*, 4304-4305. (b) Liu, J.; Alvarez, J. Kaifer, A. E. *Adv. Mater.* **2000**, *12*, 1381-1383.

[96] (a) Weisser, M.; Nelles, G.; Wohlfahrt, P.; Wenz, G.; Mittler-Neher, S. *J. Phys. Chem.* **1996**, *100*, 17893-17900; (b) Nelles, G.; Weisser, M.; Back, R.; Wohlfahrt, P.; Wenz, G.; Mittler-Neher, S. *J. Am. Chem. Soc.* **1996**, *118*, 5039-5046.

[97] Weisser, M.; Nelles, G.; Wenz, G.; Mittler-Neher, S. *Sens. Actuat. B* **1997**, *38-39*, 58-67.

[98] Henke, C.; Steinem, C.; Janshoff, A.; Steffan, G.; Luftmann, H.; Sieber, M.; Galla, H.-J. *Anal. Chem.* **1996**, *68*, 3158-3165.

[99] Michalke, A.; Janshoff, A.; Steinem, C.; Henke, C.; Sieber, M.; Galla, H.-J. *Anal. Chem.* **1999**, *71*, 2528-2533.

100 Beulen, M. W. J.; Bügler, J.; Lammerink, B.; Geurts, F. A. J.; Biemond, E. M. E. F.; Van Leerdam, K. G. C.; Van Veggel, F. C. J. M.; Engbersen, J. F. J.; Reinhoudt, D. N. *Langmuir* **1998**, *14*, 6424-6429.

101 (a) Beulen, M.W.J.; Bügler, J.; De Jong, M.R.; Lammerink, B.; Huskens, J.; Schönherr, H.; Vancso, G.J.; Boukamp, B.A.; Wieder, H.; Offenhäuser, A.; Knoll, W.; Van Veggel, F.C.J.M.; Reinhoudt, D.N. *Chem. Eur. J.* **2000**, *6*, 1176-1183; (b) Schönherr, H.; Beulen, M.W.J.; Bügler, J.; Huskens, J.; Van Veggel, F.C.J.M.; Reinhoudt, D.N. *J. Am. Chem. Soc.* **2000**, *122*, 5039-5046.

102 (a) Maeda, Y.; Fukuda, T.; Yamamoto, H.; Kitano, H. *Langmuir* **1997**, *13*, 4187-4189; (b) Yamamoto, H.; Maeda, Y.; Kitano, H. *J. Phys. Chem. B* **1997**, *101*, 6855-6860; (c) Fukuda, T.; Maeda, Y.; Kitano, H. *Langmuir* **1999**, *15*, 1887-1890.

103 Kitano, H.; Taira, Y.; Yamamoto, H. *Anal. Chem.* **2000**, *72*, 2976-2980.

104 Sabapathy, R. C.; Bhattacharyya, S.; Cleland, W. E., Jr.; Hussey, C. L. *Langmuir* **1998**, *14*, 3797-3807.

105 Israelachvili, J. N.; Tabor, D. *Proc. R. Soc. London A* **1972**, *331*, 19.

106 Binnig, G.; Rohrer, H.; Gerber, Ch.; Weibel, E. *Appl. Phys. Lett.* **1982**, *40*, 178-180.

107 Pohl, D.W.; Denk, W.; Lanz, A. *Appl. Phys. Lett.* **1984**, *44*, 651-653.

108 Binnig, G.; Quate, C. F.; Gerber, C. *Phys. Rev. Lett.* **1986**, *56*, 930-933.

109 Betzig, E.; Chichester, R.J. *Science* **1993**, *262*, 1422-1425.

110 Frisbie, C.D.; Rozsnyai, L.F.; Noy, A.; Wrighton, M.S.; Lieber, C.M. *Science* **1994**, *265*, 2071-2074.

111 Noy, A.; Vezenov, D. V.; Lieber, C. M. *Annu. Rev. Mater. Sci.* **1997**, *27*, 381-421.

112 McKendry, R.; Theoclitou, M. E.; Rayment, T.; Abell, C. *Nature* **1998**, *391*, 566-568.

113 Florin, E.-L.; Moy, V. T.; Gaub, H. E. *Science* **1994**, *264*, 415-417.

114 Lee, G. U.; Kidwell, D. A.; Colton, R. J. *Langmuir* **1994**, *10*, 354-357.

115 Hinterdorfer, P.; Baumgartner, W.; Gruber, H. J.; Schilcher, K.; Schindler, H. *Proc. Natl. Acad. Sci. USA* **1996**, *93*, 3477-3481.

116 Dammer, U.; Hegner, M.; Anselmetti, D.; Wagner, P.; Dreier, M.; Huber, W.; Güntherodt, H.-J. *Biophys. J.* **1996**, *70*, 2437-2441.

117 Ros, R.; Schwesinger, F.; Anselmetti, D.; Kubon, M.; Schäfer, R.; Plückthun, A.; Tiefenauer, L. *Proc. Natl. Acad. Sci. USA* **1998**, *95*, 7402-7405.

118 Fritz, J.; Katopodis, A. G.; Kolbinger, F.; Anselmetti, D. *Proc. Natl. Acad. Sci. USA* **1998**, *95*, 12283-12288.

119 Oesterhelt, F.; Oesterhelt, D.; Pfeiffer, M.; Engel, A.; Gaub, H. E.; Muller, D. J. *Science* **2000**, *288*, 143-146.

120 Evans, E.; Ritchie, K. *Biophys. J.* **1997**, *72*, 1541-1555.

121 Izrailev, S.; Stepaninats, S.; Balsera, M.; Oono, Y.; Schulten, K. *Biophys. J.* **1997**, *72*, 1568-1581.

[122]   Merkel, R.; Nassoy, P.; Leung, A.; Ritchie, K.; Evans,E. *Nature* **1999**, *397*, 50-53.

[123]   Lee, G. U.; Chrisey, L. a.; Colton, R. J. *Science* **1994**, *266*, 771-773.

[124]   Noy, A.; Vezenov, D.; Kayyem, J. F.; Meade, T. J.; Lieber, C. M. *Chem. Biol.* **1997**, *4*, 519-527.

[125]   Struntz, T.; Oroszlan, K.; Schäfer, R.; G:untherodt, H. J. *Proc. Natl. Acad. Sci. USA* **1999**, *96*, 11277-11282.

[126]   Essevaz-Roulet, B.; Bockelmann, U.; Heslot, F. *Proc. Natl. Acad. Sci. USA* **1997**, *94*, 11935-11940.

[127]   Rief, M.; Clausen-Schaumann, H.; Gaub, H. E. *Nat. Struct. Biol.* **1999**, *6*, 346-349.

[128]   Conti, M.; Falini, G.; Samorì, B. *Angew. Chem. Int. Ed.* **2000**, *39*, 215-218.

[129]   Schönherr, H.; Beulen, M. W. J.; Bügler, J.; Huskens, J.; Van Veggel, F. C. J. M.; Reinhoudt, D. N.; Vancso, G. J. *J. Am. Chem. Soc.* **2000**, *122*, 4963-4967.

[130]   Dickinson, T.A.; White, J.; Kauer, J.S.; Walt, D.R. *Nature* **1996**, *382*, 697-700.

Chapter 3

Guest Binding Properties of Dimeric Cyclodextrin Hosts

3.1 Introduction

Cyclodextrins are often used in supramolecular chemistry for their unique capability to complex a variety of small organic guests in aqueous environment.[1] Altering the natural selectivity of the cyclodextrins such that they are better able to complex larger guests such as steroids or polycyclic aromatics, is highly useful for sensing applications, and remains a challenge. One approach is to combine multiple cyclodextrins in one molecule. Cyclodextrin dimers were shown to have improved selectivity for elongated guests.[2,3,4,5,6] Incorporation of catalytic moieties in a cyclodextrin dimer resulted in selectivity for ester hydrolysis,[7] hydroxylation,[8] or double bond scission[9] of elongated substrates. Dimers in which the cavities are oriented at an angle with respect to each other, templated the synthesis of bent products.[10]

Although several ditopic guests that bind strongly to synthetic receptors based on multiple cyclodextrin binding sites are known, it would be useful to have a general method to identify potential guest molecules for this type of receptor. Docking is a computational method often used in medicinal chemistry to identify new leads or suggest possible binding modes of known guests.[11] In applications involving the screening of molecular databases, it requires a simplified representation of the binding pocket of a protein or receptor from a crystal structure by for instance a number of spheres or interaction site points. A large number of potential substrates are fitted into this binding site model and the docking algorithm decides whether the interaction energy of each guest in the binding site is favorable or unfavorable. This approach to identifying potential binders for a receptor might also allow the rapid screening of large numbers of guests for *synthetic* receptors.

This Chapter describes the synthesis and computational assessment of the guest binding properties of a cyclodextrin dimer using a docking procedure. The actual binding of several of the hits from the docking procedure to the dimer was tested by a fluorescence competition assay. Finally, the synthesis and initial binding studies of a dansyl-modified cyclodextrin dimer are described. The fluorescent dansyl moiety is a polarity probe, rendering this dimer potentially useful for sensing applications.[12]

3.2 Synthesis of cyclodextrin dimers

Connecting the two cavities in a cyclodextrin dimer at their wider, more accessible, secondary sides should be beneficial for the cooperativity between the cavities. The strategy employed for the preparation of such cyclodextrin dimers involved the use of β-cyclodextrin, which is protected at the primary side with *tert*-butyldimethylsilyl (TBDMS) groups. The dipropylamino β-cyclodextrin dimer **6** was obtained by deprotonating an excess of heptakis(6-*O*-TBDMS)-β-cyclodextrin **4** with lithium hydride and subsequent reaction with *N*-benzylbis(3-bromopropyl)amine **3** (Scheme 3.1). This procedure is known to yield cyclodextrin derivatives modified at C-2 (Figure 2.1),[13,14] because the C-2 hydroxyl group is more acidic than the C-3 hydroxyl group.[15] The relative simplicity of the ^{1}H and ^{13}C NMR spectra confirmed the C_2-symmetry of the dimer and thus the twofold C-2 substitution.
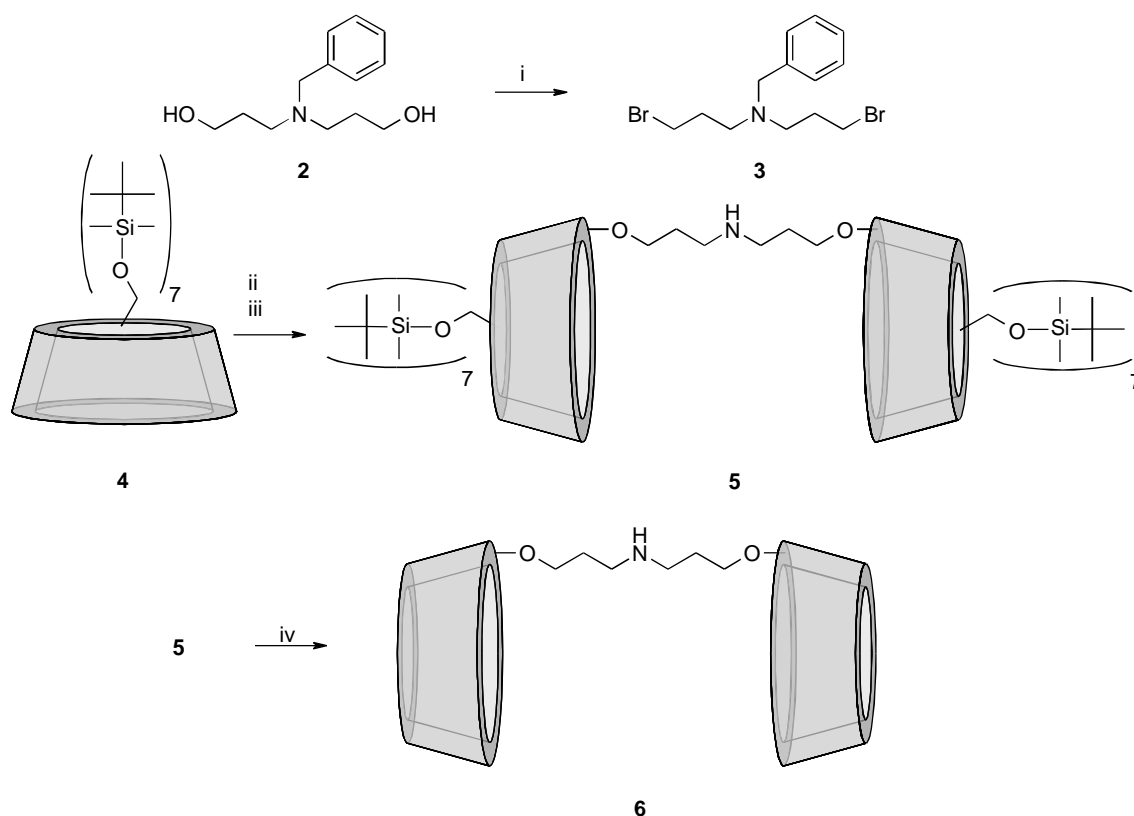
Scheme 3.1. *Synthesis of dimer **6**: i) HBr; ii) LiH, **3**; iii) Pd/C, NH₄HCOO; iv) Bu₄NF.*

Because **4** and the *N*-benzyldipropylamino β-cyclodextrin dimer co-eluted during the chromatographic purification, the benzyl group was directly removed by catalytic reduction, to give the TBDMS-protected dimer **5**. After purification, **5** was deprotected using tetrabutylammonium fluoride in THF to give the desired product **6**. The spacer **8** for the fluorescent dimer **9** (Scheme 3.2) was synthesized by reacting bis(3-hydroxypropyl)amine **7** with one equivalent of dansyl chloride and subsequently with two

equivalents of tosyl chloride. The cyclodextrin dimer was obtained by reaction of **8** with deprotonated TBDMS-β-cyclodextrin **4** followed by deprotection using tetrabutylammonium fluoride in THF.
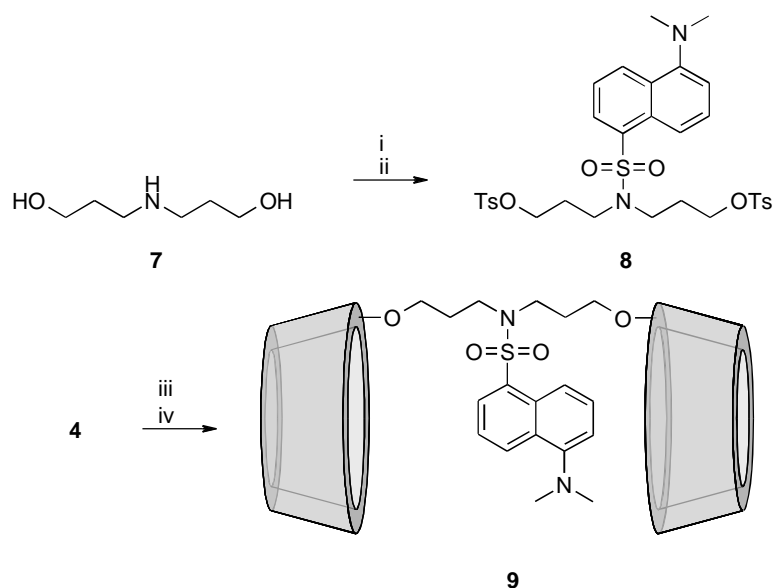
Scheme 3.2. *Synthesis of dimer **9**: i) DansCl, Et₃N; ii) TsCl, pyridine; iii) LiH, **8**; iv) Bu₄NF.*

3.3   Docking study

As no crystal structure of cyclodextrin dimer **6** was available, the conformation of the dimer to be used in the docking procedure was taken from a modeling study of **6** based on a crystal structure of native β-cyclodextrin. An extended conformation of the flexible alkyl spacer was chosen (Figure 3.1).
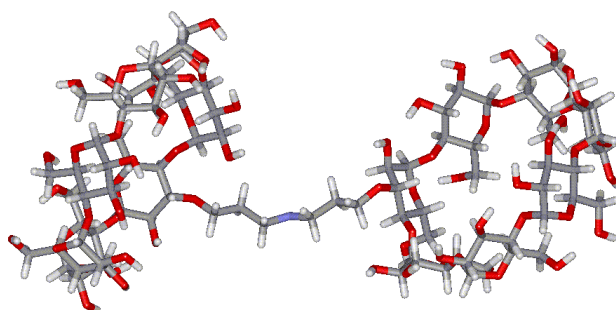
Figure 3.1.   *Conformation of dimer **6** used in the docking study.*

This conformation of the receptor was used for the docking of two databases, the available chemicals database (ACD) and the comprehensive medicinal chemistry database (CMCD). After filtering out ligands with molecular weights below 200 and compounds with more than two formal charges or reactive functionalities, 10^5 molecules from the ACD and 10^4 molecules from the CMCD were docked against the dimer. Although traditionally applied in virtual screening of protein guests,[11] molecular database docking also appears to perform well as a computational tool for identifying small molecule guests for synthetic receptors. Among the highest ranking docking solutions for molecules from the ACD, several appeared to be of sufficient length to position hydrophobic functionalities in both β-cyclodextrin cavities. In particular, phenyl, cyclohexyl, adamantyl, *tert*-butyl, and complex aliphatic ring systems (steroidal or opiate-like) were positioned in the β-cyclodextrin ring interiors. In some cases, additional hydrogen bonding with hydroxyls at the rim of the cyclodextrin rings was also suggested by the binding modes proposed by DOCK 4.0. The interaction with the linker moiety was usually minimal. Binding to both cyclodextrins appeared to be less common for the majority of ligands retrieved from the CMCD. This is due to the bias in this database for molecules of relatively low molecular weight and small size, which are more likely to penetrate biological membranes and assert their pharmacological effect. It should be noted, however, that only a single, extended, and rigid conformation of the cyclodextrin dimer was used in this study. Given the flexible nature of the linker in this system, it may well be possible that both cyclodextrins bind different portions of the same ligand. Alternatively, two ligands may bind to a single dimer.

In total, 93 docked ligands from the ACD and 125 ligands from the CMCD were selected for experimental evaluation (subject to commercial availability) after visual inspection of docking hits. Based on water solubility, cost, and commercial availability of the pure substance (CMCD), thirty guests were selected for screening, 19 from the ACD (Chart 3.1), and 11 from the CMCD (Chart 3.2).
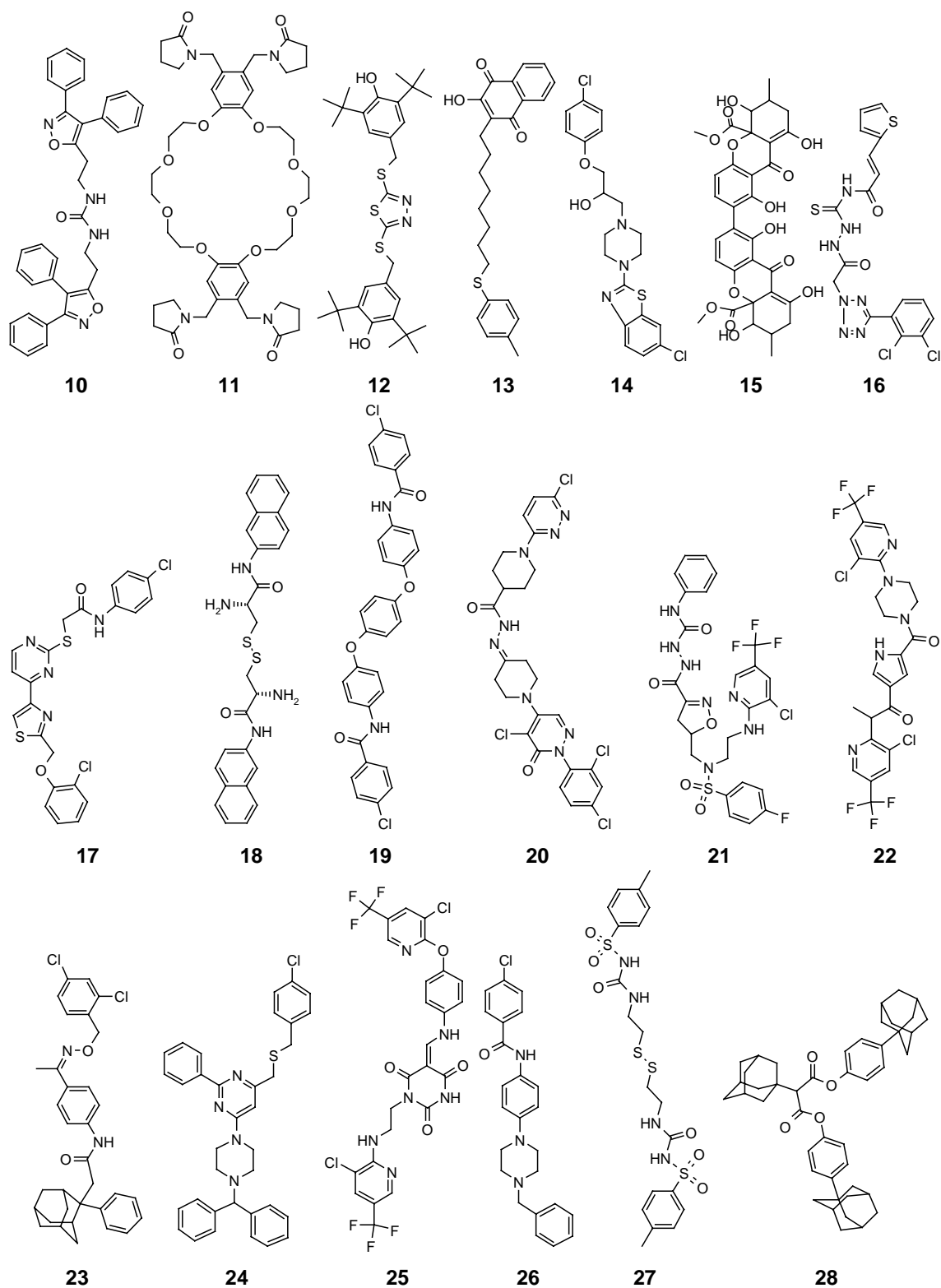
Chart 3.1. *Compounds from the ACD selected for screening.*

cholic acid
29

ursodeoxycholic acid
30

chenodeoxycholic acid
31

prednisolone
21-hemisuccinate
32

hydrocortisone
21-hemisuccinate
33

dichlorisone acetate
34

betamethasone
21-phosphate
35

clomipramine
36

hydrocodone
37

domperidone
38

imperialine
39
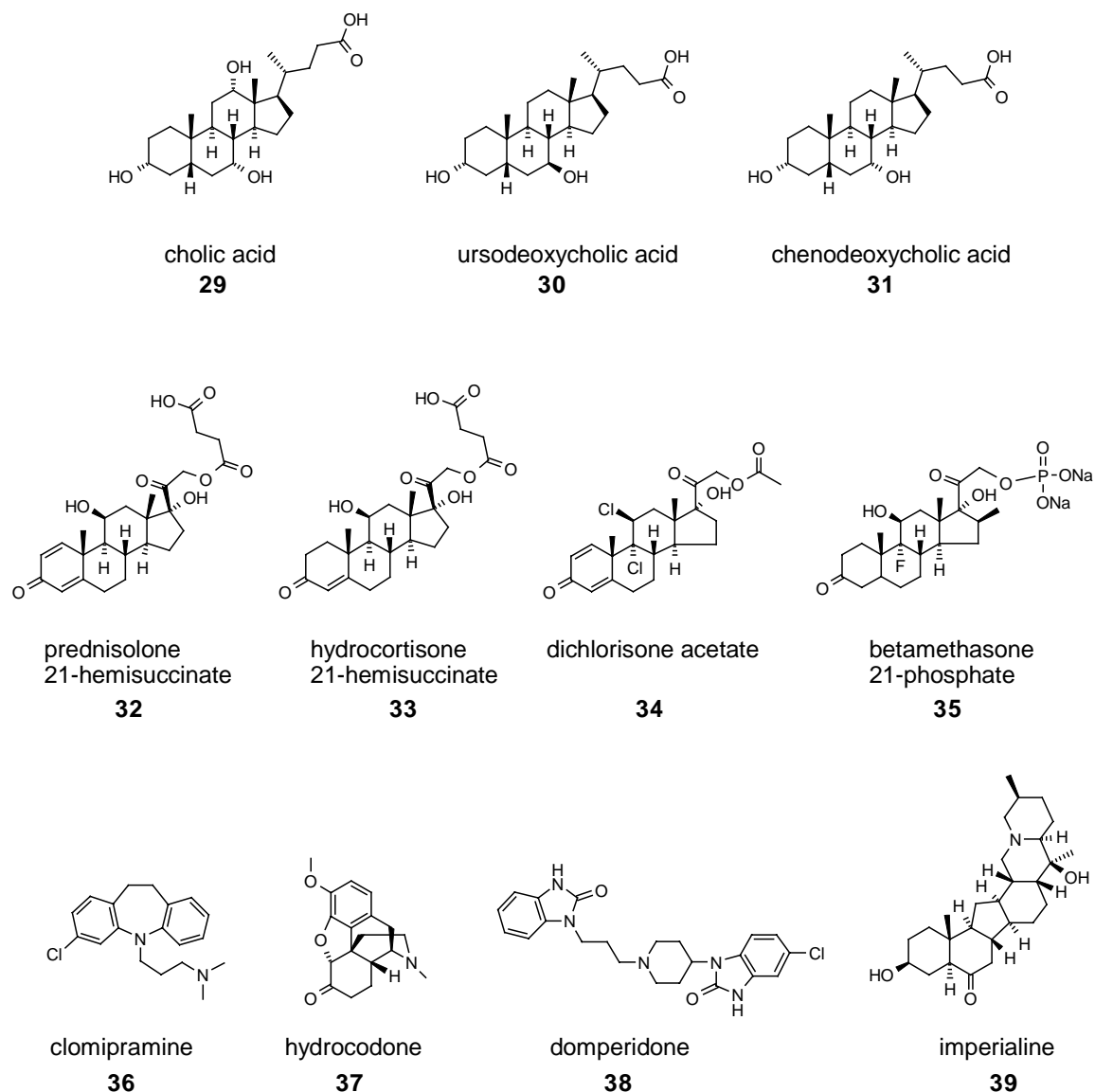
Chart 3.2. *Compounds from the CMCD selected for screening.*

To allow for rapid screening of the potential guests, a method is needed that gives an easily measurable response upon binding of a guest in dimer **6**. For most of the potential guests found by the docking procedure, no obvious method for direct generation of a signal is available. Therefore, it was decided to use a fluorescence competition assay for a rapid indication whether a guest binds or not. The polarity probe 2-*p*-toluidinylnaphthalene-6-sulfonate (TNS) is known to be cooperatively bound by cyclodextrin dimers.[6,16] Its binding constant to **6** was determined by a fluorescence titration (Figure 3.2). A curve fitting procedure yielded a 1:1 association constant of 5.3×10^4 M^{-1}.
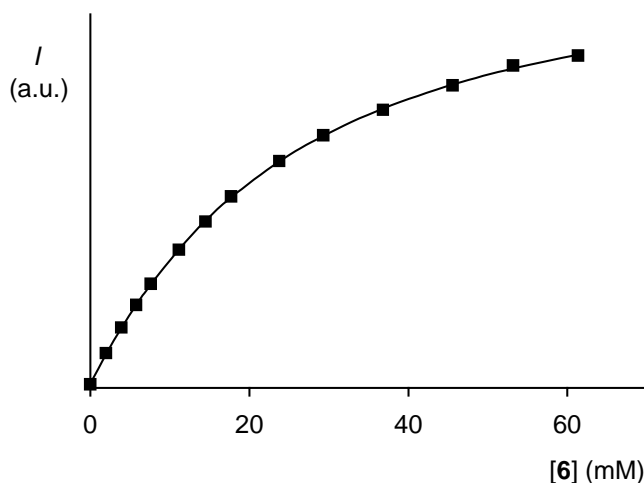
Figure 3.2. *Fluorescence intensity of TNS ([TNS] = 10 μM, λ = 454 nm) as a function of [6].*

The binding constants of most known guests in native β-cyclodextrin are in the range of 10^2 – 10^4 M^{-1}. Only a few stronger binding guests are known. Therefore, an association constant of 10^5 M^{-1} was chosen as an indication that both cavities cooperate in the binding of the guest. From the binding constant of TNS in the dimer **6** and the fluorescence intensities of bound and unbound TNS obtained by the curve fitting procedure, the expected change in total fluorescence intensity at given values for the concentrations of **6**, TNS, and competing guest was calculated (Figure 3.3).
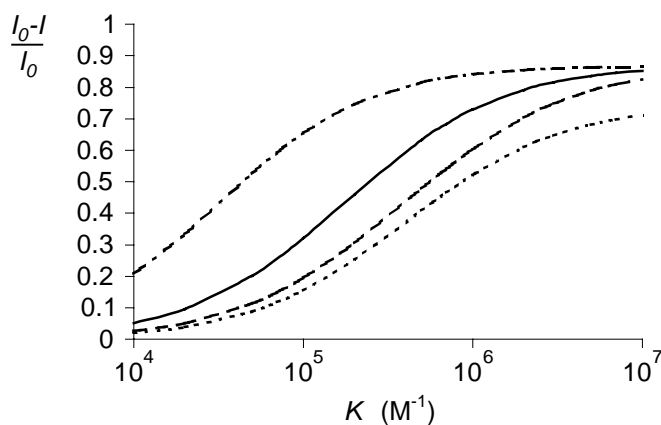
Figure 3.3. *Decrease in the fluorescence intensity of TNS as a function of the binding constant of the competing guest at 2 μM concentrations of 6. [TNS] = 10 μM, [guest] = 50 μM (— · — ·); [TNS] = 10 μM, [guest] = 10 μM (————); [TNS] = 10 μM, [guest] = 5 μM (— — —); [TNS] = 50 μM, [guest] = 10 μM (- - - - - -).*

The screening was performed at a host concentration of 2 μM. The concentrations for both guests were kept at 10 μM. The results of the screening are given in Figure 3.4.
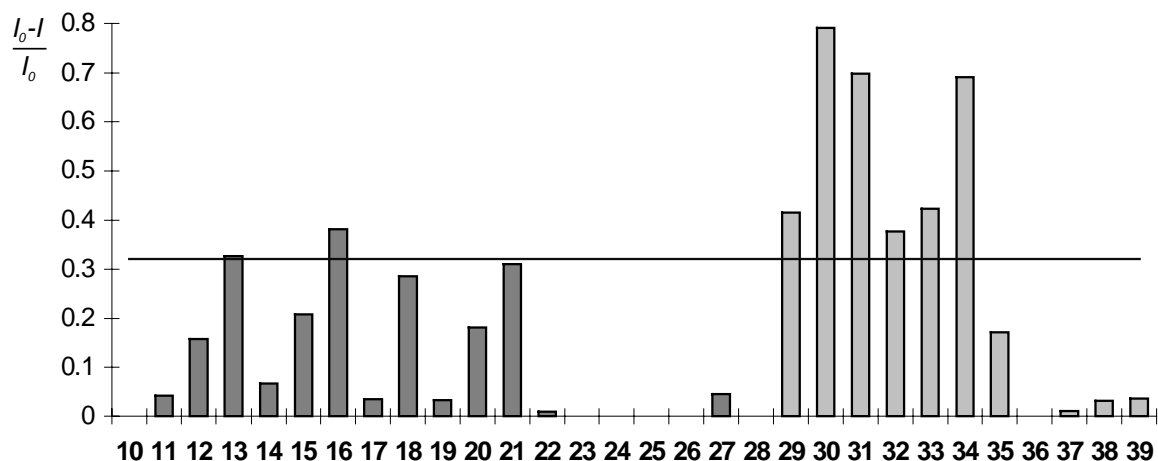
Figure 3.4. *Overview of the screening of guests found by the docking procedure. The solid line represents the expected response for a K value of the competing guest of 10^5 M^{-1}.*

Three guests from the ACD and six from the CMCD appeared to have a binding constant $> 10^5$ M^{-1} in dimer **6**. For these guests, competition fluorescence titrations were performed and association constants were determined using a curve fitting procedure. The results are given in Table 3.1.

Table 3.1. *Association constants for strongly binding guests in dimer **6** determined by competition fluorescence titrations.*

Guest	K (M^{-1})
13	$1.0 \cdot 10^5$
16	$1.9 \cdot 10^5$
21	$1.6 \cdot 10^6$
29	$2.8 \cdot 10^5$ [a]
30	$3.6 \cdot 10^6$ [a]
31	$5.2 \cdot 10^6$ [a]
32	$3.4 \cdot 10^5$
33	$4.3 \cdot 10^5$
34	$3.6 \cdot 10^6$

[a] taken from ref. [17]

From the titrations it is clear that nine out of thirty predicted guests actually bind to the dimer. This hit rate of 30% compares very favorably to the results obtained with docking of receptors to peptides, where hit rates < 10% are usually obtained. A graphical representation of the various stages that led to the identification of the nine strong binding guests is shown in Figure 3.5.

| ACD CMCD | selection criteria | 10^5 compounds | docking | 218 compounds | selection on: cost availability solubility | 30 compounds | screening | 9 hits |
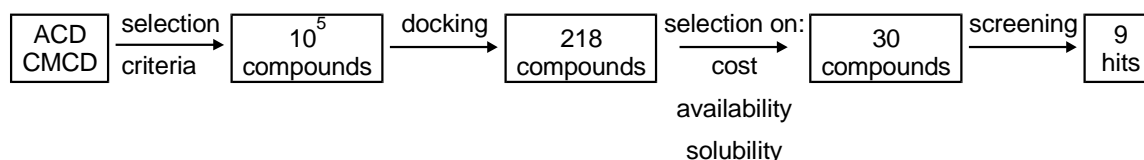
Figure 3.5. *Stages of the docking procedure.*

Molecular docking to synthetic receptors is likely to be sensitive to similar sources of error as virtual screening of molecule databases against biological receptors.[18,19] The choice of scoring function, as well as the computational implementation and amount of conformational sampling of ligands and receptor can be expected to influence results. It is encouraging, however, that using a relatively simplistic protocol, involving rigid ligand conformations and force-field scoring without correction for entropic effects, has proven to be able to identify novel ligands for cyclodextrin-derived receptors. Further improvements in terms of enriching docking results with true binders and the prediction of bound conformations through the use of alternative docking and scoring protocols requires further investigation. Another issue regarding docking to non-biological systems involves the discrimination between specific and non-specific binding. Contrary to, for instance, enzyme-inhibitor complexes, ligands may bind synthetic receptors by means of multiple configurations. In addition, the presence of solvents other than water may be of importance in the selection of relative weights for different terms in scoring functions used for docking.

3.4   Steroid binding in fluorescent cyclodextrin dimer 9

The sensing abilities of dimer **9** were tested using the guests that bind strongly to dimer **6**. The large number of hits with a steroidal structure obtained through the docking procedure, and the high binding constants of some of these steroids in dimer **6** suggested that steroids are an excellent class of molecules to test for their possibility to be detected by **9**. Therefore, some additional steroids were selected for testing as well. Dimer **9** had an emission maximum at 540 nm in aqueous solution. The blue shift compared to dansyl amide (λ_{max} = 572 nm),[20] is consistent with the partial self-inclusion of the appended fluorophore as will be discussed in Chapter 4. Addition of a tenfold excess of various steroids to a *micromolar* solution of **9** resulted in a fluorescence response to several steroids (Figure 3.6).
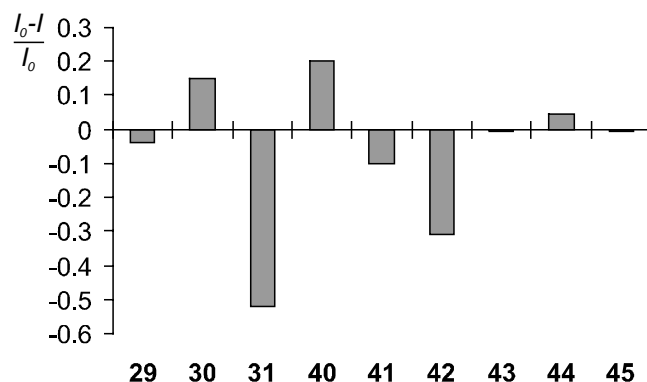
Figure 3.6. *Fluorescence response of dimer 9 on the binding of steroidal guests. 40: deoxycholic acid, 41: lithocholic acid, 42: cortexolone, 43: prednisolone, 44: prednisone, 45: corticosterone-21-acetate.*

Surprisingly, the addition of steroids did not always result in the decrease in fluorescence intensity expected when the dansyl moiety is expelled from the cavity. In some cases, a considerable increase in the fluorescence was observed. The large and opposite responses found for the closely related bile salts, prompted a closer investigation of the factors governing the fluorescence response to this class of steroids. This will be described in Chapter 4.

3.5 Conclusions

The results in this Chapter indicate that a docking procedure, which is a well established tool for identifying possible ligands or inhibitors for protein receptors, is very well suited for assessing the binding properties of synthetic host molecules based on multiple covalently connected cyclodextrin molecules. Several classes of molecules that potentially bind to cyclodextrin dimers were identified, and the strong binding of steroids was shown. The migration of computational tools commonly applied in pharmaceutical research, such as molecular docking and superpositioning, could deliver novel applications in supramolecular chemistry and nanotechnology. Docking techniques could play a role in the identification of ligands and building blocks for sensors and other complexes of synthetic organic molecules. Alternatively, they could be applied to identify molecules that can serve as connectors or to delineate the specificity of nano-devices. The work presented here provides a first demonstration of the potential for virtual screening technology to be used outside the confines of pharmaceutical lead identification and optimization.

Appending a fluorophore to a cyclodextrin dimer appeared an interesting strategy to obtain molecules that are potentially useful for application in steroid sensors. In the future, similar computational procedures as the one used here may aid in the design of cyclodextrin-based

synthetic receptors for a given analyte. The optimum orientation of the cavities with respect to each other for the analyte may be determined computationally and a host best fitting the specifications may subsequently be synthesized.

3.6   Experimental section

Materials and methods. β-Cyclodextrin was kindly donated by Wacker-Chemie, München. All chemicals were used as received, unless otherwise stated. Solvents were purified according to standard laboratory methods.[21] Solvents for fluorescence spectroscopy were of analytical grade. TLC was performed on aluminum sheets precoated with silica gel 60 F254 (E. Merck). The cyclodextrin spots were visualized by dipping the sheets in 5% sulfuric acid in ethanol followed by heating. Chromatographic separations were performed on silicagel 60 (E. Merck, 0.040-0.063 mm, 230-240 mesh). *N*-Benzylbis(3-hydroxypropyl)amine **2**,[22] bis(3-hydroxypropyl)amine **7**,[22] and TBDMS-protected β-cyclodextrin **4**[14] were prepared according to literature procedures.

Mass spectra were recorded with a Finnigan MAT 90 spectrometer using NBA/NPOE as a matrix. NMR spectra were recorded at 25 ºC using a Bruker AC 250 and a Varian Inova 300 spectrometer. ^{1}H NMR chemical shifts (250 or 300 MHz) are given relative to residual CHCl$_3$ (7.25 ppm), or HDO (4.65 ppm). [13]C chemical shifts (63 or 75 MHz) are given relative to CDCl$_3$.

N-Benzylbis(3-bromopropyl)amine 3. *N*-Benzylbis(3-hydroxy)propylamine **2** (0.35 g, 1.6 mmol) was refluxed in concentrated aqueous HBr (6 mL) for 36 h. The solution was neutralized with 1 M NaOH, after which CH$_2$Cl$_2$ was added. The organic layer was washed with water and brine, and dried (MgSO$_4$) to obtain **3** as a yellowish oil in 91% yield. ^{1}H NMR (CDCl$_3$) δ 7.37-7.27 (m, 5H), 3.58 (s, 2H), 3.47 (t, 4H, *J* = 6.5 Hz), 2.60 (t, 4H, *J* = 6.6 Hz), 2.08-1.99 (m, 4H); ^{13}C NMR (CDCl$_3$) δ 139.3, 128.7, 128.3, 127.0, 58.8, 52.0, 31.8, 30.5; MS (FAB) *m/z* calcd. for C$_{13}$H$_{19}$NBr$_2$ 347.0, found 348.1 ([M + H]$^+$).

TBDMS-protected dipropylamino cyclodextrin dimer 5. LiH (30 mg, 3.7 mmol) was added to a solution of dried (100 °C, 0.1 mbar, 5 h) **4** (6.0 g, 3.1 mmol) in dry THF (50 mL). The mixture was stirred for 1 h at room temperature and then for 1 week at reflux temperature. During the first three days, **2** (0.53 g, 1.5 mmol) was added in portions. The solvent was removed *in vacuo* and chloroform was added. The solution was washed with water and brine, and dried (MgSO$_4$). After removal of the solvent, the crude product was purified by column chromatography (eluent: ethyl acetate/ethanol/water 100:2:1), after which a mixture of **4** and benzyl-protected cyclodextrin dimer was obtained. A solution of this mixture (1.0 g) and ammonium formate (2.0 g) in EtOH (150 mL) was refluxed for 2 h

in the presence of a catalytic amount of 10% Pd/C. The catalyst was removed by filtration through Celite and the solvent was removed *in vacuo*. The product was purified by repeated column chromatography (eluent: ethyl acetate/ethanol/water 10:2:1, CH_2Cl_2/MeOH 85:15) to obtain **5** as a white powder in 5% yield (overall). [^1]H NMR ($CDCl_3$/CD_3OD) δ 4.88-4.85 (m, 14H), 4.27-3.35 (m, 92H), 2.01-1.88 (m, 4H), 1.05-0.84 (m, 126H), 0.04-0.00 (m, 84H); [^13]C NMR ($CDCl_3$/CD_3OD) δ 102.5-101.3, 82.1-79.8, 73.6-72.2, 61.9-61.5, 26.0, 25.9, 25.8, 18.5, 18.3, 18.2, 1.0, -5.0, -5.1, -5.2, -5.3, -5.4; MS (FAB) *m/z* calcd. for $C_{174}H_{347}NO_{70}Si_{14}$ 3963, found 3988.6 ($[M + Na]^+$).

Dipropylamino cyclodextrin dimer 6. TBDMS-protected dimer **5** (123 mg, 0.031 mmol) was dissolved in THF (10 mL). After addition of a 1 M solution of tetrabutylammonium fluoride in THF (1 mL) the solution was refluxed overnight. The solvent was removed *in vacuo* and the residue dissolved in water. After three washings with hexane, salts were removed over amberlite ion exchange resin. After freeze-drying the dimer was obtained as a white powder in 50% yield. [^1]H NMR (D_2O) δ 5.11-5.10 (m, 2H), 4.97-4.96 (m, 12H), 3.98-3.37 (m, 88H), 3.14-3.08 (m, 4H), 1.93-1.85 (m, 4H); [^13]C NMR (D_2O) δ, 104.8-102.0, 84.0-82.8, 75.6-75.4, 74.5-74.0, 71.7, 62.8, 48.1, 28.9; MS (FAB) *m/z* calcd. for $C_{90}H_{151}NO_{70}$ 2365.8, found 2388.9 ($[M + Na]^+$).

N,N-bis(3-tosyloxypropyl)dansylamide 8. Dansyl chloride (1.0 g, 3.7 mmol) was added to a solution of dipropanolamine (0.60 g, 4.5 mmol) and triethylamine (1.5 g, 15 mmol) in CH_2Cl_2 (20 mL). The solution was stirred at room temperature for 1 h. The organic layer was washed with a saturated aqueous solution of NH_4Cl, water, and brine, and dried over $MgSO_4$. After evaporation of the solvent N,N-bis(3-hydroxypropyl)dansylamide was obtained as a greenish oil in 96% yield. [^1]H NMR ($CDCl_3$) δ 8.53 (d, 1H, *J* = 8.7 Hz), 8.29 (d, 1H, *J* = 8.4 Hz), 8.09 (d, 1H, *J* = 7.2 Hz), 7.58-7.48 (m, 2H), 7.18 (d, 1H, *J* = 7.8 Hz), 3.62 (t, 4H), 3.45 (t, 4H), 288 (s, 6H), 1.79-1.71 (m, 4H) [^13]C NMR ($CDCl_3$) δ 151.7, 134.9, 130.3, 130.0, 129.9, 128.8, 128.2, 123.1, 119.2, 115.2, 59.1, 45.3, 44.9, 31.2; MS (FAB) *m/z* calcd. for $C_{18}H_{26}N_2O_4S$ 366.2, found 367.1 ($[M + H]^+$).

At 0 °C a solution of tosyl chloride (4.0 g, 21 mmol) in pyridine (20 mL) was added to a solution of N,N-bis(3-hydroxypropyl)dansylamide (1.3 g, 3.5 mmol) in pyridine (20 mL). The solution was stirred at 0 °C for 3 h. The mixture was shaken for 5 min with ice water and then acidified (pH 2) using concentrated HCl. The product was extracted with ethyl acetate. The organic layer was washed with water, 1 M NaOH, water, and brine, and dried over $MgSO_4$. After evaporation of the solvent, the crude product was purified by column chromatography (eluent: ethyl acetate/hexanes 1:1) to give **8** as a greenish oil in 67 % yield. [^1]H NMR ($CDCl_3$) δ 8.55 (d, 1H, *J* = 8.4 Hz), 8.18 (d, 1H, *J* = 9 Hz), 8.10 (d, 1H, *J* = 7.2 Hz), 7.73 (d, 4H, *J* = 8.1 Hz), 7.53-7.47 (m, 2H), 7.34 (d, 4H, *J* = 8.4 Hz), 7.19 (d, 1H, *J* = 7.5 Hz), 3.93 (t, 4H, *J* = 6 Hz), 3.26 (t, 4H, *J* = 7.2 Hz), 2.89 (s, 6H), 2.45 (s, 6H), 1.87-1.78 (m, 4H) [^13]C NMR ($CDCl_3$) δ 151.9, 145.0, 134.2, 132.7, 130.7, 129.9, 128.3, 127.9,

123.1, 119.0, 115.3, 67.6, 45.4, 44.8, 44.5, 28.1, 21.6; MS (FAB) *m/z* calcd. for $C_{32}H_{38}N_2O_8S_3$ 674.2, found 674.2 ($[M + H]^+$).

Fluorescent cyclodextrin dimer 9. LiH (3 mg, 0.37 mmol) was added to a solution of dried (100 °C, 0.1 mbar, 5 h) TBDMS-protected β-cyclodextrin **4** (0.50 g, 0.26 mmol) in THF (50 mL). The mixture was stirred for 1 h at room temperature and then for 2 h at reflux. A solution of **8** (68 mg, 0.10 mmol) in THF (5 mL) was added and reflux was continued for 120 h. The solvent was removed *in vacuo* and chloroform was added. The solution was washed with 1 M HCl, water, and brine, and dried (MgSO₄). After removal of the solvent and purification by column chromatography (eluent: ethyl acetate/ethanol/water 100:2:1) the TBDMS-protected fluorescent cyclodextrin dimer was obtained as a light green powder in 22% yield. ^{1}H NMR (CDCl₃/CD₃OD) δ 8.51 (d, 1H, *J* = 8.4 Hz), 8.24 (d, 1H, *J* = 8.4 Hz), 8.13 (d, 1H, *J* = 7.5 Hz), 7.55-7.45 (m, 2H) 7.15 (d, 1H, *J* = 7.8 Hz), 4.93-4.88 (m, 14H), 4.18-3.03 (m, 92H), 2.86 (s, 6H), 2.23-2.17 (m, 4H), 0.90-0.83 (m, 126H), 0.07-0.00 (m, 84H); ^{13}C NMR (CDCl₃/CD₃OD) δ 151.7, 135.4, 130.1, 130.0, 129.4, 127.9, 123.0, 119.7, 115.1, 102.4, 102.1, 101.9, 101.5, 99.1, 83.1, 82.0, 81.9, 81.8, 81.7, 80.9, 80.8, 79.5, 77.2, 73.6, 73.3, 73.2, 73.1, 72.5, 72.2, 72.0, 70.8, 62.5, 61.6, 61.1, 45.4, 43.9, 29.7, 28.1, 25.9, 25.7, 18.4, 18.3, 18.1, 1.0, -5.3, -5.3; MS (FAB) *m/z* calcd. for $C_{186}H_{358}N_2O_{72}SSi_{14}$ 4196.1, found 4221.6 ($[M + Na]^+$).

The TBDMS-protected fluorescent cyclodextrin dimer (140 mg, 0.034 mmol) was dissolved in THF (10 mL). After addition of a 1 M solution of tetrabutylammonium fluoride in THF (1 mL), the solution was refluxed overnight. The solvent was removed *in vacuo* and the residue dissolved in water. After three washings with hexane, salts were removed over amberlite ion exchange resin. After freeze-drying the dimer was obtained as a yellowish powder in 76% yield. ^{1}H NMR (D₂O) δ 8.52 (d, 1H, *J* = 7.8 Hz), 8.21-8.17 (m, 2H), 7.70-7.65 (m, 2H) 7.23 (d, 1H, *J* = 7.5 Hz), 5.01-4.91 (m, 14H), 3.96-3.27 (m, 92H), 2.79 (s, 6H), 1.88-1.65 (m, 4H); ^{13}C NMR (D₂O) δ 153.9, 135.6, 133.0, 132.4, 131.8, 129.9, 104.4, 84.4-83.6, 75.6-71.7, 62.7, 48.0, 30.6; MS (FAB) *m/z* calcd. for $C_{102}H_{162}N_2O_{72}S$ 2598.9, found 2600.8 ($[M + H]^+$).

Computational methodology.

Gas-phase minimization. Initial structures as well as visualizations were carried out with Quanta97.[23] The MD calculation was run with CHARMM 22.0 and 23.0.[24] Parameters were taken from Quanta97 and point charges were assigned with the charge template option in Quanta/CHARMm. The structure of β-cyclodextrin was taken from the Cambridge Crystallographic Database. After removal of the water molecules from the crystal structure, two cyclodextrin units were manually connected *via* a spacer in an all-trans conformation. The dimer was charged to 0, with a small "excess" charge smoothed to non-polar carbons and hydrogens. The starting structure was minimized by ABNR (Adopted-Basis set Newton-Raphson) until the RMS on the energy gradient was ≤ 0.01

kcal·mol^{-1}·Å^{-1}. No cutoff on the non-bonded interactions was applied in the gas-phase minimizations of the complexes. A constant dielectric constant with an ε of 1 was used.

Docking. In order to identify small organic molecules that bind both cyclodextrin cavities of the dimer, the molecular docking program DOCK 4.0[25] was applied. The AMBER[26] electrostatic and van der Waals force field parameters for the host molecule were encoded in a three-dimensional (3D) grid of 0.3 Å spacing using the GRID program from the DOCK 4.0 suite of software[27] to speed up the force field scoring calculations. A distance dependent dielectric of $\varepsilon=\varepsilon_0 4r$ was applied to approximate electrostatics in aqueous solvent. The grid was placed in a box of dimensions $35.8 \times 20.9 \times 22.2$ Å, encompassing the entire β-cyclodextrin dimer with an additional margin of 3 Å. The original source code of DOCK 4.0 was modified such that ligand atoms that were placed outside the box containing the receptor molecule were counted as van der Waals bumps. This modification eliminates ligand placements that are outside the area of interest at an early stage of the docking procedure.

Two chemical databases supplied by MDL Information Systems Inc. (San Leandro, USA) were considered for docking. The available chemicals database (ACD) provides a source of commercially available small organic molecules and was used to obtain a general idea of what type of molecules and chemical functionalities can bind to the dimer. The comprehensive medicinal chemistry database (CMCD) is a source of currently marketed drugs and other molecules of medical importance and was used to screen for biologically more relevant ligands. Three-dimensional structures for potential ligands from the ACD and CMCD were generated using CORINA[28]. The linear shape of the dual cyclodextrin receptor molecule suggests preferred binding of molecules in an extended conformation. It was therefore decided to directly use the extended ligand conformations commonly generated by CORINA without allowing for additional ligand flexibility during docking. All ligands were converted to SYBYL (Tripos Inc., St. Louis, USA) mol2 format with SYBYL atom types and Gasteiger-Marsili[29] partial charges. For docking of the ACD, ligands were separated based on their total, absolute formal charges. This procedure and the use of a distance-dependent dielectric provide some compensation for the tendency of force field-based scoring to favor highly charged interactions. After filtering out ligands with molecular weights below 200, more than two formal charges, and reactive functionalities, a total of 70867 molecules from the ACD and 7497 molecules from the CMCD were docked against the β-cyclodextrin dimer.

Docking of rigid ligand molecules involves their superposition onto site points in the receptor molecule. Docking site points, covering the binding pockets of both cyclodextrin host molecules, were generated with SPHGEN[30] and culled to a total of 25 by means of visual inspection using Quanta 98 (Molecular Simulations Inc., San Diego, USA). Uniform sampling,[25] generating 200 orientations per ligand, was applied during docking and three van der Waals bumps were allowed for molecules to enter the stage of force field scoring

and minimization. After positioning and scoring of each ligand, a maximum of 100 Simplex minimization steps were performed using an initial translation of 1 Å and a rotation of 0.1 rad until convergence was reached within 0.1 kcal/mol. The highest ranking 200 molecules were visually inspected using Quanta 98 and web-tools applying the Chime plug-in (MDL, San Leandro USA). Those ligands displaying good complementarity to the cyclodextrin dimer were selected for testing. Additional compounds from the ACD with more than 80 % similarity to known actives from the first screen in terms of ISIS base (MDL, San Leandro, USA) fingerprints were also selected for testing.

Fluorescence. Fluorescence measurements were performed on an Edinburgh SF 900 spectrometer. Sample solutions were prepared using a phosphate buffer (pH 7, I=0.02) in pure water (Millipore Q2). The optical density of the samples at the excitation wavelength, as determined by UV-vis spectroscopy, remained below 0.1. The fluorescence titration of **6** with TNS was performed by adding aliquots of **6** (1.6×10^{-4} M) in TNS solution (1.0×10^{-5} M) to the pure TNS solution and vice versa, thus keeping the TNS concentration constant. After each addition the fluorescence spectrum was recorded.

The screening was performed by recording fluorescence spectra before and after adding 50 µL of a solution of the guest (6.1×10^{-4} M) in methanol to 3 mL of an aqeuous solution of **6** (2.0×10^{-6} M) and TNS (1.0×10^{-5} M). Fluorescence competition titrations were performed by adding aliquots of a solution of the guest (6.1×10^{-4} M) in methanol to 3 mL of an aqeuous solution of **6** (2.0×10^{-6} M) and TNS (1.0×10^{-5} M). After each addition the fluorescence spectrum was recorded.

Fluorescence titrations with **9** were performed by adding aliquots of guest in host solution to the pure host solution and *vice versa*, thus keeping the host concentration constant. After each addition, the fluorescence spectrum was recorded.

3.7   References

[1]   (a) Wenz, G. *Angew. Chem. Int. Ed. Engl.* **1994**, *33*, 803-822. (b) Szejtli, J.; Osa, T. *Comprehensive Supramolecular Chemistry, Vol. 3*, (Eds.: J.L. Atwood, J.E.D. Davies, D.D. MacNicol, F. Vögtle, J.-M. Lehn), Pergamon, Oxford, **1996**.

[2]   Fujita, K.; Ejima, S.; Imoto, T. *Chem. Commun.* **1984**, 127-128.

[3]   Breslow, R.; Chung, S. *J. Am. Chem. Soc.* **1990**, *112*, 9659-9660.

[4]   Breslow, R.; Zhang, B.L. *J. Am. Chem. Soc.* **1996**, *118*, 8495-8496.

[5]   Venema, F.; Rowan, A.E.; Nolte, R.J.M. *J. Am. Chem. Soc.* **1996**, *118*, 257-258.

[6]   Venema, F.; Nelissen, H.F.M.; Berthault, P.; Birlirakis, N.; Rowan, A.E.; Feiters, M.C.; Nolte, R.J.M. *Chem. Eur. J.* **1998**, *4*, 2237-2250.

[7]   Zhang, B.; Breslow, R. *J. Am. Chem. Soc.* **1997**, *119*, 1676-1681.

[8]   Yang, J.; Breslow, R. *Angew. Chem. Int. Ed.* **2000**, *39*, 2962-2964.

[9]   French, R.R.; Holzer, P.; Leuenberger, M.G.; Woggon, W.-D. *Angew. Chem. Int. Ed.* **2000**, *39*, 1267-1269.

[10]   Easton, C.J.; Harper, J.B.; Lincoln, S.F. *New J. Chem.* **1998**, 1163-1165.

[11]   (a) Kuntz, D. *Science* **1992**, *257*, 1078-1082; (b) Walters, P.A.; Stahl, M.T.; Murcko, M.A. *Drug Disc. Today* **1998**, *3*,160-178; (c) Kubinyi, H. *Curr. Opin. Drug Discov. & Develop.* **1998**, *1*, 16-27.

[12]   Ueno, A. *Supramol. Sci.* **1996**, *3*, 31-36.

[13]   Nelissen, H.F.M.; Venema, F.; Uittenbogaard, R.M.; Feiters, M.C.; Nolte, R.J.M. *J. Chem. Soc., Perkin Trans. 2* **1997**, 2045-2053.

[14]   Van Dienst, E.; Snellink, B.H.M.; Von Piekartz, I.; Grote Gansey, M.H.B.; Venema, F.; Feiters, M.C.; Nolte, R.J.M.; Engbersen, J.F.J.; Reinhoudt, D.N. *J. Org. Chem.* **1995**, *60*, 6537-6545.

[15]   Yamamoto, Y.; Inoue, Y.; *J. Carbohydr. Chem.* **1989**, *8*, 29-46.

[16]   Liu., Y.; Wu, C.T.; Xue, G.P.; Li, J. *J. Incl. Phenom. Mol. Recogn.* **2000**, *36*, 95-100.

[17]   De Jong, M.R.; Engbersen, J.F.J.; Huskens, J.; Reinhoudt, D.N. *Chem. Eur. J.* **2000**, *6*, 4034-4040.

[18]   Lengauer, T.; Rarey, M. *Curr. Opin. Struct. Biol.* **1996**, *6*, 402-406.

[19]   Knegtel, R.M.A.; Wagener, M. *Proteins* **1999**, *37*, 334-345.

[20]   Bügler, J.; Engbersen, J.F.J.; Reinhoudt, D.N. *J. Org. Chem.* **1998**, *63*, 5339-5344.

[21]   Perrin, D.D.; Armarego, W.F.L. *Purification of Laboratory Chemicals*, 3rd ed.; Pergamon Press: Oxford, **1989**.

[22]   Groth, A.M.; Lindoy, L.F.; Meehan, G.V.; *J. Chem. Soc., Perkin Trans. 1* **1996**, 1553-1558.

[23]   Quanta was bought from Molecular Simulations Inc., Burlington, MA, USA.

[24]   (a) Brooks, B.R.; Bruccoleri, R.E.; Olafsen, B.D.; States, D.J.; Swaminathan, S.; Karplus, M. *J. Comput. Chem.* **1983**, *4,* 187; (b) Momany, F.A.; Klimkowski, V.J.; Schäfer, L. *J. Comput. Chem.* **1990**, *11,* 654; (c) Momany, F.A.; Rone, R.; Kunz, H.; Frey, R.F.; Newton, S.Q.; Schäfer, L. *J. Mol. Structure* **1993**, *286*, 1.

[25]   Ewing, T.J.A.; Kuntz, I.D. *J. Comput. Chem.* **1997**, *18*, 1175-1189.

[26]   Weiner, S.J.; Kollman, P.A.; Hguyen, D.T.; Case, D.A. *J. Comput. Chem.* **1986**, *7*, 230-252.

[27]   Meng, E.C.; Shoichet, B.K.; Kuntz, I.D. *J. Comput. Chem.* **1992**, *13*, 505-524.

[28]   Sadowski, J.; Gasteiger, J.; Klebe, G. *J. Chem. Inf. Comput. Sci.* **1994**, *34*, 1000-1008.

[29]   Gasteiger. J.; Marsili, M. *Tetrahedron* **1980**, *36*, 3219-3288.

[30]   Kuntz, I.D.; Blaney, J.M.; Oatley, S.J.; Langridge, R.L.; Ferrin, T.E. *J. Mol. Biol.* **1982**, *161*, 269-288.

Chapter 4

Cyclodextrin Dimers as Receptor Molecules for the Development of Steroid Sensors[*]

4.1 Introduction

The possibility to use cyclodextrins for sensor purposes by appending a fluorescent reporter molecule has been studied by several groups, as has been reviewed in Chapter 2. In this system the generation of a signal is based on the competition between the covalently attached fluorophore and an added guest for the cyclodextrin cavity. In the absence of a guest, the fluorophore (partially) resides in the cavity. Addition of a guest leads to decomplexation of the detector moiety and to a concomitant decrease in fluorescence quantum yield.[1] The selectivity of the sensing molecules mostly resembles that of the native cyclodextrin the sensor is based on. The sensitivity of this system is limited by the competition between complexation of the guest and self-inclusion of the fluorophore in the cyclodextrin cavity. This usually results in decreased binding constants for binding to the receptor compared to binding to the native cyclodextrin.

Recent research efforts in this direction focus on developing cyclodextrin sensors with altered selectivity. This can be achieved by extending the hydrophobic cavity.[2] In our group, fluorophore-appended cyclodextrin-calix[4]arene couples were used as sensing molecules with an enlarged cavity.[3] Their sensing behavior depended heavily on the aggregation state of the hosts and the host-guest complexes.[4] Ueno and coworkers have used biomolecules as large caps for cyclodextrin-based sensing molecules. Cyclodextrin derivatives with monensin moieties,[5] or biotin-modified cyclodextrins interacting with avidin,[6] were investigated as receptors with an enlarged hydrophobic cavity.

Another way to create a larger cavity with increased selectivity for ditopic guests is to couple two cyclodextrins to dimers.[7] In Chapter 3, cyclodextrin dimer **1** was synthesized and its guest-binding properties were assessed by a docking procedure. Subsequent binding experiments proved selectivity of this dimer for elongated guests, *e.g.* steroids. Addition of steroids to aqueous solutions of fluorescent cyclodextrin dimer **2** was shown to give a fluorescence response.
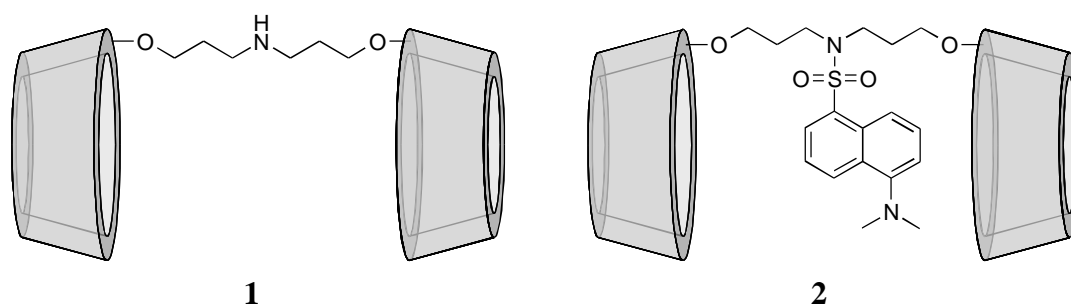
In this chapter, the steroid complexation and sensing properties of fluorescent β-cyclodextrin dimer **2**, in which the cyclodextrins are connected via their secondary sides is described in more detail. The complexation and sensing properties are compared to the dimer without the appended fluorophore **2** and to monomeric cyclodextrin derivatives.

As shown in Chapter 3, a class of steroids (the bile salts, Figure 4.1)[8,9,10,11,12,13,14] gave rise to the largest fluorescence responses when added to **2** and was therefore selected for further investigation. They are surfactant-like molecules that play a role in the metabolism and excretion of cholesterol in mammals.[15]

	Steroid	R_1	R_2	R_3
3a	Cholate	OH	H	OH
3b	Deoxycholate	H	H	OH
3c	Chenodeoxycholate	OH	H	H
3d	Ursodeoxycholate	H	OH	H
3e	Lithocholate	H	H	H
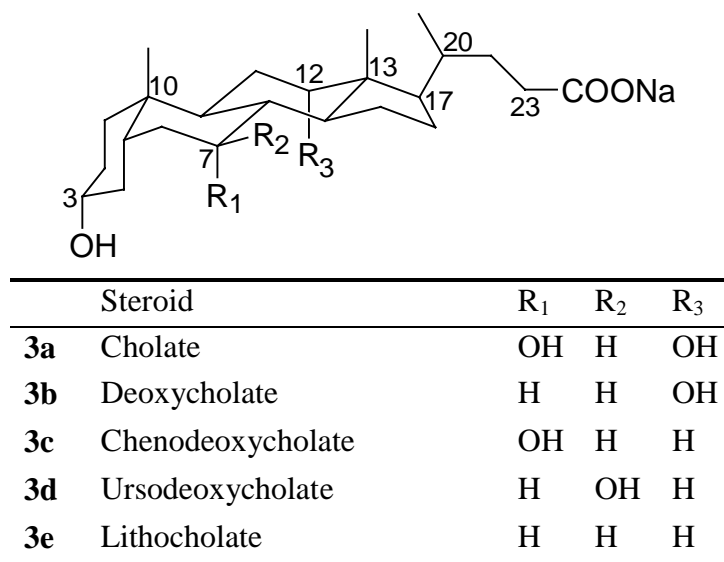
Figure 4.1. *The structure of the bile salts*

The bile salts have a characteristic structure, with a side chain at C-17, methyl groups at C-10, C-13, and C-20, and a carboxylic acid group at C-23 of the steroid skeleton. They differ in the number and position of hydroxyl groups at C-3, C-7, and C-12. The thermodynamics[11] and kinetics[12] of the inclusion of some bile salts in native β-cyclodextrins have been studied by NMR. The thermodynamics of inclusion and the effect of the presence of cyclodextrins on the thermodynamics of micelle formation have been studied by microcalorimetry.[13] The complex geometry of β-cyclodextrin with **3a**, **3b**,[14] and **3d**[8] was studied by ROESY. The aliphatic side chain of the steroid is shown to enter the cyclodextrin from the secondary side. Additional interactions of the two steroid rings closest to the side chain with the interior of the CD were observed. This leaves part of the steroid skeleton available for interaction with a second cyclodextrin. Tato and coworkers[14] also studied the formation of complexes between primary side connected β-cyclodextrin dimers and **3a** and **3b**. For **3b**, the formation of an oligomeric structure is proposed.

4.2 Synthesis of a monomeric cyclodextrin sensor

In order to allow for direct comparison between sensor molecules based on one cyclodextrin moiety and cyclodextrin sensors based on cyclodextrin dimers, a monomeric analogue of fluorescent cyclodextrin dimer **2** was synthesized. Monomeric cyclodextrin sensor **7** was synthesized employing the amine building block **6**. Following a literature procedure,[16] heptakis-6-*O*-(*tert*-butyldimethylsilyl)-β-cyclodextrin **4** was deprotonated and reacted with 1-tosyloxy-3-azidopropane **5**. Subsequent reduction yielded the amine **6**. This amine was reacted with dansyl chloride and subsequently deprotected with trifluoroacetic acid to obtain **7**.

4   **6**   **7**
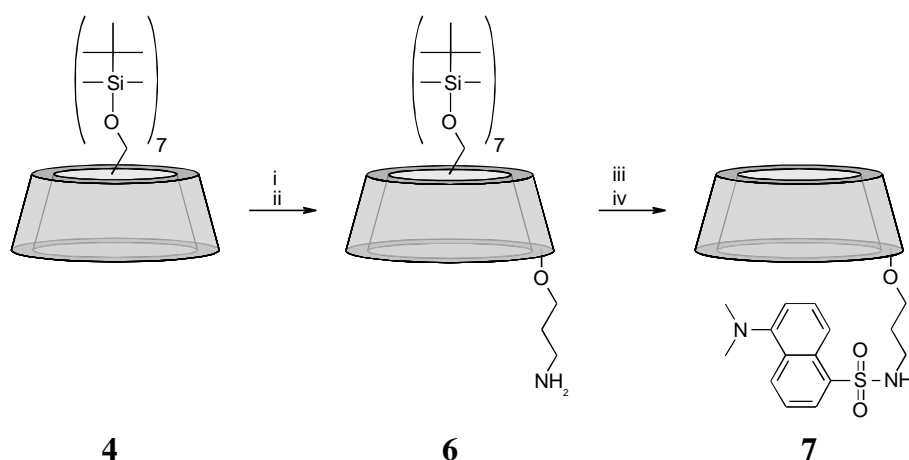
Scheme 4.1. *Synthesis of monomeric cyclodextrin sensor **7**: i) LiH, 1-tosyloxy-3-azidopropane **5**;*
ii) Pd/C, H₂; iii) DansCl, Et₃N; iv) TFA.

4.3 Complexation studies

4.3.1 Introduction

The sensing behavior of **2**, as studied by fluorescence, appeared to be complicated (Chapter 3), as witnessed by remarkable selectivity differences for binding **3a**-**3e** and the occurrence of both intensity increases and decreases. Therefore, the more universal technique of microcalorimetry was employed to study the binding stoichiometry and thermodynamics. These data were compared to data for **1** in order to elucidate the underlying binding mechanism and the role of the fluorophore. The contribution of a single cavity to the binding thermodynamics of the steroids was assessed by comparison to data for native β-cyclodextrin and for **7**.

4.3.2 Complexation of bile salts in β-cyclodextrin and the monomeric derivative 7

Dilution experiments of the bile salts proved that the titrations with β-cyclodextrin, **1**, **2**, and **7** were performed below the critical micelle concentration (cmc) of the bile salts. The titrations of steroids with β-cyclodextrin showed enthalpograms typical of 1:1 complex formation (Figure 4.2). The thermodynamic data are listed in Table 4.1.
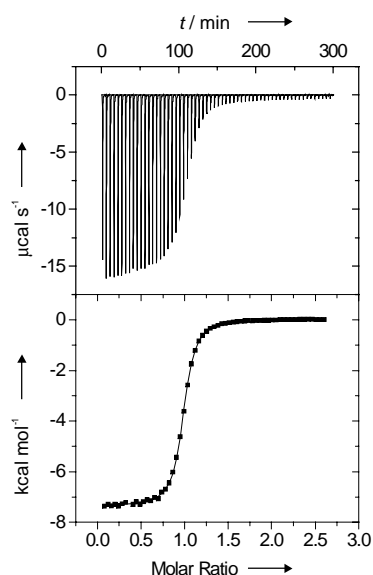
Figure 4.2. *Calorimetric titration of the binding of **3c** to β-cyclodextrin. Upper half: raw data for sequential 5 μL injections of host (13.5 mM) into guest (0.99 mM). Lower half: the integrated heat pulse data corrected for dilution (squares) and the fit (solid line) to a 1:1 binding model.*

The binding of all these guests is enthalpy-driven, indicating a good fit in the cavity. Cholate (**3a**) and deoxycholate (**3b**) have far lower stability constants than the other steroids. Although there is little agreement in the literature on the exact values for the association constants of bile salts in β-cyclodextrin, this trend usually holds.[9,11,13,14] It is thought that the hydroxyl group at C-12 of **3a** and **3b** (Figure 4.1) prevents deep inclusion of the steroid in the cyclodextrin cavity.[11]

Table 4.1. *Thermodynamic parameters (298 K) for the interaction between β-cyclodextrin and bile salts.*

Steroid	K (M^{-1})	ΔG^o (kcal mol^{-1})	ΔH^o (kcal mol^{-1})	$T\Delta S^o$ (kcal mol^{-1})
3a	$4.1 \cdot 10^3$	-4.9	-6.0	-1.1
3b	$3.6 \cdot 10^3$	-4.8	-7.0	-2.2
3c	$1.8 \cdot 10^5$	-7.1	-7.4	-0.3
3d	$7.8 \cdot 10^5$	-8.0	-9.2	-1.2
3e	$1.9 \cdot 10^6$	-8.5	-9.7	-1.2

Titrations of **3a** and **3b** with **7** revealed very weak binding of these steroids. The steroids and the sensor molecule were not soluble enough in water to achieve high concentrations of the complex to determine the binding constants accurately. Titrations of **3c**-**3e** with **7** were possible. The titration data were fitted to a 1:1 binding model (Table 4.2).

Table 4.2. *Thermodynamic parameters for the interaction between **7** and bile salts, as obtained by microcalorimetry.*

Steroid	K (M^{-1})	ΔG^o (kcal mol^{-1})	ΔH^o (kcal mol^{-1})	$T\Delta S^o$ (kcal mol^{-1})
3c	$3.0 \cdot 10^4$	-6.1	-7.6	-1.5
3d	$9.5 \cdot 10^4$	-6.8	-8.6	-1.8
3e	$6.1 \cdot 10^5$	-7.9	-10.0	-2.1

The binding strength of the steroids **3a**-**3e** to **7** is considerably lower compared to the binding to β-cyclodextrin, probably due to the competition between the dansyl moiety and the steroid for the cavity. This decrease is mainly caused by a less favorable entropy term; the binding enthalpy remains virtually unchanged. Most likely, the dansyl group is complexed weakly into the cavity, which is mainly entropy-driven, so that replacement by

the steroid causes a more unfavorable entropy change than in the case of native β-cyclodextrin.

4.3.3 Complexation of bile acid salts in cyclodextrin dimers

The complex formation of dimer **1** was studied by titration of a steroid solution to a solution of the dimer in water. The titration of **3a** and **3b** showed an inflection point at a 1:1 ratio, and the binding could be described with a 1:1 binding model (Figure 4.3a). However, the titration of chenodeoxycholate (**3c**), ursodeoxycholate (**3d**), and lithocholate (**3e**) to the dimer had an inflection point at a 1:2 host-guest ratio and could only be fitted to a sequential 1:2 binding model (Figure 4.3b).
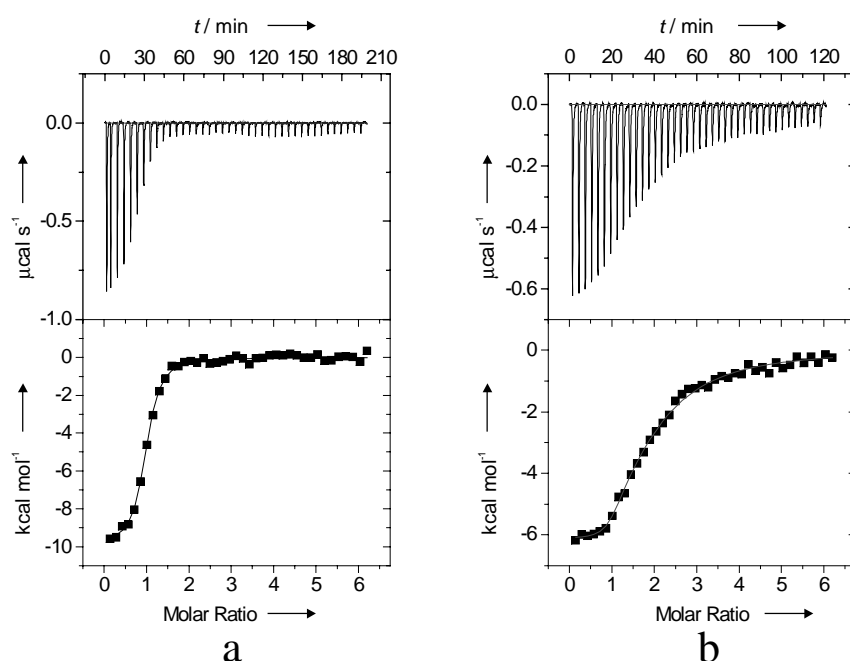
Figure 4.3. *Calorimetric titration of the binding of **3a** (a) and **3c** (b) to dimer **1**. On the upper half, raw data for sequential 7 μL injections of guest (400 μM) into host (14 μM) are shown. The lower half shows the integrated heat pulse data corrected for dilution (squares) and the fit (solid line) to the appropriate binding model.*

From Table 4.3 it can be seen that the formation of 1:1 or 1:2 complexes coincides with the presence or absence of the C-12 hydroxyl group. Steroids **3a** and **3b**, which have this group, are bound by the dimers in a 1:1 fashion. The complex stability is higher by a factor of 70 and 700, respectively, compared to binding in native β-cyclodextrin (Table 4.1).

Table 4.3. *Thermodynamic parameters (298 K) for the interaction between dimer **1** and bile salts.*

Steroid	K_1 [a]	ΔG^o [b]	ΔH^o [b]	$T\Delta S^o$ [b]	K_2 [a]	ΔG^o [b]	ΔH^o [b]	$T\Delta S^o$ [b]
3a	$2.8 \cdot 10^5$	-7.4	-5.3	2.1	-	-	-	-
3b	$2.4 \cdot 10^6$	-8.7	-9.4	-0.6	-	-	-	-
3c	$5.2 \cdot 10^6$	-9.1	-6.0	3.0	$1.4 \cdot 10^5$	-7.0	-7.2	-0.2
3d	$3.6 \cdot 10^6$	-8.9	-11.7	-2.7	$1.0 \cdot 10^5$	-6.8	-8.4	-1.6
3e	$8.9 \cdot 10^6$	-9.4	-9.4	0.0	$1.4 \cdot 10^6$	-8.3	-9.0	-0.6

[a]: values given in M^{-1}

[b]: values given in kcal mol^{-1}

These two steroids can only be partially included in a cyclodextrin cavity, because the C-12 hydroxyl group prevents deeper protrusion through the cavity.[11] Consequently, a large part of the hydrophobic skeleton is still available for complexation by a second cavity. A large fraction of the increase in binding strength compared to native β-cyclodextrin is accounted for by a more favorable entropy component. The loss of conformational flexibility for the cyclodextrin dimer, when both cavities cooperate in the binding of a single guest is apparently compensated for by the release of water molecules from the second cavity to the bulk.[17]

In the case of the other steroids, deep inclusion into a single β-cyclodextrin unit is possible, leaving the other cavity available for complexation of a second guest molecule. A sequential binding describes the binding behavior accurately. Apparently, the two binding sites in the dimer do not behave as identical, independent binding sites. Binding of a steroid in the one cavity influences the binding in the other. The increase of K_1 compared to native β-cyclodextrin indicates a small contribution of the second β-cyclodextrin in the binding of the first steroid molecule. The second steroid has to compete with the first leading to the large difference between K_1 and K_2 observed for **3c** and **3d**. The difference between K_1 and K_2 for **3c** is caused by a large positive ΔS^o upon binding of the first steroid. This suggests that this steroid causes efficient dehydration of both cavities (like in **3a**). The ΔH^o value is not so favorable as it is for **3d** and **3e**, indicating that the fit in the cavity is less tight than it is for those steroids.[17] In contrast, **3d** shows a stronger and better fit in the dimer than in β-cyclodextrin, as shown by a more favorable enthalpy, and a concomitantly larger rigidity as shown by the decrease in entropy.

Lithocholate **3e** exhibits almost independent binding of a second steroid reflected in a small difference between K_1 and K_2. Moreover, the thermodynamic parameters for both binding events are almost identical to those for the binding to native β-cyclodextrin.

Titrations with **2** as the host, performed under the same conditions as for **1**, revealed a decrease in binding strength of roughly an order of magnitude for **3a** and **3b** when compared to **1** (Table 4.4). This decrease is mainly caused by an unfavorable change in the binding entropy compared to **1**. The binding enthalpy remains almost unchanged, again suggesting weak, entropy-driven self-inclusion of the dansyl group.

Table 4.4. *Thermodynamic parameters (298 K) for the interaction between dimer **2** and bile salts.*

Steroid	K_1 [a]	ΔG^o [b]	ΔH^o [b]	$T\Delta S^o$ [b]	K_2 [a]	ΔG^o [b]	ΔH^o [b]	$T\Delta S^o$ [b]
3a	$3.6 \cdot 10^4$	-6.2	-5.1	1.1	-	-	-	-
3b	$1.9 \cdot 10^5$	-7.2	-8.9	-1.7	-	-	-	-
3c	$2.2 \cdot 10^6$	-8.6	-8.0	0.7	$1.8 \cdot 10^5$	-7.1	-9.1	-1.9
3d	$3.1 \cdot 10^6$	-8.8	-10.8	-1.9	$2.0 \cdot 10^5$	-7.2	-8.6	-1.4
3e	$1.6 \cdot 10^6$	-8.4	-11.7	--3.2	$7.6 \cdot 10^5$	-8.0	-11.1	-3.1

[a]: values given in M^{-1}

[b]: values given in kcal mol^{-1}

For the other steroids, the magnitudes of K_1 and K_2 are affected less by the presence of the dansyl group in between the two cavities. However, distinct but opposite changes in binding enthalpy and entropy were observed in nearly all cases.

The small effect of the presence of the dansyl group on K_2 for **3c**, **3d**, and **3e** indicates that the fluorophore is not penetrated deeply in one of the cavities. If it were included deeply, one would expect a reduction of K_2 due to competition of the steroid with the dansyl moiety for the second cavity.

The larger effect of the dansyl group on the association constants for **3a** and **3b**, where cooperativity of both cavities is necessary to obtain strong binding, indicates that the fluorophore hinders this cooperativity. This notion is in agreement with the mainly entropic nature of the decrease in complex stability for these steroids.

The disturbance of the cooperativity in the case of the other steroids is less pronounced, as these steroids are strongly bound in one cavity, and the second cavity offers only a moderate improvement of the binding strength. If a dansyl group is added to this system, the binding strengths of these steroids are still enhanced compared to those with native β-cyclodextrin. The changes in binding entropy and enthalpy indicate that the interactions responsible for the increase in binding strength compared to native β-cyclodextrin are not the same as those in dimer **1**. Hydrophobic interactions between the steroid and the fluorophore may play a role.

The calorimetric studies have shown, that secondary side connected cyclodextrin cavities can cooperate in the binding of bile salts. Thus, they differ from previously reported dimers that were connected via the primary side of the cyclodextrins.[14,18] These did not show the formation of strong 1:1 complexes with **3a** and **3b**. This different binding behavior can probably be attributed to the complex geometry of β-cyclodextrin with the steroids as known from NMR, which shows that part of the hydrophobic steroid skeleton protrudes from the secondary side.[14]

4.4   High Resolution NMR on cyclodextrin dimer 2

Further information about the geometry of cyclodextrin dimer **2** and its complexes with steroids was obtained by high-resolution NMR experiments. The 800 MHz 1D NMR spectrum of **2** shows seven signals for the anomeric protons (5.1-5.2 ppm), indicating that the two cavities of the dimer are equivalent, probably due to a fast exchange of the dansyl between the two cavities (Figure 4.4). The dansyl resonances (7.4-8.6 ppm) are partially overlapped.
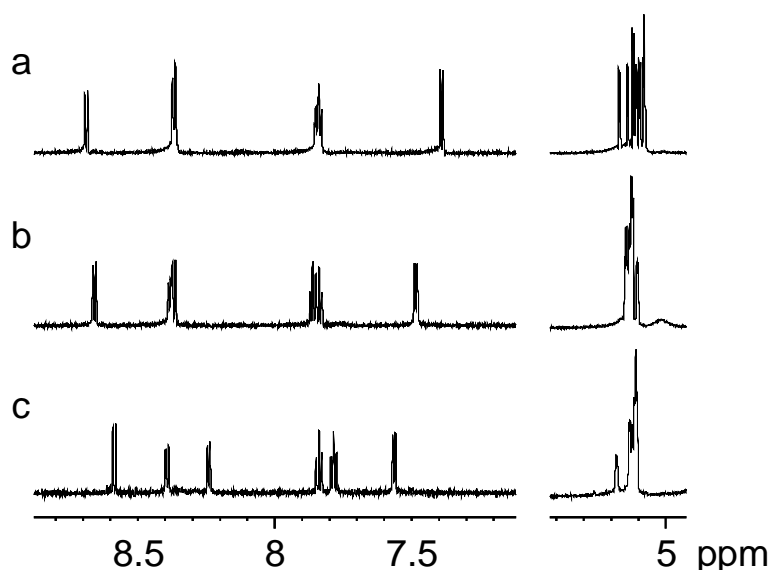
Figure 4.4. *Parts of the 1D ^{1}H NMR spectra of 2 in the absence of guests (a), the presence of 3b (b), and the presence of 3d (c).*

After the addition of **3b**, which forms a 1:1 host-guest complex with **2**, the H-1 resonances become less well dispersed. All the dansyl protons shift and become more resolved. Addition of an excess of **3d**, which forms a 1:2 complex in which the steroids are included

much deeper in the cavities, causes more pronounced shifts of the dansyl resonances and even less dispersed resonances of the anomeric protons than for **3b**.

2D ROESY experiments show NOE contacts between the dansyl protons and the protons in the interior of the cavity in the free dimer. Addition of **3b** causes these to diminish, and addition of **3d** causes them to disappear completely (Figure 4.5). Only contacts between the dansyl and the spacer protons at 3.0 ppm and 3.6 ppm and contacts between the steroid and the interior of the cavity are observed.
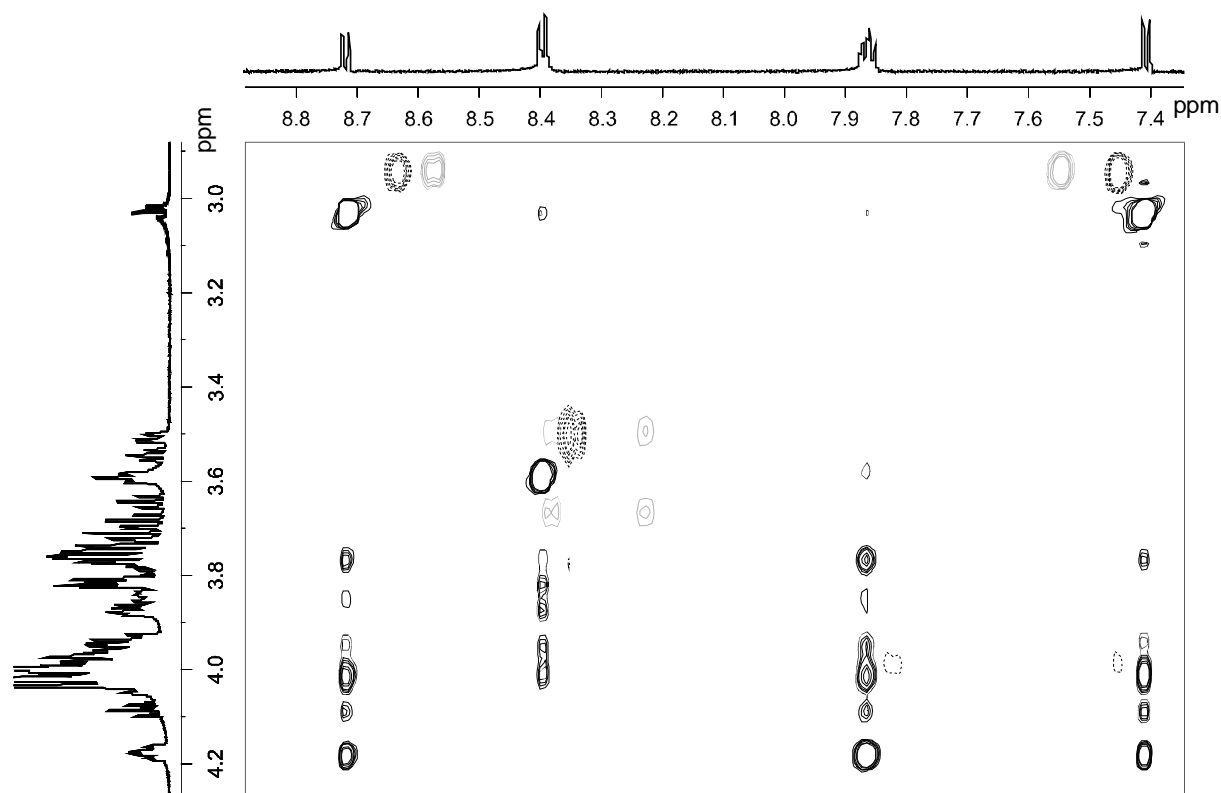
Figure 4.5. *2D NMR spectrum of **2** in the absence of guest (—), and in the presence of **3b** (----) and **3d** (—). Horizontal: dansyl region of the spectrum. Vertical: cyclodextrin region.*

The NMR data agree well with partial self-inclusion of guest in the absence of guest and expulsion of the dansyl from the cavity by the guest. For these two steroids, the dansyl does not stay very close to the guests in the complex, as evidenced by the absence of NOE contacts between the steroids and the dansyl.

4.5 Fluorescence studies

4.5.1 Steady state fluorescence

The fluorescence behavior of **2** and **7** in the presence and absence of steroids was studied by steady state fluorescence and fluorescence lifetime measurements. In aqueous solution, **7** had an emission maximum at 555 nm. The blue-shift relative to *N,N*-dimethyl dansylamide (λ_{max} = 572 nm)[3] indicates that the dansyl moiety is in a less polar environment than water, consistent with its partial self inclusion. Previously reported dansyl-modified β-cyclodextrin derivatives show larger blue-shifts, down to 520 nm.[19] With the moderate effect on the binding constants, determined by calorimetry, this indicates only weak inclusion of the dansyl moiety of **7** into the cyclodextrin cavity.

Addition of steroids that bind strongly to sensor molecule **7** gave rise to a decrease in fluorescence intensity and a concomitant shift of the wavelength of the maximum fluorescence intensity. This is attributed to the more hydrophilic environment the dansyl experiences after its expulsion from the cavity by a guest (Figure 4.6).

Figure 4.6. *Fluorescence decrease on the addition of 3e to an aqueous solution of 7 (2.7 μM).*

The fluorescence of **7** did not decrease upon titration with cholate **3a** and deoxycholate **3b** (Figure 4.7). Thus, no binding constants could be obtained. The changes in fluorescence intensity for **3c**–**3e** were large enough to allow determination of the binding constants (Table 4.5).
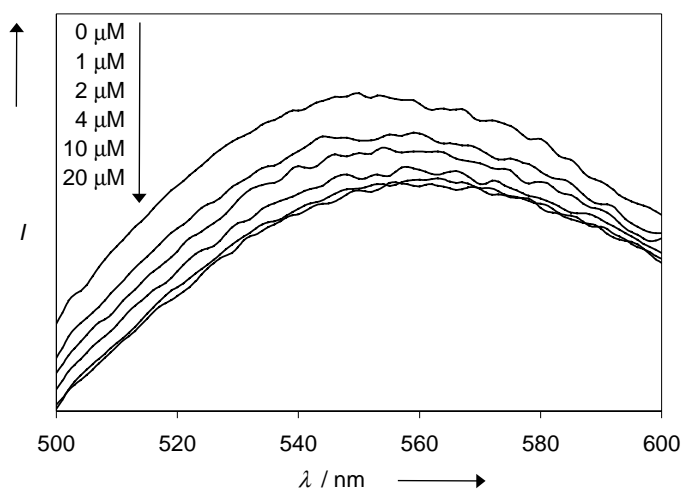
Figure 4.7. *Normalized fluorescence intensity changes of 7 (2.7 µM) at 555 nm as a function of the concentration of bile salts. (a): 3a (◊), 3b (○), 3c (∆), 3d (□), and 3e (+).*

The thermodynamic data obtained by calorimetry and fluorescence spectroscopy are in reasonable agreement. Both techniques indicate only weak or no interaction between the cyclodextrin derivative **7** and bile salts **3a** and **3b**. The binding constants obtained by fluorescence for **3c**-**3e** are slightly larger than those found by microcalorimetry, but the selectivity is the same. The most hydrophobic steroid **3e** binds strongest to cyclodextrin, **3c** has the weakest interaction. This order directly reflects the binding strengths of these steroids in native β-cyclodextrin.

Table 4.5. *Binding constants and maximum intensity changes at 555 nm for the interaction between 7 and bile salts, as obtained by fluorescence spectroscopy.*

	K (M^{-1})	I/I_0
3c	$2.1 \cdot 10^5$	0.90
3d	$3.5 \cdot 10^5$	0.70
3e	$2.2 \cdot 10^6$	0.80

The maximum emission wavelength of dimer **2** occurred at 540 nm. The blue-shift relative to **7** indicates that the dansyl group experiences more shielding from the environment in the dimer than in the monomer. Comparison to previously reported dansyl-modified β-cyclodextrin derivatives,[19] however, indicates that the dansyl moiety is still relatively weakly included by the cyclodextrin cavities of **2**.

When well-known guests for β-cyclodextrin, such as adamantanecarboxylate, adamantanamine, and 4-*tert*-butylbenzoate were added to an aqueous solution of **2**, negligible changes in fluorescence intensity were observed. In contrast, addition of the bile

salts led to a fluorescence response. In Figure 4.8a, fluorescence titration curves for the addition of **3a**, **3b**, **3c**, and **3d** to **2** are shown.

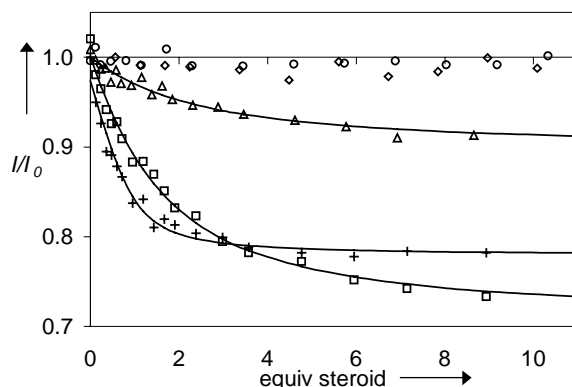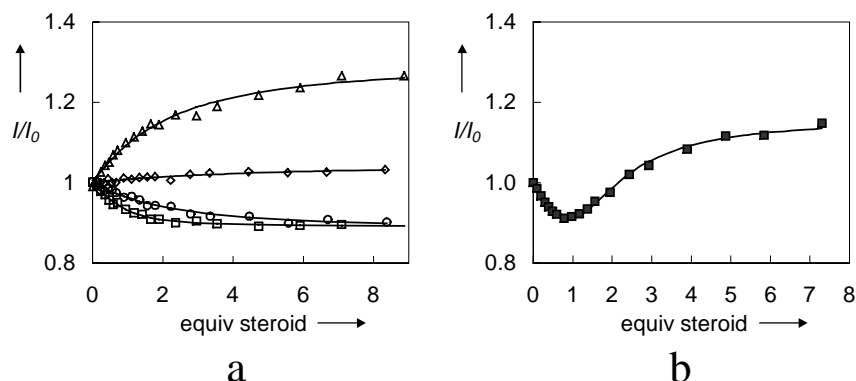**Figure 4.8.** *Normalized fluorescence intensity changes of 2 (1.5 μM) at 540 nm as a function of the concentration of bile salts (a): 3a (◊), 3b (○), 3c (∆), and 3d (□), (b): 3e (■).*

Surprisingly, some guest molecules caused an increase in fluorescence intensity. For sensor molecules based on a single dansyl-modified β-cyclodextrin cavity such as **7** and the sensor molecules reported by Ueno, addition of guests was always found to lead to a decrease in fluorescence intensity. Apparently, the location between the cyclodextrins that the dansyl moiety occupies after its expulsion from the cavities by the steroid (**3a**) or steroids (**3c**) is more hydrophobic than the cavity itself, possibly because of the proximity of the steroid(s). The interaction of the hydroxyl groups in the steroid may play a role in the quenching.

An interesting observation is that an increase in fluorescence intensity coincides with a positive entropic contribution to the binding strength. Possibly, efficient cavity dehydration (positive entropy) destroys a solvent shell in the vicinity of the complex[17] leading to a more hydrophobic environment for the fluorophore.

The cooperatively bound **3b** is detected with comparable selectivity by **2** as **3d**. In contrast, the monomeric β-cyclodextrin receptor **7** (*vide supra*) and the dimer which is connected via the primary side,[18] which lack the possibility of cooperative binding of bile salts, show a strong preference for **3d**.

The data from these titrations were fitted to a 1:1 binding model. Independent Job's plot analyses confirmed the presence of 1:1 complex for **3b** and **3c**. It is remarkable that the titrations with **3c** and **3d** could be fitted well to a 1:1 binding model, as the binding constants obtained using calorimetry imply the presence of a substantial amount of 1:2 complex at the concentrations used. Apparently, inclusion of a second steroid does not lead to an additional change in fluorescence intensity. The calculated values for the association constants are shown in Table 4.6. They are similar to the K_1 values found by the calorimetric titrations.

Table 4.6. *Binding constants and sensitivities ([2] = 1.3 μM, [Guest] = 6.5 μM) for the interaction between dimer **2** and bile salts, as obtained by fluorescence spectroscopy.*

	K_1 (M^{-1})	I/I_0	K_2 (M^{-1})	I/I_0
3a	$1.2 \cdot 10^5$	1.05	-	-
3b	$5.8 \cdot 10^5$	0.88	-	-
3c	$6.5 \cdot 10^5$	1.31	-	-
3d	$2.5 \cdot 10^6$	0.89	-	-
3e	$6.2 \cdot 10^6$	0.80	$1.0 \cdot 10^6$	1.20

Only in the titration of **3e** with **2** the presence of complexes of higher stoichiometry is shown by fluorescence. Up to one equivalent of guest the fluorescence intensity decreases, after one equivalent it starts to increase (Fig. 4b). The data of this titration could be fitted to a 1:2 binding model (Table 4.6) and the *K* values obtained are similar to those found by calorimetry.

4.5.2 Fluorescence lifetimes

In aqueous solution, the dansyl groups of fluorescent cyclodextrin derivatives are usually flexible.[20] In most cases, conformations with the fluorophore inside the cavity as well as outside the cavity are possible. The interconversion between the two occurs on the timescale of nanoseconds. This is faster than the NMR timescale, which explains the shifting resonance observed by NMR (*vide supra*), but analysis of the fluorescence decay can give information about the conformation of the fluorophore. Usually, the fluorescence intensity *I* at time *t* of a dansyl-appended cyclodextrin can be fitted to a double-exponential decay function with lifetimes τ_1 and τ_2 and fractions A_1 and A_2 (Equation 4.1).

$$I(t) = A_1 e^{-t/\tau_1} + A_2 e^{-t/\tau_2}$$

Equation 4.1

In this equation, the longer lifetime is thought to originate from the conformation with an included fluorophore, and the shorter one from the conformation with the fluorophore in the bulk. Addition of a guest usually causes a decrease in the fraction of the long-lifetime component. This is attributed to an increase in the amount of time the dansyl spends outside the cavity as a result of the competition with the added guest for the cavity (Figure 4.9).
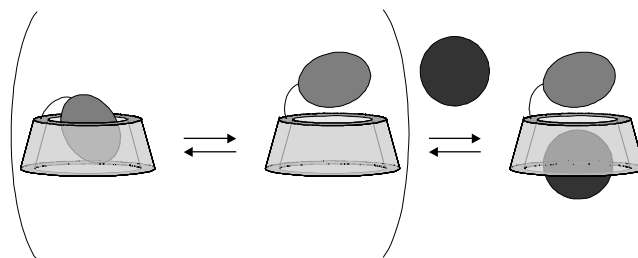
Figure 4.9. *Conformational equilibria in solution and guest-induced conformational change commonly used to explain the fluorescence lifetime behavior of cyclodextrin derivatives.*

The fluorescence of the sensor molecules **2** and **7** showed double-exponential decay curves. In both cases, the fractions of the fluorescence of the longer lifetime that is expected for a dansyl moiety that is shielded from the aqueous environment (Table 4.7 and Table 4.8) were relatively small. Moreover, compared to other dansyl-appended cyclodextrin derivatives the long lifetime is relatively short. This is consistent with the data from calorimetry and steady state fluorescence that suggested rather weak self-inclusion of the dansyl moiety.

Table 4.7. *Fluorescence lifetimes of **7** (10 μM) in the absence and presence of steroids (100 μM).*

Guest	A_1	τ_1 (ns)	A_2	τ_2 (ns)
-	0.9	7.3	0.1	11.8
3a	0.7	6.6	0.3	10.0
3b	0.7	6.8	0.3	10.2
3c	0.6	5.0	0.4	9.1
3d	0.8	4.2	0.2	9.3
3e	0.4	5.8	0.6	8.8

The decrease in fluorescence of **7** on the addition of **3c**-**3e** seems to be caused mainly by a decrease in the fluorescence lifetimes of both components (Table 4.7). This contrasts most fluorescent cyclodextrin sensors reported in literature, where the decrease in fluorescence is caused by a decrease in the fraction of the long-lifetime component of the fluorescence. The difference between **7** and the dansyl-appended cyclodextrin derivatives whose dynamic fluorescence behavior has been studied before, is that the dansyl is appended on the secondary side rather than on the primary side. As the hydrophobic region of the steroidal guest also protrudes from the secondary side, the new lifetimes may possibly be attributed to two species with more or less shielding of the dansyl from the aqueous environment by the complex of cyclodextrin and steroid (Figure 4.10).
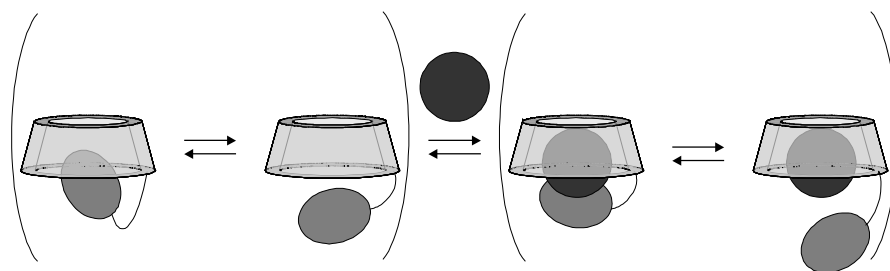
Figure 4.10. *Possible conformational equilibria for a cyclodextrin with the fluorophore appended at the secondary side.*

Table 4.8. *Fluorescence lifetimes of **2** (10 μM) in the absence and presence of steroids (50 μM).*

guest	A_1	τ_1 (ns)	A_2	τ_2 (ns)
-	0.6	6.1	0.4	10.2
3a	0.5	5.7	0.5	12.6
3b	0.6	4.4	0.4	10.6
3c	0.4	6.7	0.6	14.7
3d	0.6	5.0	0.4	9.5
3e	0.5	5.6	0.5	10.0

The decreases in fluorescence intensity of **2** after addition of **3b** and **3d** are again caused by changes in the lifetimes rather than by a decrease of the fraction of the long-lifetime component. For **3c**, that caused a large increase in the fluorescence of **1**, both the contribution of the long-lived component and the long lifetime itself increased markedly. This is consistent with the notion of shielding of the dansyl from the environment by the steroid rather than the cyclodextrin after complexation.

4.6   Conclusions

Cyclodextrin dimers **1** and **2** are very efficient hosts for the complexation of steroids. The stoichiometry of a given steroid-cyclodextrin dimer complex depends on the complex geometry of that steroid with native β-cyclodextrin. The fluorescence response of dimer **2** on a given steroid has changed markedly when compared to monomeric sensing molecule **7**. The fluorescence intensity may increase or decrease upon addition of a guest, depending on very subtle variations in complex geometry. Thus, cyclodextrin dimers are interesting hosts for the creation of sensing molecules. Optimization of this receptor molecule type may lead to sensors with 'on' rather than 'off' signaling. This can be attributed to the

proper positioning of the fluorescent reporter group at the secondary side and to a shielding interaction of the analyte with the reporter group.

4.7   Experimental section

For a general introduction on synthetic procedures, see Chapter 3.7. Mono-2-*O*-(3'-aminopropyl)-heptakis-6-*O*-(*tert*-butyldimethylsilyl)-β-cyclodextrin **6** was prepared according to literature procedures.[16] Mass spectra were recorded with a Finnigan MAT 90 spectrometer using NBA/NPOE as a matrix. NMR spectra were recorded at 25 ºC using a Bruker AC 250 and a Varian Inova 300 spectrometer. ^{1}H NMR chemical shifts (250 or 300 MHz) are given relative to residual $CHCl_3$ (7.25 ppm), or HDO (4.65 ppm). [13]C chemical shifts (63 or 75 MHz) are given relative to $CDCl_3$. High resolution NMR experiments were performed on a Bruker DRX spectrometer (18.6 T; 800 MHz for ^{1}H spectra). The 2D maps were acquired by an off-resonance ROESY sequence. Calorimetric titrations were performed at 25 ºC using a Microcal VP-ITC titration microcalorimeter. Sample solutions were prepared using 1 mM NaOH in pure water (Millipore Q2). Titrations were performed by adding aliquots of a guest solution to the host solution. The titrations were analyzed using a least squares curve fitting procedure. Control experiments involved addition of guest to 1 mM NaOH solution and addition of 1 mM NaOH to a host solution. Fluorescence measurements were performed on an Edinburgh SF 900 spectrometer. Sample solutions were prepared using a phosphate buffer (pH 7, I=0.02) in pure water (Millipore Q2). Fluorescence titrations were performed by adding aliquots of guest in host solution to the pure host solution and vice versa, thus keeping the host concentration constant. After each addition the fluorescence spectrum was recorded. The optical density of the samples at the excitation wavelength, as determined by UV-vis spectroscopy, remained below 0.1.

Mono-2-*O*-[3'-(5''-dimethylaminonaphthalene-1''-sulfonamido)-propyl]heptakis-6-*O*-(*tert*-butyldimethylsilyl)-β-cyclodextrin 7a. Dansyl chloride (220 mg, 82 μmol) and triethylamine (0.10 g, 1 mmol) were added to a solution of TBDMS-cyclodextrinpropylamine **4** (100 mg, 50 μmol) in dichloromethane (10 mL). The solution was stirred at room temperature for 15 h. The reaction mixture was washed with 1 M HCl (2 ×), water, a saturated solution of $NaHCO_3$, water, and brine, and dried ($MgSO_4$). After evaporation of the solvent and purification by column chromatography (eluent EtOAc/EtOH/H_2O, 50:2:1) **7a** was obtained as a light yellow solid in 58% yield. ^{1}H NMR ($CDCl_3$/CD_3OD) δ 8.49 (d, 1 H, J = 8.4 Hz), 8.37 (d, 1 H, J = 8.7 Hz), 8.19 (d, 1 H, J = 6.6 Hz), 7.55-7.49 (m, 2 H) 7.12 (d, 1 H, J = 7.2 Hz), 5.03-4.82 (m, 7 H), 4.15-3.28 (m, 46 H),

2.85 (s, 6 H), 1.65-1.61 (m, 2 H), 0.92-0.84 (m, 63 H), 0.06--0.01 (m, 42 H); ^{13}C NMR (CDCl$_3$/CD$_3$OD) δ 151.8, 135.5, 129.9, 129.1, 128.1, 123.3, 119.3, 115.0, 102.4, 102.0, 101.8, 101.1, 99.4, 82.8, 82.0, 80.4, 79.2, 76.6, 73.6, 72.5, 72.3, 72.0, 79.7, 62.8, 61.6, 61.3, 45.4, 26.0, 25.9, 25.8, 18.5, 18.3, -5.1, -5.2; MS (FAB) *m/z* calcd. for C$_{99}$H$_{186}$N$_2$O$_{37}$SSi$_7$ 2223.1, found 2246.9 [M + Na]$^+$.

Mono-2-*O*-[3'-(5''-dimethylaminonaphthalene-1''-sulfonamido)-propyl]-β-cyclodextrin 7. Mono-2-*O*-[3'-(5''-dimethylaminonaphthalene-1''-sulfonamido)-propyl]heptakis-6-*O*-(*tert*-butyldimethylsilyl)-β-cyclodextrin **7a** (58 mg, 40 μmol) was dissolved in TFA. After 5 min at room temperature, the solvent was removed in vacuo. Methanol was added and evaporated three times to remove residual TFA. The product was dissolved in water and washed three times with hexanes. After lyophilization, **7** was obtained as a light yellow powder in 81% yield. ^{1}H NMR (D$_2$O) δ 8.55 (d, 1 H, *J* = 8.4 Hz), 8.35 (d, 1 H, *J* = 8.4 Hz), 8.28 (d, 1 H, *J* = 7.5 Hz), 7.74-7.67 (m, 2 H) 7.22 (d, 1 H, *J* = 7.8 Hz), 5.10-4.82 (m, 7 H), 3.97-3.04 (m, 46 H), 2.79 (s, 6 H), 1.55-1.33 (m, 2 H); MS (FAB) *m/z* calcd. for C$_{57}$H$_{88}$N$_2$O$_{37}$S 1424.5, found 1425.5 ([M + H]$^+$).

4.8   References

[1] Ueno, A. *Supramol. Sci.* **1996**, *3*, 31-36.

[2] Van Dienst, E.; Snellink, B. H. M.; Von Piekartz, I.; Grote Gansey, M. H. B.; Venema, F.; Feiters, M. C.; Nolte, R. J. M.; Engbersen, J. F. J.; Reinhoudt, D. N. *J. Org. Chem.* **1995**, *60*, 6537-6545.

[3] Bügler, J.; Engbersen, J. F. J.; Reinhoudt, D. N. *J. Org. Chem.* **1998**, *63*, 5339-5344.

[4] Bügler, J. H.; Sommerdijk, N. A. J. M.; Visser, A. J. W. G.; van Hoek, A.; Nolte, R. J. M.; Engbersen, J. F. J.; Reinhoudt, D. N. *J. Am. Chem. Soc.* **1999**, *121*, 28-33.

[5] Ueno, A.; Ikeda, A.; Ikeda, H.; Ikeda, T.; Toda, F. *J. Org. Chem.* **1999**, *64*, 382-387.

[6] Ikunaga, T.; Ikeda, H.; Ueno, A. *Chem. Eur. J.* **1999**, *5*, 2698-2704.

[7] (a) Breslow, R.; Greenspoon, N.; Guo, T.; Zarzycki, R.; *J. Am. Chem. Soc.* **1989**, *111*, 8296-8297; (b) Breslow, R.; Zhang, B. *J. Am. Chem. Soc.* **1996**, *118*, 8495-8496; (c) Venema, F.; Nelissen, H. F. M.; Berthault, P.; Birlirakis, N.; Rowan, A. E.; Feiters, M. C.; Nolte, R. J. M. *Chem. Eur. J.* **1998**, *4*, 2237-2250.

[8] Mucci, A.; Schenetti, L.; Vandelli, M. A.; Forni, F.; Ventura, P.; Salvioli, G. *J. Chem. Soc, Perkin Trans. 2* **1996**, 2347-2349.

[9] Tan, X.; Lindenbaum, S. *Int. J. Pharm.* **1991**, *74*, 127-135.

[10]   Vandelli, M. A.; Salvioli, G.; Mucci, A.; Panini, R.; Malmusi, L.; Forni, F. *Int. J. Pharm.* **1995**, *118*, 77-83.

[11]   Tan, Z. J.; Zhu, X. X.; Brown, G. R. *Langmuir* **1994**, *10*, 1034-1039.

[12]   Yim, C. T.; Zhu, X. X.; Brown, G. R. *J. Phys. Chem. B* **1999**, *103*, 597-602.

[13]   Cooper, A.; Nutley, M. A.; Camilleri, P. *Anal. Chem.* **1998**, *70*, 5024-5028.

[14]   Ramos Cabrer, P.; Alvarez-Parrilla, E.; Meijide, F.; Seijas, J. A.; Rodríguez Núñez, E.; Vázquez Tato, J. *Langmuir* **1999**, *15*, 5489-5495.

[15]   Danielsson, H.; Sjövall, J. *Sterols and Bile Acids*; Elsevier Sci. Ltd., Amsterdam, The Netherlands, **1985**, Chapter 13.

[16]   Nelissen, H. F. M.; Schut, A. F. J.; Venema, F.; Feiters, M. C.; Nolte, R. J. M. *Chem. Commun.* **2000**, 577-578.

[17]   Rekharsky, V.; Inoue, Y. *Chem. Rev.* **1998**, *98*, 1875-1917.

[18]   Nakamura, M.; Ikeda, T.; Nakamura, A.; Ikeda, H.; Ueno, A. *Chem. Lett.* **1995**, 343-344.

[19]   Nelissen, H. F. M.; Venema, F.; Uittenbogaard, R. M.; Feiters, M. C.; Nolte, R. J. M. *J. Chem. Soc., Perkin Trans. 2* **1997**, 2045-2053.

[20]   Ikeda, H.; Nakamura, M.; Ise, N.; Oguma, N.; Nakamura, A.; Ikeda, T.; Toda, F.; Ueno, A. *J. Am. Chem. Soc.* **1996**, *118*, 10980-10988.

Chapter 5

Cyclodextrin Dimers in Radiopharmaceutical Applications[*]

5.1   Introduction

As has been discussed in the previous Chapters, β-cyclodextrin and cyclodextrin dimers can be used for the complexation of a variety of guest species.[1] Usually, complexation in a cyclodextrin cavity improves the solubility of hydrophobic guests in water, a property that is of interest for applications in medicine.[2,3,4,5] The advantageous effects of cyclodextrin complexation of certain drugs have often been described.[6,7,8] Cyclodextrins are attractive carriers in drug delivery or controlled release systems,[9] due to their low toxicity and the possibility to tune their delivery properties through chemical modification. The known beneficial properties of cyclodextrins for pharmaceutical applications have prompted research efforts to go one step further. In combination with other carrier materials cyclodextrins may offer the possibility to deliver drugs to a targeted site. Several large biologically active peptides have been coupled to cyclodextrins.[10] If a spacer is introduced, neither the interaction of the peptide with its receptor nor the guest binding ability of the cyclodextrin is influenced substantially.[11]

Much research has been done over the last decades on the use of technetium and rhenium for radiopharmaceutical applications,[12] because of the favorable nuclear properties and the easy availability of ^{99m}Tc, ^{186}Re, and ^{188}Re. Radiopharmaceuticals, like other drugs, usually need to be water-soluble in order to be of practical use. Furthermore, complexes must be synthesized starting from an aqueous solution of sodium perrhenate, as this is the sole source of radioactive rhenium. Like the analogous technetium(V) gluconate,[13] rhenium(V) gluconate[14] is often prepared from the perrhenate and subsequently used as a precursor for the preparation of rhenium(V) complexes. Exchange reactions with appropriate ligands may be carried out in aqueous or aqueous/organic solutions and the resulting Re complexes are, as a rule, of high (radiochemical) purity. However, the required water-solubility limits the use of lipophilic ligands and thus of lipophilic metal-complexes capable of crossing the blood-brain barrier.[12,15]

Examples of the use of cyclodextrins in combination with radiopharmaceuticals are scarce.
[15,16] This Chapter describes possible roles of cyclodextrin dimers in radiopharmaceutical applications. The complexation properties of native β-cyclodextrin and β-cyclodextrin dimers were used for enhancing the water-solubility of lipophilic rhenium complexes. Furthermore, cyclodextrin mediated synthesis[17] has been used for the preparation of a variety of rhenium complexes in water, improving access to lipophilic rehenium complexes. Using a cyclodextrin dimer, stereoselective templation of the formation of a complex has been accomplished. Finally, the first results in the development of a supramolecular strategy for the radiolabeling of biomolecules are presented.

5.2 Cyclodextrin complexes of rhenium compounds

5.2.1 Synthesis

The synthesis and characterization of the lipophilic NS-bidentate ligands **1**, **2a**, and **2b**, along with the formation of the rhenium complexes **3**, **4a**, and **4b** in organic media have been described.[18] The *trans*-configuration of the metal complexes was proven by ^{1}H NMR and in some cases X-ray crystal structure determination.[18]
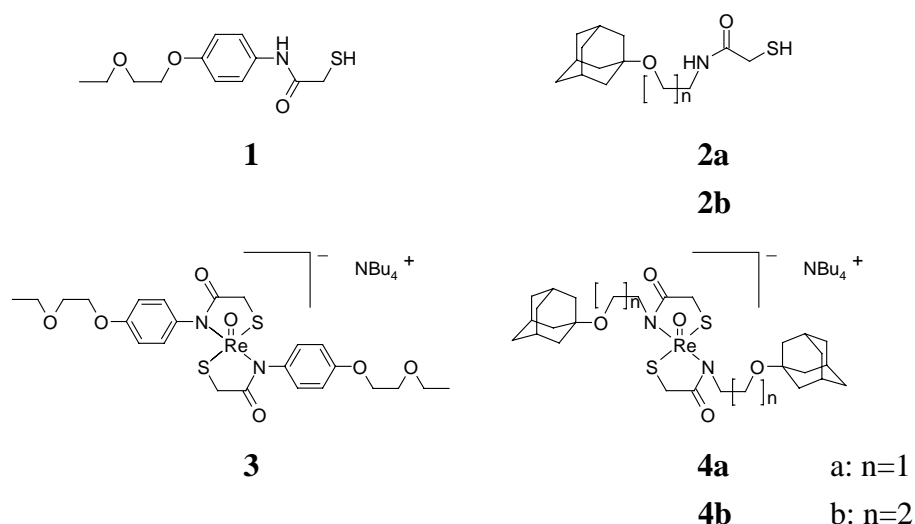
Chart 5.1. *Structures of NS-ligands and their rhenium complexes.*

Three different 2'-connected β-cyclodextrin dimers have been used (Chart 5.2). The synthesis of dimers containing a dipropylamine spacer (**5**) and a dipropylaminodansyl spacer (**6**) has been described in Chapter 3. The dimer that contains a benzophenone spacer (**7**) was prepared following the same strategy. β-Cyclodextrin, which was protected at the primary side with *tert*-butyldimethylsilyl (TBDMS) groups, was deprotonated and reacted

with 4,4'-bis(bromomethyl)benzophenone. Subsequent deprotection using tetrabutylammonium fluoride in THF yielded the desired dimer.
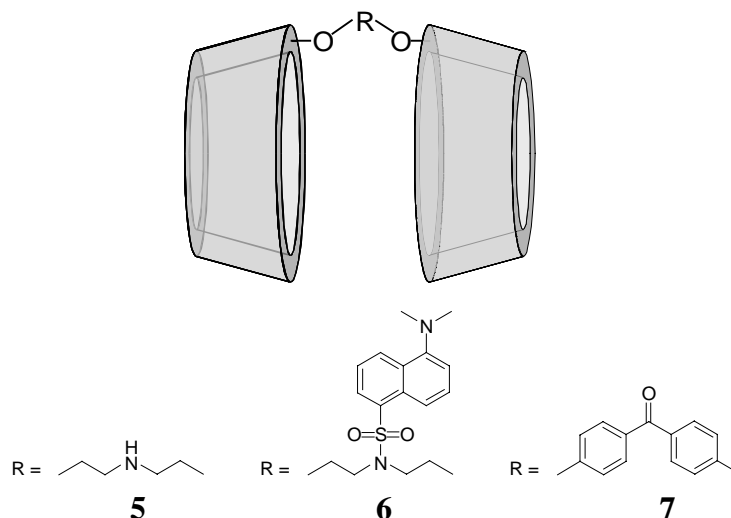
Chart 5.2.   *β-Cyclodextrin dimers used for the complexation of small rhenium complexes.*

5.2.2 Complexes with native β-cyclodextrin

The rhenium complex **3** was designed to form a 2:1 inclusion complex with native β-cyclodextrin through complexation of the two ethylene glycol tails and the connected aromatic rings inside the β-cyclodextrin cavities. It could be dissolved in D_2O at room temperature up to a concentration of 1.0 mM. Upon the addition of cyclodextrin distinct changes in the ^1H NMR spectrum of **3** were observed. indicating the formation of an inclusion complex of cyclodextrin and **3**.

NMR titration data for the complex of *β*-cyclodextrin and **3** could be fitted well to a 2:1 binding model with stepwise association constants of $(1.9 \pm 0.3) \times 10^3$ M^{-1} and $(1.0 \pm 0.3) \times 10^3$ M^{-1} for the first and the second *β*-cyclodextrin unit, respectively (Figure 5.1).[19] This confirmed the formation of the three-component inclusion complex and showed the independence of the *β*-cyclodextrin binding sites of **3**.
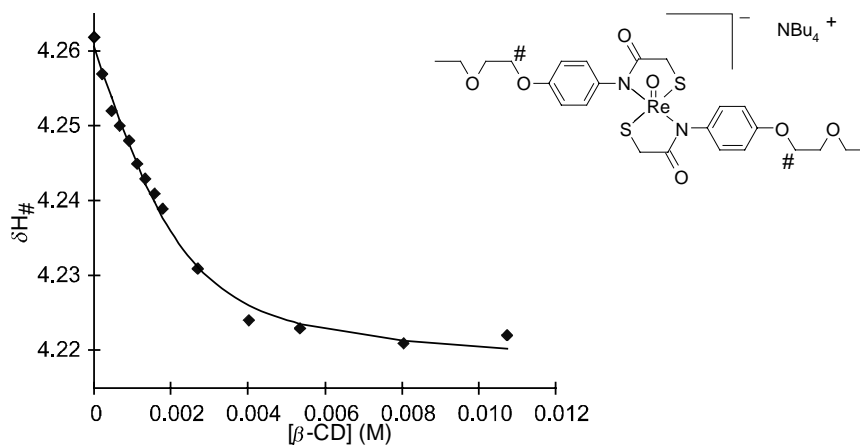
Figure 5.1. *Titration curve for the determination of the stepwise association constants for the complexation of **3** by β-cyclodextrin. (◆: experimental, ▬: calculated).*

The complexes **4a** and **4b** each bearing two adamantyl moieties, were also designed to form a 1:2 inclusion complex with native β-cyclodextrin, but with much higher association constants. Typical association constants for the complexation of adamantane moieties by native β-cyclodextrin are known to be in the range of 10^4-10^6 M^{-1}.[20] Due to the insolubility of **4a** and **4b** in water, it was not possible to perform a titration as was done in the case of compound **3**. Although no association constant was obtained, **4a** and **4b** could be made water-soluble by the addition of β-cyclodextrin. Complexation of the two adamantane compounds by native cyclodextrin was proven by ^{1}H NMR (ROESY), which showed strong NOE contacts between the protons of the adamantane moieties and the protons H-3 and H-5, at the inside of the cyclodextrin cavity (Figure 5.2).
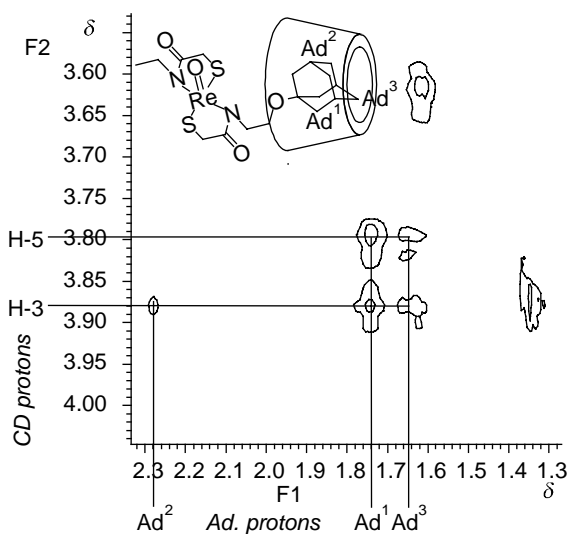
Figure 5.2. *Part of the ROESY spectrum of the inclusion complex of **4a** and β-cyclodextrin.*

5.2.3 Complexes with cyclodextrin dimers

The three different 2'-connected cyclodextrin dimers that have been used, possess different properties. The β-cyclodextrin dimer **7** was designed to form complexes with large hydrophobic guests, by a cooperative effect of the two β-cyclodextrin moieties. The benzophenone spacer makes this dimer rather rigid and hence not very capable of adjusting itself to facilitate binding of guest species that do not exactly fit. The cyclodextrin dimer **5** has a more flexible dipropylamine spacer, allowing it to adjust itself in order to facilitate binding of different guest species. Finally, the dimer **6** has a built-in sensing moiety, which allows the assessment of the binding strengths of rhenium complexes through fluorescence titrations, as has been shown in Chapter 4.

The complexation behavior of **3** with the cyclodextrin dimer **7** was studied in water using the continuous variation method (Job's plot) (Figure 5.3).[21] The concentration of supercomplex **3·7**, as calculated from the change in chemical shift of the protons *ortho* to the carbonyl of the benzophenone spacer of **7**, was plotted against the molar fraction of **7**. The plot shows a maximum close to 0.5, proving the expected 1:1 stoichiometry.[22] The corresponding association constant is $(5.5 \pm 0.6) \times 10^3$ M^{-1}, showing a weakly cooperative binding when compared to the binding in native β-cyclodextrin.
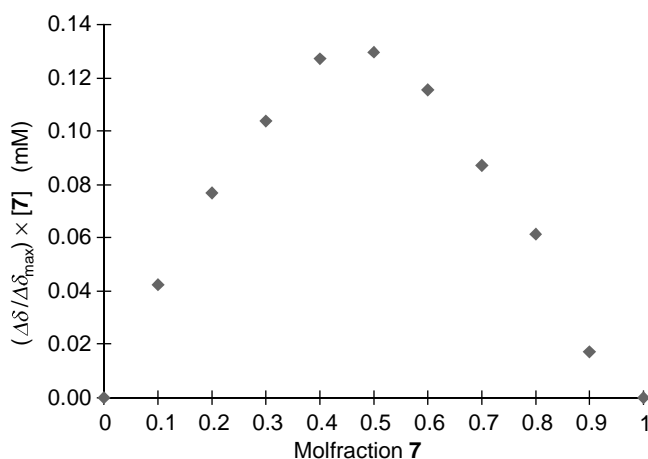
Figure 5.3. *Job's plot to determine the stoichiometry of the inclusion complex of 3 with 7. The shift of the aromatic protons* ortho *to the carbonyl of the benzophenone spacer of 7 was followed.*

The most likely mode of complexation would be the threading of the ethylene glycol tails through the β-cyclodextrins, followed by binding of the aromatic rings inside the β-cyclodextrin.[23] Although both components show substantial changes in their ^{1}H NMR signals upon complexation of **3** by dimer **7**, no NOE contacts between **3** and **7** could be observed. This is probably due to a rather loose fit of **3** in **7**, as also suggested by the

moderate association constant and the weak cooperative effect. Although no conclusive structural information could be obtained for the superstructure of **3·7**, the large chemical shifts observed upon mixing of **3** and **7** and the observed 1:1 stoichiometry, strongly suggest that complexation occurs inside the *β*-cyclodextrin cavities.

Due to the aforementioned insolubility of complex **4a** in water, ^{1}H NMR titration experiments could not be performed to determine the binding constants of **4a** with the dimers **5** and **7**. However, ^{1}H NMR experiments showing strong NOE contacts between the protons of the adamantane moieties and the protons H-3 and H-5 on the inside of the *β*-cyclodextrin moieties of both dimers, proved the formation of the supercomplexes **4a·5** and **4a·7**. To be able to determine the association constant for the complexation of AdEt$_2$Re (**4a**) by a cyclodextrin dimer, dimer **6** was used. Possessing comparable structures, the two dimers display similar binding behavior, as shown in Chapter 4. The presence of a fluorescent probe in **6** makes it possible to determine association constants by means of fluorescence. Titrations were performed in different water/methanol mixtures, since complex **4a** could be dissolved in mixtures with up to 80% of water. Similarly, association constants were determined for **4b**, which differs from **4a** only in the length of the carbon chains linking the adamantane moieties to the ligating part of the complex. The association constants found for the complexation of the *bis(*adamantane) guests by the *β*-cyclodextrin dimer ranged from about 10^6 M^{-1} in MeOH:H$_2$O = 50:50 to about 10^8 M^{-1} in MeOH:H$_2$O = 20:80 (Figure 5.4).[24]

The influence of a binary solvent medium on the association constants for binding of a guest by *β*-cyclodextrin has been studied by Connors *et al.*, who dissected the free energy change for complex formation in contributions stemming from solvent-solvent interactions (the general medium effect), solvent-solute interactions (the solvation effect), and solute-solute interactions (the intersolute effect).[25] In order to find the association constant for the binding of **4a** and **4b** by the cyclodextrin dimer in 100% water, an extrapolation of the binding constants observed in the methanol/water mixtures is needed. Of the three factors described by Connors *et al.*, the part describing the solvent-solvent interactions can be used as is, since in both cases a methanol-water system is studied. Although the system described by Connors deals with complexation of a guest by *α*-cyclodextrin, the interactions between *β*-cyclodextrin (used here) and the solvents are here assumed identical. Since the factor describing the solute-solute interactions is considered to be independent of the medium (i.e. the ΔG of complex formation in pure water), it is possible to fit a curve to the experimental datapoints, which can be extrapolated to give the association constant in 100% water. Both in the case of **4a** and **4b**, the same set of parameters[26] was used to fit the curves to the datapoints.
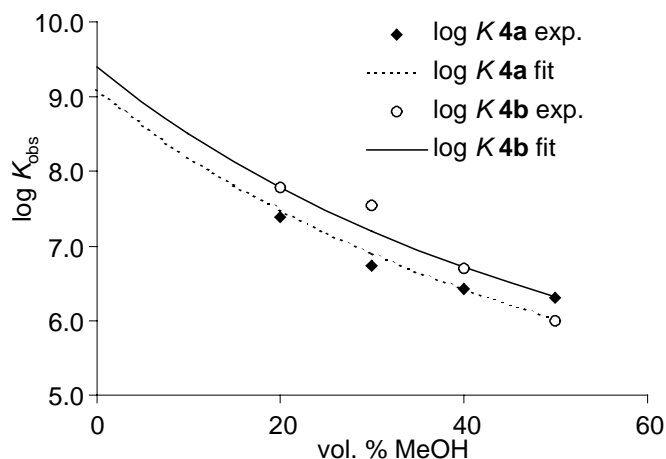
Figure 5.4. *Determination of the association constants for the complexation of **4a** and **4b**, by β-cyclodextrin dimer **6**.*

By extrapolation of the curve, K values of 10^9-10^{10} M^{-1} for the complexation of **4a** and **4b** by **6** in 100% water (Figure 5.4) were found.[27] The large increase in binding constant compared to the binding of **7** proves the introduction of better ligands for β-cyclodextrin to be an effective tool to increase the interaction of rhenium complexes with cyclodextrin dimers. The difference in binding strength between **4a** and **4b** shows that fine-tuning of the association constant is possible by relatively small adjustments to the structure of the guest. The association constants for guests in dimer **5** are generally larger than those obtained using **6**, owing to enhanced cooperativity of the cavities in **5** (Chapter 4). With binding constants of this magnitude, supercomplexes like **4a·5** rather than the "guest complex" **4a** may be considered the actual radiopharmaceutical.[5]

These results show that the addition of *β*-cyclodextrin and especially cyclodextrin dimers very effectively increases the water solubility of lipophilic metal complexes, thus widening the range of complexes that can be used in nuclear medicine. The numerous possibilities to tune the strength of the association complexes using different ligands for cyclodextrin or different geometries of cyclodextrin hosts offer interesting opportunities for the controlled release of radiopharmaceuticals.[28]

5.3   Cyclodextrin-mediated complex formation

The metal complexes whose inclusion in cyclodextrin dimers has been described in the previous section were synthesized in organic media. The efficient water solubilization by cyclodextrins suggested that cyclodextrins may mediate the formation of metal complexes of water-insoluble ligands in aqueous solution. This would allow the preparation of

lipophilic complexes starting from the precursor rhenium(v) gluconate,[29] as is the case for the radiopharmaceuticals presently used.

Being slightly water-soluble, the NS-ligand functionalized with an ethylene glycol chain (**1**) could be used to synthesize the analytically pure complex **3** from rhenium gluconate under aqueous conditions in good yield. The ligand **1** was added to the reaction mixture in a minimal amount of MeOH or as its β-cyclodextrin complex in water. The highest yield of **3** was obtained by the latter procedure. The more lipophilic adamantane ligand **2a** could only be dissolved in water by complexing it with *β*-cyclodextrin. After allowing metal complex formation to take place for 1 h at room temperature, a mixture of two products was isolated in an overall yield of 95%. These products could not be separated, so analyses were done on the mixture, rather than the pure compounds. The ¹H NMR spectrum showed that one of these products was identical to **4a** that was synthesized in organic solvents. The other product displayed very similar signals, but at different positions. Both FAB-MS and elemental analysis indicated a composition identical to **4a**. This strongly suggested that the second product is the *cis* configuration of complex **4a**.[30] The formation of both isomers of the complex (i.e. *trans*-**4a** and *cis*-**4a**) is depicted schematically in Scheme 5.1. The ratio of *cis*-**4a** : *trans*-**4a**, as determined by integration of their ¹H NMR signals, was 15:85 (entry 1, Table 5.1).
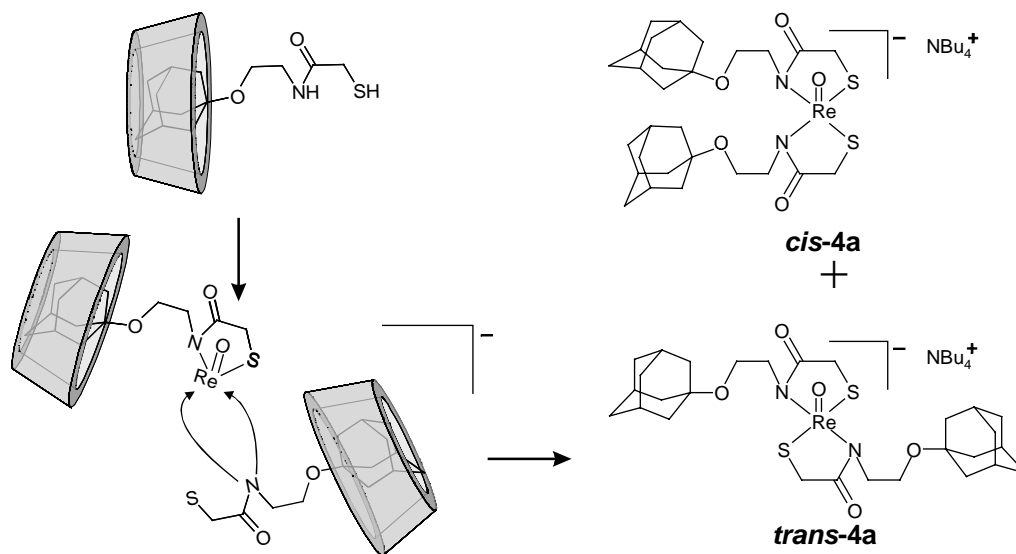
Scheme 5.1. *β-Cyclodextrin-facilitated formation of **4a** (cis and trans).*

To investigate the time and temperature dependence of this ratio, the same reaction was performed for different times and at different temperatures, keeping all other conditions the same (Table 5.1). For all entries the total yield of isolated complex (*cis* + *trans*) was >95%. An increase in the reaction time or the reaction temperature results in a shift in the ratio *cis*-**4a** : *trans*-**4a** in favor of the latter. Apparently, the complex formation reaction initially gives a mixture of the *cis* and *trans* products, followed by complete conversion into the thermodynamically more stable *trans* product. Applying the reaction conditions of entry 5

of Table 5.1 (*i.e.* 2.5 h at 55 °C) to the formation of **4b** in water, starting from the ligand **2b**, gave exclusively the expected *trans* complex in 95% yield.

Table 5.1. *Relative yields of* cis-**4a** *and* trans-**4a** *for different* t *and* T *(total yields for all entries > 95%).*

Entry	t_1 (h)	T_1 (°C)	t_2 (h)	T_2 (°C)	% *cis* [a]	% *trans* [a]
1	1	25	-	-	15	85
2	1	0	-	-	51	49
3	1	0	1.5	0	22	78
4	1	0	1.5	55	6	94
5	1	55	1.5	55	<1	>99

[a] Determined by ^{1}H NMR; error ± 2%.

Refluxing a chloroform solution of the *cis/trans* mixture of entry 2 for a period of 5 h (61 °C) did not result in a change of the ratio of *cis*-AdEt$_2$Re : *trans*-AdEt$_2$Re. Redissolving the same mixture in a basic solution of β-cyclodextrin and sodium gluconate and stirring this at 0 °C for 1.5 h, resulted in a *cis* to *trans* ratio of 25:75. After identical reaction periods and times as those used for entry 3 (i.e. 1 h + 1.5 h at 0 °C), this sample shows a ratio that is in good agreement with the ratio observed for entry 3. Redissolving several *cis*:*trans* mixtures in aqueous solutions only containing *β*-cyclodextrin (i.e. no sodium gluconate and NaOH) and stirring for 24 h at room temperature, never resulted in a change of these ratios. These results clearly show that the *cis/trans* conversion can only take place under the reaction conditions used for the complex formation and that when a mixture is isolated and subsequently resubjected to these reaction conditions this conversion can again take place. This strongly suggests the fast formation of a kinetic product or product mixture that is unstable under the reaction conditions, allowing it to be slowly interconverted to the thermodynamic product.

Owing to the orientation of the *β*-cyclodextrin cavities in the dimers, they should be capable of preorganizing two molecules of the bidentate ligand **2a** in such a way that complex formation can only take place in a *trans* fashion rather than a *cis* fashion (Scheme 5.2).[31] To investigate whether dimer **5** could indeed template[32] the formation of *trans*-**4a**, a reaction was performed under exactly the same conditions as used for entry 2 of Table 5.1 (0 °C, 1 h), but using **5** instead of native cyclodextrin (0.55 eq. per ligand). Whereas for entry 2 the *cis* to *trans* ratio was 51:49, the ^{1}H NMR spectrum of the product obtained using the dimer, showed 100% of the *trans* product and no detectable signals of the *cis* product. The complex was obtained in 96% yield and the template **5** could be recovered in 83% yield by dialysis of the aqueous phase. This proves that dimer **5** is an efficient and reusable supramolecular template for the stereoselective formation of a metal complex.
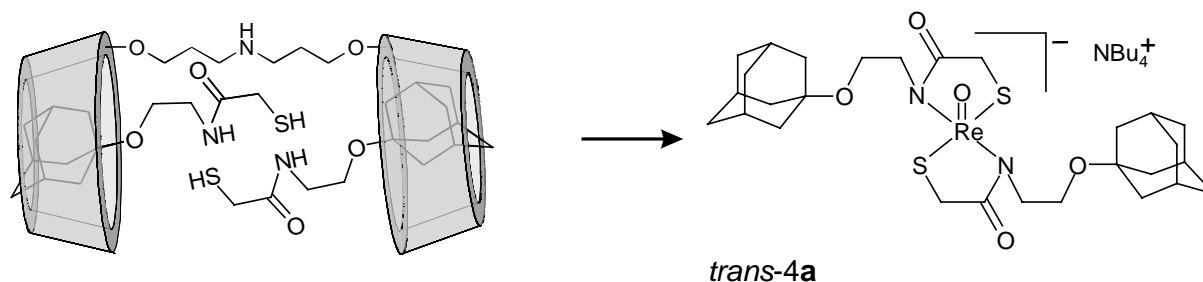
trans-4**a**

Scheme 5.2. *Templated formation of* trans-**4a** *by dimer* **5**.

In all cases described, the yields for cyclodextrin-mediated rhenium complex formation in water are much higher than those for the synthesis of the same complexes in organic solvents. This demonstrates cyclodextrin-mediated synthesis to be a powerful new tool, granting easy access to a range of lipophilic rhenium complexes that can be further extended by using α- or γ-cyclodextrin. The rapid reaction and absence of impurities render this method interesting for radiopharmaceutical applications, as these characteristics reduce loss of radioactivity to a minimum. Adding to the versatility of the method is the control over the stereochemistry of the product. The *trans* isomer of the complex can be obtained exclusively by performing the reaction at elevated temperatures. If heating is prohibited because the ligand systems used are prone to decomposition or racemization, a β-cyclodextrin dimer may be used to template the formation of this isomer. Conversely, shorter reaction times or cyclodextrin dimers with another geometry may enable the isolation of the *cis* complex.

5.4   Supramolecular labeling of biomolecules

In nuclear medicine, target-specific radiopharmaceuticals are synthesized through both pre- and postlabeling of biomolecules.[33] Although widely used, both methods have the inherent disadvantage, that a certain degree of radiolysis of the biomolecules will occur since both radioisotope and biomolecule will be present in relatively high concentrations for an extended period of time (*i.e.* the time required for the conjugation or chelation step, respectively).

The results presented here sofar may offer the possibility of a novel, supramolecular approach toward the radiolabeling of biomolecules. Hereto a cavity-containing moiety, *i.e.* a cyclodextrin containing functionality (Scheme 5.3) is first linked to a biomolecule. The actual labeling step is now the complexation of a small radioisotope complex, which can be synthesized separately. As the complexation will take place almost instantaneously, this approach has the potential to decrease damage to the biomolecule to an absolute minimum. In order for this approach to be successful, a strong complex between the cavity-containing

molecule and the radiopharmaceutical is necessary to prevent rapid dissociation of the complex.
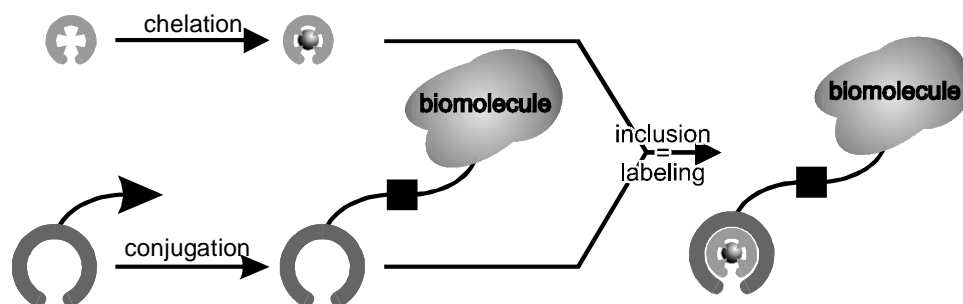
Scheme 5.3. *Supramolecular labeling approach.*

5.4.1 Bioconjugation of a cyclodextrin dimer

Biomolecules are often coupled through the reaction between a thiol and a maleimide,[34] usually after coupling of these moieties to free amino groups of lysine residues. Thus, the amino group of dimer **5** was functionalized with a thiol group by reaction with the *N*-hydroxysuccinimide ester of *S*-acetylthioacetic acid (SATA), followed by basic hydrolysis of the thioester using NH_2OH, to give **8** (Scheme 5.4).[35]

Cytochrome C (Cyt C), although not a protein used in drug targeting, was used as a model biomolecule because of the high purity in which it is commercially available. The bifunctional reagent succinimidyl 6-(*N*-maleimido)-*n*-hexanoate (MHS) was linked to Cyt C by reaction with free lysine NH_2 moieties.[34] After reaction with an excess of MHS, the Cyt C was purified using a PD-10 desalting column packed with Sephadex G-25. Subsequently, the thiol-functionalized β-cyclodextrin dimer **8** was reacted with the maleimide-functionalized Cyt C, followed by dialysis (cutoff MW 10000) to give the dimer-functionalized Cyt C (**10**).
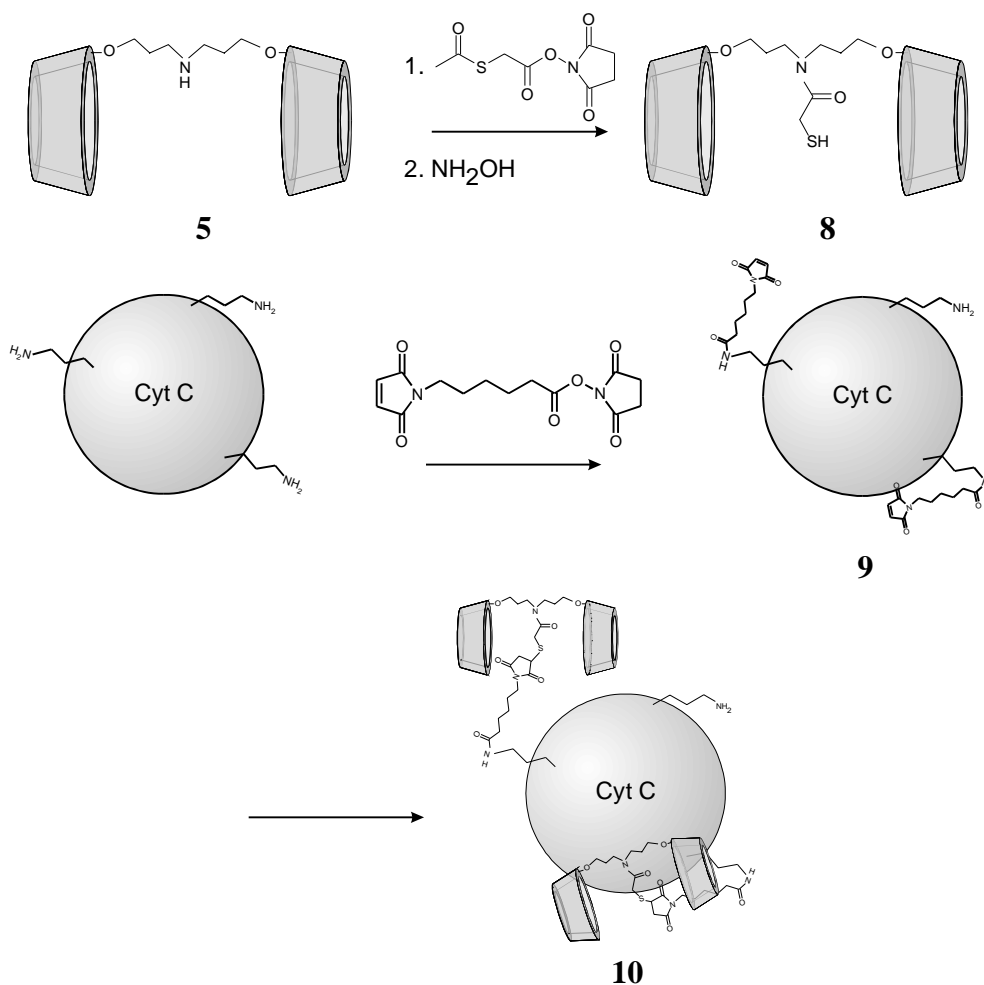
Scheme 5.4. *Synthesis of the cytochrome C-β-cyclodextrin dimer conjugate* **10** *(schematical representation, not to scale).*

The MALDI-TOF spectrum showed a large cluster of signals around $m/z = 13301$, belonging to Cyt C functionalized with an average of five maleimide moieties (**9**). The smaller cluster around $m/z = 15868$ corresponds to reaction of **9** with one β-cyclodextrin dimer, indicating that the strategy to functionalize Cyt C was indeed successful. Microcalorimetric titrations showed that the first additions of a known ditopic guest for cyclodextrin (sodium deoxycholate, see Chapter 4) to the obtained mixture caused larger exothermic heat effects than the reference experiments, strongly suggesting inclusion of the guest by the cyclodextrin dimer. Although binding constants could not be obtained due to the unknown ratio of functionalized to non-functionalized Cyt C, this proves the principle of the supramolecular labeling of radiopharmaceuticals.

5.5 Conclusions

Several small rhenium complexes, synthesized in organic solvents, have been shown to form inclusion complexes with native β-cyclodextrin, thus becoming water-soluble. Several *β*-cyclodextrin dimers form 1:1 inclusion complexes with these rhenium complexes, with association constants $>10^9$ M^{-1} for the supercomplex **4b·6**.

Water-solubilizing only the ligands has been shown a powerful new tool for the synthesis of very lipophilic rhenium complexes, affording high yields without the need for tedious purification steps. Through cyclodextrin mediated synthesis, homo- as well as heterodimeric bis(bidentate) rhenium complexes could be synthesized, as was proven by their X-ray crystal structures.[18] Variation of reaction time, reaction temperature, or the cyclodextrin derivative used, provided excellent control over the configuration of the rhenium complex obtained. Using a cyclodextrin dimer afforded the first example of a stereoselective formation of a metal complex that is templated by a supramolecular system. The high degree of configurational control might make this an interesting new tool not only in pharmacology, but also in the field of coordination chemistry in general. The use of different ligands and of α– and γ-cyclodextrin can further widen the scope of this approach.

Finally, the use of very strong supercomplexes like those presented here could be the basis for a novel, supramolecular method for the labeling of biomolecules.

5.6 Experimental section

NMR experiments were performed using Varian Inova and Varian Unity 400 WB NMR spectrometers. Residual solvent protons were used as internal standard and chemical shifts are given in ppm relative to tetramethylsilane (TMS). ^{1}H, ^{13}C, COSY,[36] clean-TOCSY (MLEV17),[37] NOESY,[38] and HMQC[39] experiments were used for the assignment of the ^{1}H and ^{13}C resonances. All 2D spectra were collected as 2D hyper-complex data.[40] After weighting with shifted sine-bell functions, the COSY data were Fourier transformed in the absolute value mode while the clean-TOCSY (MLEV17) and HMQC data were transformed in the phase sensitive mode. All data processing was performed using standard Varian VnmrS/VnmrX software packages. COSY and TOCSY spectra were accumulated with 256 increments and 32 scans per increment, typically. In the clean-TOCSY experiments the mixing time of the MLEV17-pulse was arrayed between 30 and 100 ms; in the NOESY experiments mixing times of 30 to 90 ms were applied. Fast atom bombardment (FAB) mass spectra were measured on a Finnigan MAT 90 spectrometer using *m*-nitrobenzyl alcohol (NBA) as a matrix. Identification of the Cyt C compounds was performed by Matrix Assisted Laser Desorption Ionization (MALDI) Time-of-Flight

(TOF) mass spectrometry[41,42,43] using a PerSeptive Biosystems Voyager-DE-RP MALDI-TOF mass spectrometer (PerSeptive Biosystems, Inc., Framingham, MA, USA) equipped with delayed extraction.[44] A 337 nm UV Nitrogen laser producing 3 ns pulses was used and the mass spectra were obtained both in the linear and reflectron mode. Mass assignments were performed with unmanipulated spectra (no smoothing or centering, etc.) for an optimal correlation between observed and calculated masses.

All solvents were purified by standard procedures. All other chemicals were analytically pure and were used without further purification. All reactions were carried out under an inert argon atmosphere. The presence of solvent in the analytical samples was confirmed by ^{1}H NMR spectroscopy. Melting points (uncorrected) of all compounds were obtained on a Reichert melting point apparatus. The synthesis of compounds **5** and **6** is described in Chapter 3. 4,4'-Bis(bromomethyl)benzophenone[45] and TBDMS-protected β-cyclodextrin[46] were prepared by literature procedures.

***Trans*-adamantane-rhenium complex (4a).** To a nitrogen flushed solution of **5** (40 mg, 16.9 μmol) in water (5 mL) was added a solution of **2a** (10 mg, 8.4 μmol) dissolved in a minimal amount of THF. The resulting mixture was flushed with nitrogen for 5 min, after which NaRe(gluc)$_2$ solution (0.22 mL, 4.2 μmol), adjusted to pH = 10 by the addition of 1 N NaOH (aq), was added to the mixture. The resulting mixture was flushed with nitrogen for an additional 5 min and then stirred for 1 h at 0 °C. NBu$_4$OAc (0.17 g, 0.56 mmol) was added and the mixture was extracted with CH$_2$Cl$_2$ (3 × 50 mL). The combined extracts were washed with water and brine and dried using MgSO$_4$. The solvent was removed under reduced pressure, giving **4a** as a brown-red oil. Yield: 96%. The ^{1}H NMR spectrum was identical to that of **4a** synthesized in organic solvent: ^{1}H NMR: δ = 4.86 and 4.23 (2 × m, 2 × 2 H; NCH$_2$), 3.94 and 3.58 (ABq, $^2J_{AB}$ = 17.5 Hz, 2 × 2 H; CH$_2$S), 3.70 and 3.58 (2 × m, 2 × 2 H; CH$_2$O), 3.17 (m, 8 H; NCH$_2$), 2.12 (bs, 6 H; Ad), 1.76 (bs, 12 H; Ad), 1.61 (m, 20 H; Ad and NCH$_2$C*H*$_2$), 1.43 (m, 8 H; C*H*$_2$CH$_3$), 1.02 (t, J = 7.3 Hz, 12 H; CH$_3$); ^{13}C NMR: δ = 196.0, 72.0, 58.6, 58.5, 54.1, 41.7, 41.1, 41.1, 38.8, 36.4, 30.5, 23.8, 21.1, 19.6, 13.5; FAB-MS: *m/z* [^{187}Re, correct isotope pattern], (%): 737.5 (100) (negative mode, [*M*-NBu$_4$]$^-$), 242.1 (100) (positive mode, [NBu$_4$]$^+$).

The cyclodextrin dimer **5** was recovered in 83% yield through dialysis of the aqueous phase (Sigma-D7884, benzoylated cellulose tubing, cutoff ca. 1200 Da.; 3 days). ^{1}H NMR spectroscopy and FAB-MS proved it identical to the starting material.

TBDMS-protected benzophenone-spaced cyclodextrin dimer (7a). NaH (60% dispersion in oil, 84 mg, 2.1 mmol) was added to a solution of dried (100 °C, 0.1 mbar, 5 h) TBDMS-protected *β*-cyclodextrin (4.0 g, 2.1 mmol) in THF (100 mL). The mixture was stirred for 1 h at room temperature and then for 2 h at reflux. After addition of 4,4'-*bis*(bromomethyl)benzophenone (100 mg, 0.27 mmol) reflux was continued for 5 days. The solvent was removed in vacuo and chloroform was added. The solution was washed

with 1 M HCl, water, and brine, and dried (MgSO$_4$). After removal of the solvent and purification by column chromatography (eluent: ethyl acetate/ethanol/water 100:2:1) the product was obtained as a colorless powder in 9% yield. ^{1}H NMR (300 MHz, CDCl$_3$/CD$_3$OD, 25 ºC) δ 7.80 (d, 4 H, J = 7.7 Hz; Ar-H), 7.52 (d, 4 H, J = 7.7 Hz; Ar-H), 5.07-4.84 (m, 14 H; H-1), 4.34-3.15 (m, 88 H; H-2, H-3, H-4, H-5, H-6, Ar-CH$_2$), 0.95-0.81 (m, 126 H; CH$_3$-C), 0.11-0.00 (m, 84 H; CH$_3$-Si); MS (FAB) *m/z* calcyclodextrin. for C$_{183}$H$_{346}$O$_{71}$Si$_{14}$ 4075.1, found 4099.1 ([M + Na]$^+$).

Benzophenone-spaced cyclodextrin dimer (7). The TBDMS-protected dimer **7a** (80 mg, 0.020 mmol) was dissolved in THF (5 mL). After addition of a 1 M solution of tetrabutylammonium fluoride in THF (0.7 mL) the solution was stirred overnight at ambient temperature. The solvent was removed in vacuo and the residue dissolved in water. After three washings with hexane, salts were removed over amberlite ion exchange resin. After freeze-drying the dimer was obtained as a colorless powder in 70% yield. ^{1}H NMR (300 MHz, D$_2$O, 25 ºC) δ 7.62 (d, 4 H, J = 7.8 Hz; Ar-H), 7.46 (d, 4 H, J = 7.9 Hz; Ar-H), 4.91-4.86 (m, 14 H; H-1), 3.96-3.15 (m, 88 H; H-2, H-3, H-4, H-5, H-6, Ar-CH$_2$); MS (FAB) *m/z* calcyclodextrin. for C$_{99}$H$_{150}$O$_{71}$ 2474.7, found 2476.8 ([M + H]$^+$).

Cyclodextrin-modified cytochrome C (10). To a solution of cyclodextrin dimer **5** (10 mg, 4.2 μmol) in aqueous phosphate buffer (0.05 M, pH 7.5, 1 mL) was added a solution of *N*-succinimidyl *S*-acetylthioacetate (2 mg, 8.4 μmol) in DMF (50 μL). After 10 min at room temperature, the modified dimer was purified using a PD-10 column. To the cyclodextrin-containing fractions, a solution of NH$_2$OH·HCl (300 μL, 0.5 M) in phosphate buffer pH 7.5 was added and allowed to react for 1 h to obtain the free thiol **8**.

While vortexing, a solution of *N*-succinimidyl-6-maleimidocaproate (0.9 mg, 3 μmol) in DMF (10 μL) was added to a solution of cytochrome C (9 mg, 0.7 μmol) in phosphate buffer pH 8 (0.5 mL). After vortexing 5 min at room temperature, phosphate buffer pH 6 (0.5 mL) was added and the product **9** was purified over a PD-10 column that had previously been equilibrated at pH 6.

At room temperature, the solution of the thiol-containing cyclodextrin dimer was slowly added to the solution of the modified cyctochrome C and allowed to react for 2 h. After dialysis against phosphate buffer pH 6.9 (2 × 2.5 L, 24 h) and purified water (2.5 L, 24 h), lyophilization yielded a mixture of products as a red powder (6 mg, 67%). MALDI-MS: *m/z* calcyclodextrin. for [Cyt C + 5 × maleimide + **8**] = 15868, found 15868, 13301 [Cyt C + 5 × maleimide], 6652 [Cyt C + 5 × maleimide]$^{2+}$, 7934 [Cyt C + 5 × maleimide + **8**]$^{2+}$, 26728 ($\cong$ 2 × 13301), and 29196 ($\cong$ 13301 + 15868). The last two masses are minor peaks, probably caused by formation of disulfide bonds between two cytochrome C molecules.

Determination of the association constants by fluorescence titrations. Fluorescence measurements were performed on an Edinburgh SF 900 spectrometer. Sample solutions

were prepared using a phosphate buffer (pH = 7, I = 0.02 M) in pure water (Millipore Q2). To a solution of **6** (7.2×10^{-7} respectively, 7.0×10^{-7} M) in a certain MeOH/water mixture were added aliquots of guest (**4a** or **4b**) (4.7×10^{-5} respectively, 1.3×10^{-4} M) in MeOH. A correction for the MeOH addition was done by performing the same titration using pure MeOH and subtracting these values from the values obtained for the methanolic solution of the guest (λ_{ex} = 335 nm). The optical density of the samples at the excitation wavelength, as determined by UV-vis spectroscopy, remained below 0.1.

5.7 References and Notes

[1] For reviews on cyclodextrin chemistry see *Chem. Rev.* **1998**, *98*, Issue 5.

[2] J. Szejtli, *Med. Res. Rev.* **1994**, *14*, 353-386.

[3] K. Uekama, F. Hirayama, T. Irie, *Chem. Rev.* **1998**, *98*, 2045-2076.

[4] S. D. Eastburn, B. Y. Tao, *Biotech. Adv.* **1994**, *12*, 325-339.

[5] β-Cyclodextrin dimer complexes with potential applications in photodynamic therapy have been reported: a) J. G. Moser, A. Ruebner, A. Vervoorts, B. Wagner, *J. Incl. Phenom. Macromol. Chem.* **1996**, *25*, 29-34; b) A. Ruebner, J. G. Moser, D. Kirsch, B. Spengler, S. Andrees, S. Roehrs, *J. Incl. Phenom. Macromol. Chem.* **1996**, *25*, 35-38; c) A. Ruebner, D. Kirsch, S. Andrees, W. Decker, B. Roeder, B. Spengler, R. Kaufmann, J. G. Moser, *J. Incl. Phenom. Macromol. Chem.* **1997**, *27*, 69-84; d) A. Ruebner, Z. Yang, D. Leung, R. Breslow, *P. Natl. Acad. Sci. U.S.A.* **1999**, *96*, 14692-14693.

[6] K. H. Frömming, J. Szejtli, *Cyclodextrins in Pharmacy*, Kluwer Academic Publisher, Dordrecht, **1993**, p. 324.

[7] J. Szejtli, *Cyclodextrin Technology*, Kluwer Academic Publisher, Dordrecht, **1988**, p. 450.

[8] G. N. Kalinkova, *Int. J. Pharm.* **1999**, *187*, 1-15.

[9] F. Hirayama, K. Uekama, *Adv. Drug Deliver. Rev.* **1999**, *36*, 125-141.

[10] a) F. Djedaïni-Pilard, J. Désalos, B. Perly, *Tetrahedron Lett.* **1993**, *34*, 2457-2460; b) M. K. Hristova-Kazermieski, P. Horan, P. Davis, H. I. Yamamura, T. Kramer, R. Horvath, W. M. Kazermieski, F. Porreca, V. J. Hruby, *Biorg. Med. Chem. Lett.* **1993**, *3*, 831-834; c) N. Schaske, S. Fiori, E. Weyher, C. Escrieut, D. Fourmy, G. Muller, L. Moroder, *J. Am. Chem. Soc.* **1998**, *120*, 7030-7038.

[11] a) N. Schaske, I. Assfalg-Machleidt, W. Machleidt, T. Lassleben, C. P. Sommerhoff, L. Moroder, *Biorg. Med. Chem. Lett.* **2000**, *10*, 677-680; b) C. Péan, C. Créminon, A. Wijkhuisen, J. Grassi, P. Guenot, P. Jéhan, J.-P. Dalbiez, B. Perly, F. Djedaïni-Pilard, *J. Chem. Soc., Perkin Trans. 2* **2000**, 853-863.

[12] For recent reviews of medicinal inorganic chemistry in general, or (rhenium) radiopharmaceuticals in specific see: a) *Chem. Rev.* **1999**, *99*, Issue 9; b) Z. Guo, P.

J. Sadler, *Angew. Chem.* **1999**, *111*, 1610-1630; *Angew. Chem. Int. Ed.* **1999**, *38*, 1513-1531; c) K. Schwochau, *Angew. Chem.* **1994**, *106*, 2349-2358; *Angew. Chem. Int. Ed. Engl.* **1994**, *33*, 2258-2267; d) J. R. Dilworth, S. J. Parrot, *Chem. Soc. Rev.* **1998**, *27*, 43-55.

[13] B. Johannsen, R. Syhre, *Radiochem. Radioanal. Lett.* **1978**, *36*, 107-110.

[14] B. Noll, T. Kniess, M. Freibe, H. Spies, B. Johannsen, *Isotopes Environ. Health Stud.* **1996**, *32*, 21-29.

[15] D. W. Oliver, I. C. Dormehl, W. Louw, E. Kilian, V. de Beco, J. L. Morretti, *Arzneimittel Forsch.* **2000**, *50*, 758-764.

[16] C. Bolzati, A. Boschi, L. Uccelli, A. Duatti, R. Franceschini, A. Piffanelli, *Nucl. Med. Biol.* **2000**, *27*, 309-314

[17] K. Takahashi, *Chem. Rev.* **1998**, *98*, 2013-2033.

[18] Van Bommel, K.J.C. *Ph.D. Thesis*, University of Twente, The Netherlands, **2000**.

[19] $K_1 = \dfrac{[HG]}{[H][G]}$ and $K_2 = \dfrac{[H_2G]}{[H][HG]}$, where H (host) is β-cyclodextrin and G (guest) is **3**.

A least squares fitting procedure was used while independently varying K_1, K_2, and the free and bound shift values, using a spreadsheet methodology developed before: J. Huskens, H. van Bekkum, J. A. Peters, *Comp. Chem.* **1995**, *19*, 409-416.

[20] K. A. Connors, *J. Pharm. Sci.* **1995**, *84*, 843-848.

[21] K. A. Connors, *Binding Constants, the measurement of molecular complex stability*; John Wiley & Sons, New York, **1987**, Chapter 4.

[22] The deviation from 0.5 may be caused by the presence of small amounts of **3 ⊂ 7**.

[23] CPK molecular models suggest that only one of the two aromatic rings can be complexed at any given time, due to the distance between the β-cyclodextrin moieties. NMR spectra indicate that there is a rapid exchange between the extremes *i.e.* either one of the aromatic rings inside a β-cyclodextrin cavity.

[24] The error in the individual log K_{obs} values is estimated to be ± 0.3.

[25] K. A. Connors, M. J. Mulski, A. Paulson, *J. Org. Chem.* **1992**, *57*, 1794-1798.

[26] The formula $\delta_M \Delta G^0 = \dfrac{[g\Delta A(\gamma_2 - \gamma_1) + kT \ln K_1]K_1 x_1}{x_1 + K_1 x_2}$, as derived by Connors et al. (ref. 25) was used to obtain the association constants for the complexation of the bisadamantane guests by **6** in pure water.

ΔG^o	=	total free energy change
g	=	curvature correction factor to the surface tension
ΔA	=	decrease in surface area resulting from the coalescence of two solvent cavities (containing substrate and ligand molecules)
γ	=	solvent surface tension
K_1	=	K_M / K_W, with K_M and K_W being the equilibrium constants for the

following two equilibria: L + W $\rightleftharpoons$ LW and

L + M $\rightleftharpoons$ LM, respectively. In these equilibria, L = ligand,

W = water, and M = methanol.

x_1, x_2 = bulk mole fractions of water and organic cosolvent.

Using $\gamma_1 - \gamma_2 = 6.5 \times 10^{-22}$ J·Å^{-2} and K_1 = 4.9 (values used by Connors et al.), the following value was obtained for -$g\Delta A$: 50 Å^2·molec^{-1}. A similar value was obtained by Connors et al.: -$g\Delta A$ = 43 Å^2·molec^{-1}. (Since the error in the fitting procedure proved not very sensitive to changes in K_1, the reported value of 4.9 could be used for the fitting procedure.)

[27] When the fitting parameters are optimized independently for the two datasets of Figure 5.4, the optimized log *K* value for the binding of **4b** by dimer **6** is 10.3 ± 1.0.

[28] For the different aspects of rhenium radiopharmaceuticals see the review of Dilworth and Parrot, ref. 1d.

[29] Rhenium(V) gluconate was synthesized according to an adapted literature procedure (Ref. 14), using $NaReO_4$ instead of NBu_4ReO_4.

[30] Due to the degree of symmetry present in both the *cis* as well as the *trans* complex, the structure of the two complexes could not be proven with NMR.

[31] Only one example of preferential product formation using a cyclodextrin-dimer has been reported, however, without stereoselectivity: C. J. Easton, J. B. Harper, S. F. Lincoln, *New J. Chem.* **1998**, 1163-1165.

[32] a) D. H. Busch, A. L. Vance, A. G. Kolchinkski, in *Comprehensive Supramolecular Chemistry, Vol. 9* (Eds.: J.-P. Sauvage, M. W. Hosseini), Elsevier Science, Amsterdam/New York, **1996**, p. 1; b) R. G. Chapman, J. C. Sherman, *Tetrahedron* **1997**, *53*, 15911-15945.

[33] S. Liu, S. Edwards, *Chem. Rev.* **1999**, *99*, 2235-2268.

[34] J. M. Peeters, T. G. Hazendonk, E. C. Beuvery, G. I. Tesser, *J. Immunol. Methods* **1989**, *120*, 133-143.

[35] R. J. S. Duncan, P. D. Weston, R. Wrigglesworth, *Anal. Biochem.* **1983**, *132*, 68-73.

[36] A. Bax, R. Freeman, *J. Magn. Reson.* **1981**, *44*, 542-546.

[37] A. Bax, D. G. Davis, *J. Magn. Reson.* **1985**, *65*, 355-60.

[38] J. Jeener, B. M. Meier, P. Bachmann, R. R. Ernst, *J. Chem. Phys.* **1979**, *71*, 4546-4553.

[39] A. Bax, R. H. Griffey, B. L. Hawkins, *J. Magn. Reson.* **1983**, *55*, 301-315.

[40] D. J. States, R. A. Haberkorn, D. J. Ruben, *J. Magn. Reson.* **1982**, *48*, 286-292.

[41] M. Karas, D. Bachmann, U. Bahr, F. Hillenkamp, *Int. J. Mass Spectrom. Ion Processes* **1987**, *78*, 53-68.

[42] F. Hillenkamp, M. Karas, *Anal. Chem.* **1991**, *63*, A1193-A1202.

[43]   K. Tanaka, H. Waki, Y. Ido, S. Akita, Y. Yoshida, T. Yoshida, *Rapid Commun. Mass Spectrom.* **1988**, *2*, 151-153.

[44]   M. L. Vestal, P. Juhasz, S. A. Martin, *Rapid Commun. Mass Spectrom.* **1995**, *9*, 1044-1050.

[45]   H.-F. Gruetzmacher, W. Husemann, *Tetrahedron* **1987**, *43***,** 3205-3212.

[46]   E. van Dienst, B. H. M. Snellink, I. Von Piekartz, M. H. B. Grote Gansey, F. Venema, M. C. Feiters, R. J. M. Nolte, J. F. J. Engbersen, D. N. Reinhoudt, *J. Org. Chem.* **1995**, *60*, 6537-6545.

Chapter 6

Guest Binding at Cyclodextrin Monolayers[*]

6.1 Introduction

Self-assembled monolayers (SAMs)[1] on gold are easily prepared and highly stable. Combined with the possibility to introduce functional groups, this makes them attractive for the modification of surface properties, *e.g.* for sensing purposes. Our group has previously reported the self-assembly of various receptor molecules, including resorcin[4]arenes[2] and crown ethers[3] on gold. Interactions of resorcin[4]arene monolayers with organic guests have been monitored by quartz crystal microbalance (QCM)[2a] and surface plasmon resonance (SPR) spectroscopy both in the gas phase[2e] and in aqueous solution.[4] The binding of metal ions from solution by SAMs of crown ethers was studied by electrochemical impedance spectroscopy.[3]

Cyclodextrins[5] possess a hydrophobic cavity that enables the complexation of organic guests in aqueous solution. Sulfur-modified α-[6] and β-cyclodextrin[7] derivatives have been used by several groups for the preparation of SAMs on gold. Kaifer *et al.* used per-6-deoxy-(6-thio)-β-cyclodextrin with seven thiol moieties for binding to the gold surface.[7a] Their binding properties with metallocenes were studied on surfaces[7a] and on colloids.[8] Galla *et al.* reported cyclodextrins with one thiol moiety as attachment point.[7e] Binding studies at SAMs of these adsorbates revealed that guest binding did not follow a Langmuir isotherm due to the disorder in the layers.[7f]

In our group, the strategy to obtain dense, well-packed monolayers of receptor molecules involves filling the space underneath a headgroup by alkyl chains using multiple attachment points. For example, a resorcin[4]arene[2a] was substituted with four thioether units (4×40 Å^2) to match the size of the cavity head group (160 Å^2). Recently, the same approach was used for monolayers of α-, β-, and γ-cyclodextrin (Figure 6.1a).[9,10] Electrochemistry and AFM proved that the adsorbates are ordered and packed with their cavity pointing outward. The β-cyclodextrin adsorbates with free hydroxyl groups at the 2-

and 3-positions complex guests from aqueous solution. The binding of 1-anilinonaphthalene-8-sulfonate, a well-known guest for β-cyclodextrin, to these monolayers was best described by a Langmuir isotherm,[10a] indicating the presence of only one type of binding site.
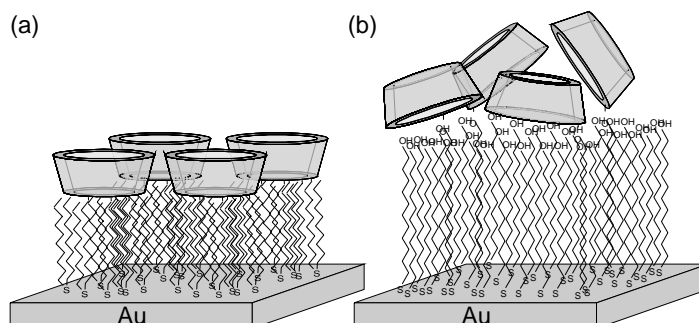

Figure 6.1. *Architectures of cyclodextrin monolayers employed in this study.*

In this Chapter, the binding of several structurally different guests to cyclodextrin monolayers is measured, and the binding by the monolayer is compared to the binding by cyclodextrin in solution. A β-cyclodextrin heptasulfide and a β-cyclodextrin monoalkylthiol were used to prepare self-assembled monolayers on gold. The latter cyclodextrin adsorbate was used in an alternative strategy to obtain well-packed monolayers of receptor adsorbates. It consists of filling the space left under a head group that is attached to the gold only through a single thiol moiety with mercaptoalcohols (Figure 6.1b).[11] The mercaptoalcohols should prevent the formation of a quasi-two-layer system that is predicted by molecular dynamics calculations for pure monolayers of cyclodextrin adsorbates monosubstituted with a long alkyl chain.[12] The monolayers were characterized by a variety of techniques to verify that densely packed monolayers are obtained through both strategies employed. Surface plasmon resonance (SPR) spectroscopy was used to monitor the host-guest interactions of a variety of guests with the cyclodextrins in the monolayers. Guests were chosen that bind *in* the cavity, *through* the cavity, or require two cavities for strong binding.

In Chapters 3 and 4, guest binding by cyclodextrin dimers in solution was studied. Dimer complexation was shown to have a large effect on the selectivity of cyclodextrin-based hosts. The monolayer architecture shown in Figure 6.1b might also allow two cavities to act as one binding site. Therefore, the binding behavior of the guests to the different monolayers will be discussed focusing on the possibility of dimer complexation at an interface.

6.2   Synthesis of adsorbates and monolayer characterization

Previously, our group reported an amide-connected cyclodextrin heptathioether prepared from heptakis-6-deoxy-6-amino-β-cyclodextrin and a thioether carboxylic acid with a methyl-terminated chain that was one carbon atom shorter than the carboxylic acid terminated chain.[10a] The β-cyclodextrin heptathioether **1** described here was synthesized by the same procedure using a thioether carboxylic acid with alkyl chains of equal length.

A protected precursor of cyclodextrin monoalkylthiol **2** was synthesized by deprotonating β-cyclodextrin, protected at the primary side with *tert*-butyldimethylsilyl groups, with lithium hydride and subsequent reaction with 12-bromo-1-(*S*-trityl)mercaptododecane. All protecting groups were removed in one step with a solution of triethylsilane in trifluoroacetic acid to obtain **2**. All compounds were characterized by NMR and FAB or MALDI-MS.
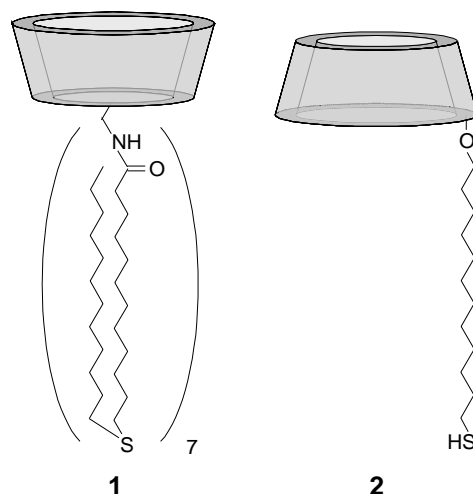
Chart 6.1.   *β-Cyclodextrin adsorbates used.*

The monolayers of the cyclodextrin adsorbates were characterized by electrochemistry and wettability studies (Table 6.1). The monolayers of **1** closely resembled those reported before.[9, 10a] The charge-transfer resistance (R_{CT}) towards the $Fe(CN)_6^{3-}$ / $Fe(CN)_6^{4-}$ external redox couple was higher than that reported before,[10a] reflecting the slightly better packing expected for thioethers with two alkyl chains of identical length.[87c] Although the contact angles are higher than those reported before, they are still indicative of a rather hydrophilic surface.

Monolayers with varying ratios of **2** to mercaptoundecanol were prepared. The surface area occupied by the cyclodextrin head groups is smallest when they are oriented with the rims of the cavities perpendicular to the surface, rather than parallel. At 17% of **2**, we calculated that the cyclodextrin cavities are tightly packed even in this orientation.[13] In the more dilute layers, the cyclodextrin cavities have more orientational freedom. Wettability studies

show that the outer surfaces of all mixed monolayers of **2** and mercaptoundecanol are hydrophilic. The R_{CT} and capacitance values of mixed monolayers of **2** and mercaptoundecanol are similar to those of monolayers of mercaptoundecanol. The slightly lower capacitance values compared to monolayers of mercaptoundecanol are indicative of a thicker monolayer in the case of the mixed monolayers, in agreement with the cyclodextrin headgroups resting on top of the closely packed alkyl part of the monolayer.

Table 6.1. *Properties of self-assembled monolayers of **1** and of self-assembled monolayers containing varying ratios of mercaptoundecanol and **2**.*

Monolayer	θ_a/θ_r (H$_2$O, °)	C_{ML} (μF/cm^2)	R_{CT} (10^5 Ω)
1	55/<20	2.6	1.1
HO-(CH$_2$)$_{11}$-SH	<20	2.7	4.4
2% **2**[a]	<20	2.4	8.0
4.5% **2**[a]	<20	2.4	8.1
9% **2**[a]	<20	2.3	10.1
17% **2**[a]	<20	2.6	6.1
2	<20	7.1	2.0

[a]: Percentages given are molar percentages in solutions used for monolayer preparation

In AFM images of the mixed monolayers no phase-segregated domains were observed (Figure 6.2), and this also suggests the formation of well-mixed, densely packed monolayers. At 17% of **2**, the packing properties of the layers start to deteriorate, as shown by increasing capacitance and decreasing R_{CT} values. Possibly, the very tight packing of the cyclodextrin head groups is giving rise to the introduction of more defects.
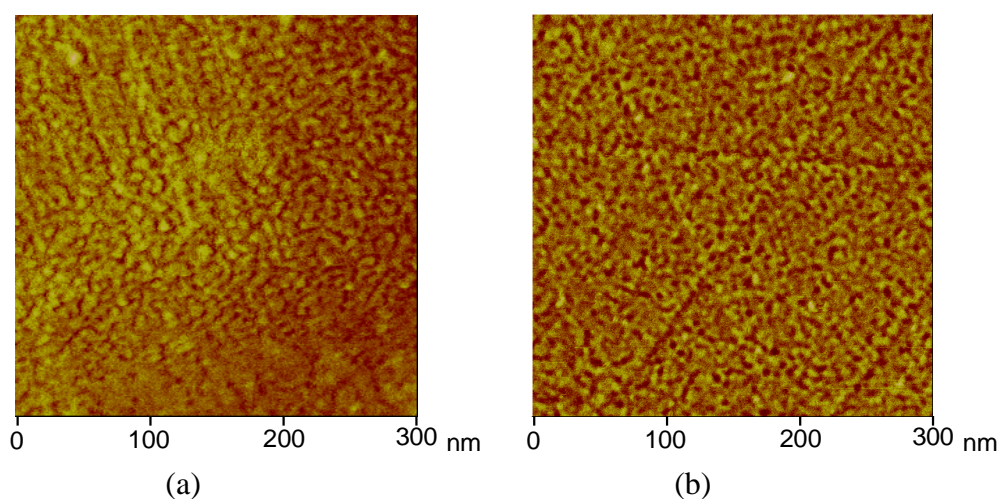

(a)   (b)

Figure 6.2. *Tapping mode AFM images of a monolayer of **1** (a), and of a mixed monolayer of 9% of **2** and mercaptoundecanol (b).*

The monolayers of pure **2** have a considerably lower R_{CT} than the mixed monolayers, showing that the absence of the mercaptoundecanol causes more defects in the monolayer. In accordance, the capacitance value is much higher than that of the mixed monolayers, which means that the pure layer is thinner than the mixed monolayers. The capacitance is slightly lower than the previously reported values for monolayers of short-chain heptathioethers.[10a] This is tentatively assigned to the formation of two layers of cyclodextrins, as predicted by molecular dynamics.[12] Alternatively, it can be the result of the cavities being at a larger average distance from the surface owing to the long S-alkyl spacer. The characterization of these cyclodextrin monolayers reveals that (except for pure **2**) they are densely packed with their cavities exposed to the outer surface of the monolayer.

6.3   Guest binding at monolayers of 1

We used SPR spectroscopy to monitor host-guest interactions between steroids and cyclodextrin monolayers.[14] Changes in the refractive index and thickness near an interface can be detected readily by SPR. Experimentally, the plasmon resonance angle is determined, which is the angle under which light, reflected at a prism/metal interface in the so-called Kretschmann configuration, exhibits a minimum in the reflectance. The change of the plasmon angle during a surface binding experiment is proportional to the amount of material bound to the surface.[15]

The addition of ferrocenemethanol (**3**), 4-*tert*-butylphenylacetanilide (**4**), and 1-acetamidoadamantane (**5**) (Chart 6.2), all of which contain known binding motifs for β-cyclodextrin in solution, to a monolayer of **1** gave rise to rapid and reversible changes in the SPR angle. The interaction of monolayers of **1** with small neutral organic guests was studied in detail by titrations (Figure 6.3). The experimental data could be fitted to Langmuir isotherms (solid lines), confirming the previous finding that only one type of binding site is present on the monolayer and that the cavities behave independently.[10a] When monolayers of mercaptoundecanol were contacted with the same guest concentrations, no change in the SPR angle was observed, proving that the change in SPR angle is indeed the result of host-guest complexation at the monolayer of **1**.
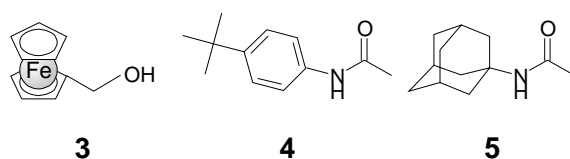

3   **4**   **5**
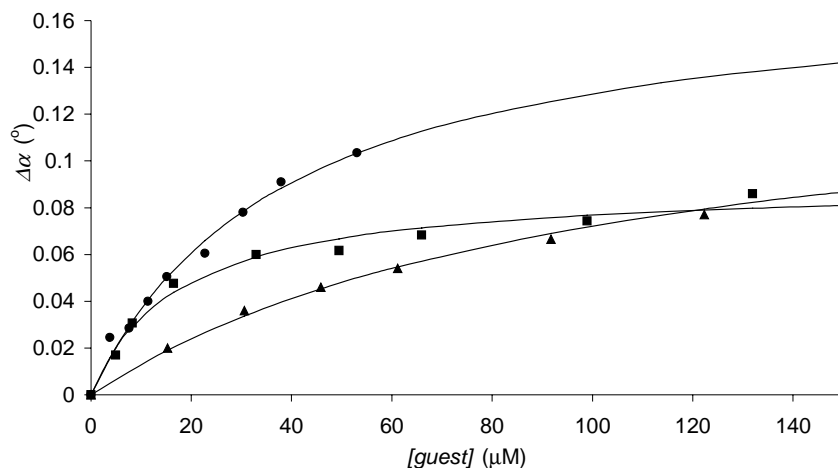
Chart 6.2.   *Small guests for cyclodextrins used.*

Figure 6.3. *Change in SPR angle ($\Delta\alpha$) of a monolayer of **1** as a function of the concentration of ferrocenemethanol **3** (▲), 4-tert-butylphenylacetanilide **4** (●), and 1-acetamidoadamantane **5** (■).*

In order to compare the binding of these guests by surface-confined cyclodextrins to the binding of these molecules by β-cyclodextrin in solution, the binding constants in solution were determined by microcalorimetry. The association constants for these small guests obtained at a monolayer and in solution are in surprisingly good agreement (Table 6.2). This indicates that the interior of the cavity is hardly affected by the perfunctionalization of the primary rim and that the microenvironment of a cavity in the monolayer is comparable to that of a cavity in solution. It shows that cyclodextrin heptathioether **1** is an excellent receptor adsorbate for the detection of small organic compounds, that bind *in* the cyclodextrin cavity.

Table 6.2. *The interaction of guests **3**-**5** with monolayers of **1** and with β-cyclodextrin in solution.*

| Guest | 1 | | solution | | |
| | K | $\Delta\alpha_{sat}$ | K | ΔH^o | $T\Delta S^o$ |
	(M^{-1})	(°)	(M^{-1})	(kcal mol^{-1})	(kcal mol^{-1})
3	$9.9{\cdot}10^3$	0.145	$1.0{\cdot}10^4$	-6.1	-0.7
4	$2.6{\cdot}10^4$	0.179	$3.0{\cdot}10^4$	-5.2	0.9
5	$5.7{\cdot}10^4$	0.090	$6.8{\cdot}10^4$	-5.9	0.7

Steroids are present in all eukaryotic organisms, where they play a role in numerous processes.[16] Their biological importance and hence their detection has attracted great scientific interest.[17] Our group has shown that resorcin[4]arene-based receptors complex steroids in chloroform solutions.[18] When we incorporated this class of receptors in monolayers, the interaction with steroids appeared to be largely governed by the

hydrophobicity of the guest.[19] A class of steroids whose interaction with cyclodextrins has been well studied is that of the bile salts (Chart 6.3). Their recognition by cyclodextrin derivatives has been studied both by our group[20] and others.[21] NMR experiments have shown that these steroids are complexed *through* the cavity, with the aliphatic side chain of the steroid entering the cyclodextrin from the secondary side.[22] Steroids **6a** and **6b** are not complexed as deeply as the others, due to the presence of the hydroxyl group at C12 of the steroid skeleton.[23]
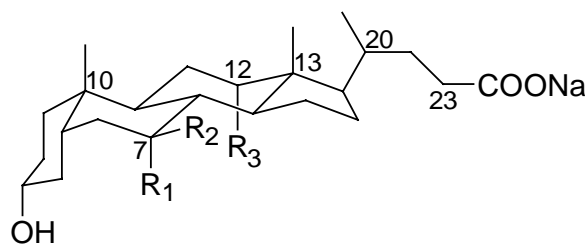
	Steroid	R_1	R_2	R_3
6a	Cholate	OH	H	OH
6b	Deoxycholate	H	H	OH
6c	Chenodeoxycholate	OH	H	H
6d	Ursodeoxycholate	H	OH	H
6e	Lithocholate	H	H	H

Chart 6.3. *Structures of bile salts.*

Also the interaction of monolayers of **1** with these steroids was studied by SPR spectroscopy. The changes in the SPR angle ($\Delta\alpha$) as a function of the concentration of steroids for a monolayer of **1** are plotted in Figure 6.4. The experimental $\Delta\alpha$ data could be fitted to Langmuir isotherms (solid lines). The titration data for steroid **6e** deviated from the fitted curve at higher concentrations, where $\Delta\alpha$ started to increase linearly. Titration of the steroids to a monolayer of mercaptoundecanol showed a linear increase in $\Delta\alpha$ for the higher concentrations of steroid **6e** and no change for the other steroids. Although the concentrations of the steroids were chosen to be below the critical micelle concentration (cmc), steroid **6e**, the most hydrophobic one, apparently has some aspecific interaction with the layers. Thus, for **6e** the last points of the titration were not considered in the Langmuir fitting procedure.
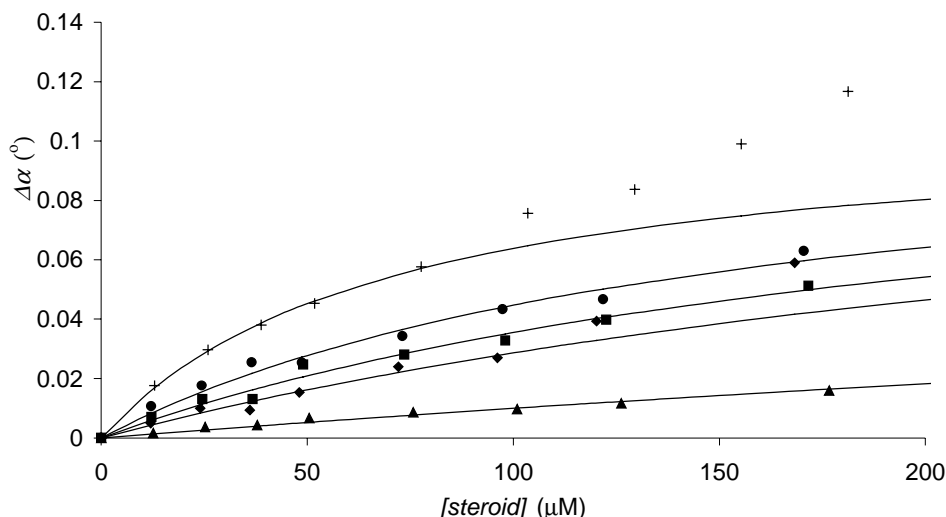
Figure 6.4. *Change in SPR angle (Δα) at a monolayer of **1** as a function of the concentration of **6a** (▲), **6b** (●), **6c** (■), **6d** (♦), **6e** (+). For **6e**, the last three points were not incorporated in the Langmuir fit.*

The association constants obtained from the fitting procedure are shown in Table 6.3. Comparison with the previously reported solution data[20] for the complexation of these steroids by β-cyclodextrin reveals that the association constants in solution are higher than those at the surface. More interestingly, there is a difference in selectivity. In solution, **6a** and **6b** have far lower stability constants than the other steroids. In contrast, the monolayers of **1** complex steroid **6b** more strongly than its isomers **6c** and **6d**. The difference in selectivity between solution and monolayers for the steroids may be due to the fact that these relatively large guests are complexed *through* the cavity instead of *in* the cavity. The persubstitution of the primary side blocks one side of the cyclodextrin and prevents protrusion through the cavity. Steroid **6b** is affected less by the blocking of the primary side, as in solution it is already less deeply included than **6c** and **6d**.[23]

Table 6.3. *The interaction of bile salts with cyclodextrin monolayers and with β-cyclodextrin and a β-cyclodextrin dimer in solution.*

Guest	**1**		9% **2**		solution[a]	
	K (M^{-1})	Δα$_{sat}$ (°)	K (M^{-1})	Δα$_{sat}$ (°)	K$_{\beta\text{-}CD}$ (M^{-1})	K$_{dimer}$ (M^{-1})
6a	$9.7 \cdot 10^2$	0.110	$6.8 \cdot 10^3$	0.053	$4.1 \cdot 10^3$	$2.8 \cdot 10^5$
6b	$6.4 \cdot 10^3$	0.114	$1.1 \cdot 10^4$	0.072	$3.6 \cdot 10^3$	$2.4 \cdot 10^6$
6c	$4.5 \cdot 10^3$	0.115	$1.9 \cdot 10^4$	0.108	$1.8 \cdot 10^5$	$5.2 \cdot 10^6$
6d	$4.2 \cdot 10^3$	0.124	$4.8 \cdot 10^4$	0.107	$7.8 \cdot 10^5$	$3.6 \cdot 10^6$
6e	$1.3 \cdot 10^4$	0.109	$8.6 \cdot 10^4$	0.120	$1.9 \cdot 10^6$	$8.9 \cdot 10^6$

[a] taken from Chapter 4.

It is noteworthy that the saturation values obtained by the fitting procedure were approximately the same ($\Delta\alpha_{max} \approx 0.115$ °) for all steroids. This is in agreement with expectation, as the amount of material bound at the surface for these similar steroids is nearly identical. The absolute value of the change in SPR angle can be related to a mass change.[24] Although this relationship is dependent on the type and thickness of the metal, the mass increase for the formation of a 1:1 host-guest complex should give rise to approximately this saturation value in the system used.[25]

6.4   Guest binding at monolayers of 2

Mixed monolayers of **2** and mercaptoundecanol containing 9% of **2** have close to the same surface concentration of cyclodextrins as monolayers of **1**. The binding of steroids to a monolayer with 9% of **2** was compared to the binding to monolayers of **1**. In these mixed monolayers, the cyclodextrins are spaced sufficiently apart for the cavities to be readily accessible, and concentrated enough to ensure reasonable changes in the SPR angle upon complexation of guests in the cavities. The titration data for the addition of bile salts **6a**-**6e** to this layer are shown in Figure 6.5. Again, steroid **6e** showed some aspecific interaction at higher concentrations. It can be easily seen that these mixed monolayers interact more strongly with **6c**-**6e** than with **6a** and **6b**. This is in accordance with the complexation behavior known from solution and supports the notion that the different selectivity of monolayers of **1** towards the various bile salts is caused by the persubstitution on the primary rim and the resulting architecture of the monolayer.
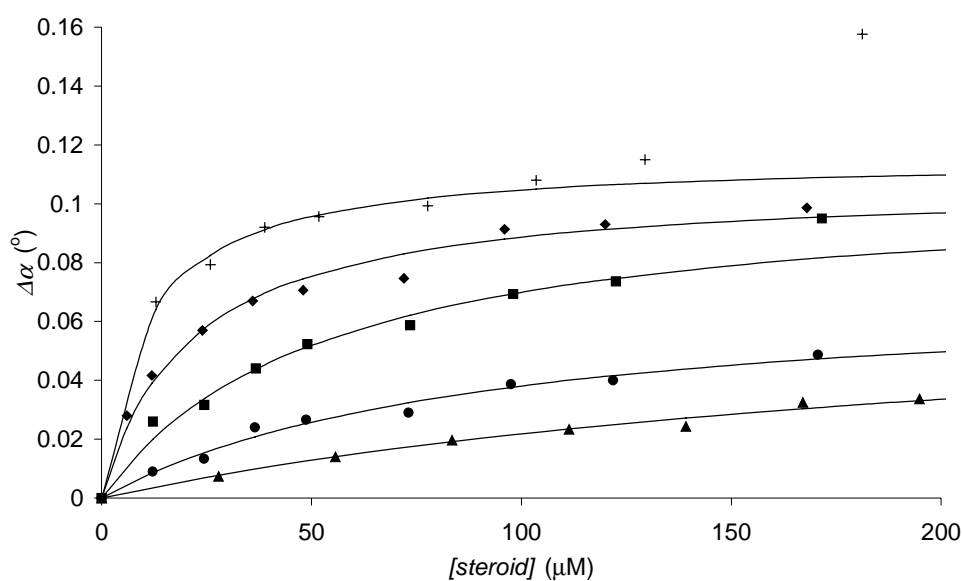

Figure 6.5. *Change in SPR angle ($\Delta\alpha$) at a mixed monolayer containing 9% of **2** as a function of the concentration of **6a** (▲), **6b** (●), **6c** (■), **6d** (♦), **6e** (+). For **6e**, the last two points were not incorporated in the Langmuir fit.*

When the titration data were fitted to Langmuir isotherms, the saturation values of the various steroids varied (Table 6.3). For **6a** and **6b**, far lower values were found than for the other steroids. This difference may be explained by looking at the binding behavior in solution. In solution, steroids **6a** and **6b** are known to require a β-cyclodextrin dimer for strong complexation,[20] whereas the other steroids are already complexed strongly by native β-cyclodextrin. At the 9% cyclodextrin surface, the cavities are fairly close to each other. Therefore, we assume that two processes can occur:

$$H + G \; \rightleftharpoons \; HG \qquad K_1 = \frac{[HG]}{[H][G]}$$

Equation 6.1.

$$H_2 + G \; \rightleftharpoons \; H_2G \qquad K_2 = \frac{[H_2G]}{[H_2][G]}$$

Equation 6.2.

In these equations, *[H]* and *[H$_2$]* are the surface concentrations of monomeric and dimeric binding sites, respectively, *[G]* is the guest concentration in solution, and *[HG]* and *[H$_2$G]* are the surface concentrations of the 1:1 complexes of a guest in a monomeric and dimeric binding site, respectively. Here, we assume that the binding behavior of all dimeric binding sites can be described by a single, average binding constant K_2.

If we define surface coverages θ_1 and θ_2:

$$\theta_1 = \frac{[HG]}{H_{tot}}, \; \theta_2 = \frac{[H_2G]}{[H_2]_{tot}} = \frac{[H_2G]}{\frac{1}{2}[H]_{tot}}$$

Equation 6.3.

it follows that

$$K_1 = \frac{\theta_1}{(1-\theta_1-\theta_2)[G]}, \; K_2 = \frac{\theta_2}{(1-\theta_1-\theta_2)[G]}$$

Equation 6.4.

If the presence of guest molecules at the surface causes the same change in SPR angle independent of the number of cavities they are bound by, the total change will be

$$\Delta\alpha = (\theta_1 + \frac{1}{2}\theta_2)\Delta\alpha_{max}$$

Equation 6.5.

Where *Δα$_{max}$* is the maximum possible SPR angle change, reached for purely monomeric complexation. Therefore, Langmuir binding curves are expected with saturation values

between $\frac{1}{2}\Delta\alpha_{max}$ and $\Delta\alpha_{max}$. From the comparison with the monolayer of **1**, $\Delta\alpha_{max}$ is estimated to be approximately 0.145° for a 9% layer of **2**.[26] Using this value, we calculated the ratio of monomer complexation to dimer complexation at the surface for steroids **6a-6e** (Table 6.4).[27] Steroids **6a** and **6b** are bound by two cyclodextrin cavities rather than one. This is in agreement with the strong preference of these guests to be complexed by a dimer in solution.[20] It should be noted, however, that K values for a dimer cannot be directly compared to K_2 values obtained here, since the conformation a dimer adopts to bind a guest in solution may be entirely different from the orientation of and distance between the cavities in a monolayer. Moreover, the surface case merely represents an average situation. A mixture of monomer and dimer complexation is observed for **6c-6e**, also in qualitative agreement with the binding behavior in solution.[20]

Table 6.4.   *Ratio of monomer to dimer complexation by mixed monolayers of **2**.*

	9% **2**	4.5% **2**
Guest	$\theta_1:\theta_2$	$\theta_1:\theta_2$
6a	0:100	0:100
6b	0:100	0:100
6c	48:52	67:33
6d	48:52	69:31
6e	59:41	85:15

Further evidence for 2:1 binding at the surface came from diluting the monolayer. The K_1 values are unaffected by this dilution, but the K_2 values should decrease because of the increased distance between the cyclodextrin cavities.[28] This should therefore be reflected in a change of the $\theta_1:\theta_2$ ratio (Equation 6.4) and thus to a change in the saturation value of $\Delta\alpha$ (Equation 6.5). For steroids **6c-6e** dilution of the monolayer indeed led to a markedly increased ratio of monomer to dimer complexation (Table 6.4), supporting the model of both dimer and monomer complexation at the surface. Further dilution of the cyclodextrin adsorbate in the monolayer, which might have enabled the observation of monomer complexation even for **6a** and **6b**, reduced the SPR signal so that it was too small to obtain reproducible results.

Titrations of steroids to monolayers containing 17% of **2** were not described well by a Langmuir isotherm. Possibly, the lack of freedom of the cyclodextrin cavities in these layers causes the presence of different absorption sites as observed for pure cyclodextrin monothiol layers.[7f]

6.5   Conclusions

Densely packed monolayers can be prepared by filling the space under the cyclodextrin head group, either through persubstitution of the primary rim or through coadsorption of a monosubstituted cyclodextrin with a simple mercaptoalcohol. These monolayers have well-defined host-guest interactions with known guests for β-cyclodextrin. In all cases, the response to a certain concentration of an analyte is rapid and reversible, making these monolayers excellent candidates for on-line sensing applications. The selectivity of the monolayers depends on their architecture. Monolayers of the β-cyclodextrin heptathioether have excellent recognition properties for small organic guests that bind *in* the cavity, *e.g.* 1-acetamidoadamantane and ferrocenemethanol. For larger guests, like steroids, the selectivity of monolayers of monofunctionalized cyclodextrin more closely resembles the binding by native β-cyclodextrin in solution. Such cyclodextrin derivatives organized in a monolayer appear to be capable of cooperativity. The mode of incorporation of a cyclodextrin into a monolayer is a method for altering its selectivity. This offers the possibility to screen sensor molecules for selectivity for a certain guest by assembling receptors on a monolayer, rather than by first synthesizing the optimal receptor and then incorporating it into a monolayer.

6.6   Experimental section

Materials. β-Cyclodextrin was dried prior to use. All other chemicals were used as received, unless otherwise stated. Solvents were purified according to standard laboratory methods.[29] All reactions were carried out in an inert atmosphere. NMR spectra were taken on a 300 MHz NMR spectrometer, using residual solvent protons or TMS as an internal standard. TLC was performed on aluminum sheets precoated with silica gel 60 F_{254} (E. Merck). The cyclodextrin spots were visualized by dipping the sheets in 5% sulfuric acid in ethanol followed by heating. Chromatographic separations were performed on silica gel 60 (E. Merck, 0.040-0.063 mm, 230-240 mesh). Matrix assisted laser desorption ionization time-of-flight (MALDI-TOF) mass spectrometry was carried out using a Perseptive Biosystems Voyager-DE-RP MALDI-TOF mass spectrometer. FAB-mass spectra were obtained with a Finnigan MAT 90 spectrometer. For MALDI-TOF mass spectrometry α-cyano-4-hydroxycinnamic acid and for FAB-mass spectrometry *m*-nitrobenzylalcohol were used as the matrix. TBDMS-protected β-cyclodextrin (TBDMS-CD) was prepared according to a literature procedure.[30]

Heptakis-{6-deoxy-6-[12-(thiododecyl)dodecanamido]}-β-cyclodextrin   (1)   was synthesized analogous to a procedure published before.[10a] Yield 45%. TLC R_f = 0.56

(CH$_2$Cl$_2$/MeOH 30% v/v). ^{1}H NMR (CDCl$_3$): δ 7.06 (s, 7 H), 6.56 (s, 7 H), 5.12 (s, 7 H), 4.80 (s, 7 H), 3.96-3.08 (m, 42 H), 2.42 (t, ^3J(H,H) = 7.5 Hz, 28 H), 2.22-2.05 (m, 14 H), 1.52-1.45 (m, 42 H), 1.29-1.19 (m, 238 H), 0.83 (t, ^3J(H,H) = 6.5 Hz, 21 H); ^{13}C NMR (CDCl$_3$): δ 173.6, 103.4, 84.1, 72.7, 52.6, 36.0, 31.7, 3149, 29.1, 29.0, 28.8, 28.6, 28.5, 25.5, 22.2, 13.6; MS (MALDI-ToF) *m/z*: calcd. for C$_{210}$H$_{399}$N$_7$O$_{35}$S$_7$: 3807, found 3830 [*M*+Na]$^+$.

12-Bromo-1-(*S*-trityl)mercaptododecane.[31] A mixture of 1,12-dibromododecane (5.00 g, 3.68 mmol), triphenylmethylmercaptane (17.8 g, 0.111 mmol), and potassium carbonate (3 g) in 300 ml acetonitrile was refluxed over night. After evaporation of the solvent, the residue was dissolved in dichloromethane and washed with HCl (1 M), NaOH (1 M) and brine, and dried over MgSO$_4$. After removal of the solvent the crude product was purified by repeated crystallization from hexane to give 12-bromo-1-(*S*-trityl)mercaptododecane as a colorless solid in 45% yield. ^{1}H NMR (CDCl$_3$): δ 7.45 (d, 6 H, *J* = 7.8 Hz), 7.35-7.09 (m, 9 H), 3.33 (t, 2 H, *J* = 7.5 Hz), 2.06 (t, 2 H, *J* = 7.5 Hz), 1.82-1.72 (m, 2 H), 1.45-1.10 (m, 18 H); ^{13}C NMR (CDCl$_3$): δ 174.2, 102.5, 84.3, 73.4, 71.1, 54.3, 43.1, 37.2, 36.4, 32.2, 31.9, 29.7, 29.6, 29.5, 29.3, 29.0, 26.0, 22.7, 14.2. FAB-MS: *m/z* calcd. for C$_{31}$H$_{39}$BrS: 522.2 found: 523.3 [*M*+H]$^+$.

Heptakis(6-*O*-*tert*-butyldimethylsilyl)mono-2-O-(12-thiotrityl-dodecyl)-β-cyclodextrin. LiH (18 mg, 2.3 mmol) was added to a solution of dried (100 ºC, 0.1 mbar, 5 h) TBDMSCD[30] (2.0 g, 1.03 mmol) in dry THF (30 mL). The mixture was refluxed for 2 h. 1-Bromo-12-(*S*-trityl)mercaptododecane (0.87 g, 1.7 mmol) was added and reflux was continued for 16 h. The solvent was removed *in vacuo* and the residue was dissolved in dichloromethane. The solution was washed with HCl (1 M), water, and brine, and dried over MgSO$_4$. After removal of the solvent and purification by column chromatography (ethyl acetate/ethanol/water 100:2:1) the product was obtained as a white powder in 30% yield. ^{1}H NMR (CDCl$_3$): δ = 7.40-7.14 (m, 15 H), 4.88-4.84 (m, 7 H), 4.12-3.13 (m, 44 H), 2.07 (t, 2 H, *J* = 8 Hz), 1.58-1.03 (m, 18 H), 0.86-0.79 (m, 63 H), 0.02 - -0.04 (m, 42 H). FAB-MS: *m/z* calcd for C$_{115}$H$_{206}$O$_{35}$SSi$_7$: 2373.2 found: 2374.2 [*M* - H]$^-$.

Mono-2-O-(12-thiododecyl)-β-cyclodextrin (2). A solution of triethylsilane in trifluoroacetic acid was added to a solution of heptakis(6-O-*tert*-butyldimethylsilyl)mono-2-O-(12-thiotrityl-dodecyl)-β-cyclodextrin (0.40 g, 0.17 mmol) in trifluoroacetic acid until it decolored. The solvent was removed in vacuo and methanol was added and evaporated three times to remove residual acid. The residue was dissolved in water and washed three times with ether. After lyophilization the product was obtained as a white powder in 76% yield. ^{1}H NMR (D$_2$O): δ = 5.06-4.88 (m, 7 H), 3.84-3.39 (m, 44 H), 2.38 (t, 2 H, *J* = 9 Hz), 1.42-1.12 (m, 18 H). FAB-MS: *m/z* calcd for C$_{54}$H$_{94}$O$_{35}$S: 1334.5 found: 1333.8 [*M* - H]$^-$.

Calorimetry. Titrations were performed at 25 ºC using a Microcal VP-ITC titration microcalorimeter. Sample solutions were prepared using pure water (Millipore Q2). Titrations were performed by adding aliquots of a β-cyclodextrin solution to the guest (**3**, **4**, **5**) solution. The titrations were analyzed using a least squares curve fitting procedure. Control experiments involved addition of β-cyclodextrin to water and addition of water to a guest solution.

Monolayers. Gold Substrates. Gold substrates were prepared by evaporating 200 nm gold on a glass slide of 25 mm diameter with a 2 nm chromium layer for adhesion. Before use, the gold substrates were cleaned in an oxygen plasma for 5 min. The resulting oxide layer was removed by leaving the substrates in EtOH for 10 min.[32] For SPR measurements 47.5 nm thick gold-coated glass substrates were used. For AFM measurements, gold substrates were purchased from Metallhandel Schröer GmbH, Lienen, Germany (200 nm gold on 5 nm chromium on glass substrates [11×11 mm^2]). These samples were stored under nitrogen. Prior to use, substrates were flame annealed with a H$_2$ flame (quality 6). The annealing yielded reproducibly large Au(111) terraces of a few square micrometers in size. After annealing, the substrates were allowed to cool to room temperature and transferred with minimal delay into the adsorption solution.

Monolayer preparation. All glassware used to prepare monolayers was immersed in *piraña* at 70 ºC for 1 h. **Warning**: *piraña* solution should be handled with caution; it has detonated unexpectedly. Next, the glassware was rinsed with large amounts of high purity water (Millipore). Cleaned gold substrates were immersed with minimal delay into a 0.1 mM adsorbate solution in EtOH and H$_2$O (2:1, v/v) for 16 h. The sulfide monolayers were prepared at 60 ºC in EtOH and CHCl$_3$ (1:2, v/v) for 16 h. Subsequently, the substrates were removed from the solution and rinsed repeatedly with chloroform, ethanol, and water to remove any physisorbed material.

Monolayer characterization. The advancing and receding contact angles with water were measured on a Krüss G10 Contact Angle Measuring Instrument, equipped with a CCD camera. The contact angle measurements were measured during the growth and shrinkage of a droplet.

Electrochemical measurements (cyclic voltammetry and impedance spectroscopy) were performed on an Autolab PGSTAT10 (ECOCHEMIE, Utrecht, The Netherlands) in a three electrode system consisting of a gold working electrode (clamped to the bottom of the cell, exposing a geometric area of 0.44 cm^2 to the electrolyte solution), a platinum counter electrode, and a mercurous sulfate reference electrode (+0.61 V$_{NHE}$). Cyclic voltammetric capacitance measurements were conducted in 0.1 M K$_2$SO$_4$ between -0.35 V$_{MSE}$ and -0.25 V$_{MSE}$ at scan rates ranging from 0.1 V/s to 2.0 V/s. Impedance spectroscopy measurements were performed in 1 mM K$_3$Fe(CN)$_6$ / K$_4$Fe(CN)$_6$ and 0.1 M K$_2$SO$_4$ at -0.2 V$_{MSE}$ with an amplitude of 5 mV using a frequency range from 50 kHz to 0.1 Hz. The charge-transfer resistance of the monolayer was obtained by fitting the experimental data to an equivalent

circuit consisting of the monolayer resistance parallel with the monolayer capacitance, in series with the solution resistance.[33]

The AFM measurements were carried out with a Nanoscope III AFM (Digital Instruments, Santa Barbara, California, USA) in tapping mode. AFM scans were performed in water using a liquid cell. Silicon nitride cantilevers with nominal spring constants of 0.38 N/m and 0.06 N/m were used.

SPR measurements were performed in a two-channel vibrating mirror angle scan set-up based on the Kretschmann configuration, described by Kooyman *et al.*[34] Light from a 2-mW HeNe Laser is directed onto a prism surface by means of a vibrating mirror. The intensity of the light is measured by means of a large-area photodiode. This set-up allows determination of changes in plasmon angle with an accuracy of 0.002°. The gold substrate with the monolayer was optically matched to the prism using an index matching oil. A cell placed on the monolayer was filled with 800 mL of a 1 mM KOH solution. After stabilization of the SPR signal, titrations were performed by removing an amounts of KOH solution and adding the same amounts of stock solutions of the bile salts in KOH. Between additions, the cell was cleaned by repeated washings with KOH solution (700 μL, three or four times). SPR measurements were repeated three times for each monolayer guest system.

6.7 References

1   (a) Ulman, A.; *An Introduction to Ultrathin Organic Films*; Academic Press: San Diego, CA, **1991**; (b) Finklea, H.O.; in *Electroanalytical Chemistry*, *Vol. 19* (Eds.: A. J. Bard, I. Rubinstein), Marcel Dekker: New York, **1996**, p 109-335.

2   (a) Schierbaum, K.-D.; Weiss, T.; Thoden van Velzen, E.U.; Engbersen, J.F.J.; Reinhoudt, D.N.; Göpel, W. *Science* **1994**, *265*, 1413-1415; (b) Thoden van Velzen, E.U.; Engbersen, J.F.J.; Reinhoudt, D.N. *Synthesis* **1995**, *8*, 989-1008; (c) Thoden van Velzen, E.U.; Engbersen, J.F.J.; de Lange, P.J.; Mahy, J.W.; Reinhoudt, D.N.; *J. Am. Chem. Soc.* **1995**, *117*, 6853-6862; (d) Thoden van Velzen, E.U.; Engbersen, J.F.J.; Reinhoudt, D.N. *J. Am. Chem. Soc.* **1994**, *116*, 3597-3598; (e) Huisman, B.-H.; Kooyman, R.P.H.; Van Veggel, F.C.J.M.; Reinhoudt, D.N. *Adv. Mater.* **1996**, *8*, 561-564.

3   (a) Flink, S.; Boukamp, B.A.; Van den Berg, A.; Van Veggel, F.C.J.M.; Reinhoudt, D.N. *J. Am. Chem. Soc.* **1998**, *120*, 4652-4657; (b) Flink, S.; Van Veggel, F.C.J.M.; Reinhoudt, D.N. *J. Phys. Chem. B* **1999**, *103*, 6515-6520.

4   Friggeri, A.; Van Veggel, F.C.J.M.; Reinhoudt, D.N.; Kooyman, R.P.H. *Langmuir* **1998**, *14*, 5457-5463.

5   (a) Wenz, G. *Angew. Chem. Int. Ed. Engl.* **1994**, *33*, 803-822. (b) *Chem. Rev.* **1998**, *98*, Issue 5. (c) Szejtli, J.; Osa, T. *Comprehensive Supramolecular Chemistry, Vol.*

3, (Eds.: Atwood, J.L.; Davies, J.E.D.; MacNicol, D.D.; Vögtle, F.; Lehn, J.-M.), Pergamon, Oxford, **1996**.

6   (a) Maeda, Y.; Fukuda, T.; Yamamoto, H.; Kitano, H. *Langmuir* **1997**, *13*, 4187-4189; (b) Yamamoto, H.; Maeda, Y.; Kitano, H. *J. Phys. Chem. B* **1997**, *101*, 6855-6860. (c) Fukuda, T.; Maeda, Y.; Kitano, H. *Langmuir* **1999**, *15*, 1887-1890. (d) Kitano, H.; Taira, Y.; Yamamoto, H. *Anal. Chem.* **2000**, *72*, 2976-2980.

7   (a) Rojas, M.T.; Köninger, R.; Stoddart, J.F.; Kaifer, A.E. *J. Am. Chem. Soc.* **1995**, *117*, 336-343; (b) Nelles, G.; Weisser, M.; Back, R.; Wohlfahrt, P.; Wenz, G.; Mittler-Neher, S. *J. Am. Chem. Soc.* **1996**, *118*, 5039-5046; (c) Weisser, M.; Nelles, G.; Wohlfahrt, P.; Wenz, G.; Mittler-Neher, S. *J. Phys. Chem.* **1996**, *100*, 17893-17900; (d) Weisser, M.; Nelles, G.; Wenz, G.; Mittler-Neher, S. *Sens. Actuat. B* **1997**, *100*, 58-67; (e) Henke, C.; Steinem, C.; Janshoff, A.; Steffan, G.; Luftmann, H.; Sieber, M.; Galla, H.-J. *Anal. Chem.* **1996**, *68*, 3158-3165; (f) Michalke, A.; Janshoff, A.; Steinem, C.; Henke, C.; Sieber, M.; Galla, H.-J.; *Anal. Chem.* **1999**, *71*, 2528-2533; (g) He, P.; Ye, J.; Fang, Y.; Suzuki, L.; Osa, T. *Anal. Chim. Acta* **1997**, *337*, 217-233; (h) Lahav, M.; Ranjit, K.T.; Katz, E.; Willner, I. *Chem. Commun.* **1997**, 259-260.

8   (a) Liu, J.; Mendoza, S.; Roman, E.; Lynn, M.J.; Xu, R.L.; Kaifer, A.E. *J. Am. Chem. Soc.* **1999**, *121*, 4304-4305. (b) Liu, J.; Alvarez, J.; Kaifer, A.E. *Adv. Mater.* **2000**, *12*, 1381-1383.

9   Beulen, M.W.J.; Bügler, J.; Lammerink, B.; Geurts, F.A.J.; Biemond, E.M.E.F.; van Leerdam, K.G.C.; Van Veggel, F.C.J.M.; Engbersen, J.F.J.; Reinhoudt, D.N. *Langmuir* **1998**, *14*, 6424-6429.

10   (a) Beulen, M.W.J.; Bügler, J.; De Jong, M.R.; Lammerink, B.; Huskens, J.; Schönherr, H.; Vancso, G.J.; Boukamp, B.A.; Wieder, H.; Offenhäuser, A.; Knoll, W.; Van Veggel, F.C.J.M.; Reinhoudt, D.N. *Chem. Eur. J.* **2000**, *6*, 1176-1183; (b) Schönherr, H.; Beulen, M.W.J.; Bügler, J.; Huskens, J.; Van Veggel, F.C.J.M.; Reinhoudt, D.N. *J. Am. Chem. Soc.* **2000**, *122*, 5039-5046.

11   (a) Motesharei, K.; Myles, D.C. *J. Am. Chem. Soc.* **1994**, *116*, 7413-7414; (b) Motesharei, K.; Myles, D.C. *J. Am. Chem. Soc.* **1998**, *120*, 7328-7336. (c) Wenz suggested coadsorbing hexanethiol and cyclodextrin monothiols as a method to improve the binding properties of monolayers of cyclodextrin, without performing guest-binding studies. See ref 7d

12   Qian, X.; Hentschke, R.; Knoll, W. *Langmuir* **1997**, *13*, 7092-7098.

13   The surface areas of β-cyclodextrin with the rim parallel or perpendicular to the surface are 190 Å^2 and 120 Å^2, respectively (see Figure 2.1). The surface area occupied by a thiol is approximately 20 Å^2.

14   Previously, we measured the complexation of 1-anilinonaphthalene-8-sulfonate in monolayer-confined β-cyclodextrin by electrochemical impedance spectroscopy.[10a] Addition of less highly charged organic guests to monolayers of heptathioether **1**

did not lead to a change in the charge transfer resistance. Interactions of guests with the cavities in the monolayer may require a large electrostatic interaction between the reporter redox couple and the guest to give a reponse in an impedance spectroscopy experiment. This may in part be caused by the very high charge transfer resistance of the monolayers.

[15] Raether, H. in *Physics of Thin Films*, *Vol. 9* (Eds.: Has, G.; Francombe, M.; Hoffman, R.), Academic Press: New York, **1977**.

[16] (a) Fieser, L.F.; Fieser, M. *Steroids*, Reihold, New York, **1959**. (b) Templeton, W. *An Introduction to the Chemistry of the Terpenoids and Steroids*, Buttworth, London, **1969**.

[17] Danielsson, H.; Sjövall, J.; *Sterols and Bile Acids*; Elsevier Sci. Ltd., Amsterdam, The Netherlands, **1985**

[18] Higler, I.; Timmerman, P.; Verboom, W.; Reinhoudt, D. N. *J. Org. Chem.* **1996**, *61*, 5920-5931.

[19] Friggeri, A.; Van Veggel, F.C.J.M.; Reinhoudt, D.N. *Chem. Eur. J.* **1999**, *5*, 3595-3602.

[20] De Jong, M.R.; Engbersen, J.F.J.; Huskens, J.; Reinhoudt, D.N. *Chem. Eur. J.* **2000**, *6*, 4034-4040.

[21] Ueno, A. *Supramol. Sci.* **1996**, *3*, 31 and references herein

[22] (a) Mucci, A.; Schenetti, L.; Vandelli, M.A.; Forni, F.; Ventura, P.; Salvioli, G. *J. Chem. Soc., Perkin Trans. 2* **1996**, 2347-2349. (b) Ramos Cabrer, P.; Alvarez-Parrilla, E.; Meijide, F.; Seijas, J.A.; Rodríguez Núñez, E.; Vázquez Tato, J. *Langmuir* **1999**, *15*, 5489-5495.

[23] Tan, Z.J.; Zhu, X.X.; Brown, G.R. *Langmuir* **1994**, *10*, 1034-1039.

[24] Kooyman, R.P.H.; Kolkman, H.; Van Gent, J.; Greve, J. *Anal. Chim. Acta* **1988**, *213*, 35-45

[25] Using the relationship derived for silver in ref 24, SPR sensitivity is calculated to be approximately 6° for every ng mm^{-2}.

[26] Monolayers of **1** which give $\Delta\alpha_{max} = 0.115°$ have 14 alkyl chains per cavity, giving them the same cyclodextrin concentration as mixed monolayers of 7% of **2** with mercaptoundecanol.

[27] Using $K_1 : K_2 = \theta_1 : \theta_2$, Which follows from equation 6.4.

[28] We have previously shown that dilution of a monolayer of crownethers hinders the formation of a sandwich complex between two crown ethers and potassium ions, resulting in a loss of potassium over sodium selectivity for these monolayers. See ref. 3a.

[29] Perrin, D.D.; Armarego, W.F.L. *Purification of Laboratory Chemicals*, third edition, Pergamon Press: Oxford, **1989**.

30   Van Dienst, E.; Snellink, B.H.M.; Von Piekartz, I.; Grote Gansey, M.H.B.; Venema, F.; Feiters, M.C.; Nolte, R.J.M.; Engbersen, J.F.J.; Reinhoudt, D.N. *J. Org. Chem.* **1995**, *60*, 6537-6545.

31   This compound has been synthesized before, by a different procedure: Tam-Chang, S.-W.; Mason, J.C. *Tetrahedron* **1999**, *55*, 13333-13344. The presented spectral data closely resemble those described previously.

32   Ron, H.; Rubinstein, I. *Langmuir* **1994**, *10*, 4566-4573.

33   (a) Boukamp, B.A. *Solid State Ionics* **1986**, *18-19*, 136. (b) Boukamp, B.A. *Solid State Ionics* **1986**, *20*, 31.

34   Lenferink, A.T.M.; Kooyman, R.P.H.; Greve, J. *Sens. Act. B* **1991**, *3*, 261-265.

Chapter 7

Probing Individual Cyclodextrin-Guest Interactions with AFM

7.1   Introduction

The advent of scanning probe techniques such as atomic force microscopy (AFM) has given rise to an increasing interest to measure individual molecular interactions. Numerous interactions have been studied by AFM, *e.g.* between biotin and (strept)avidin[1,2] and between complementary DNA strands.[3] The interactions of these large systems usually have very slow unbinding kinetics. Evans *et al.* showed that this renders the force of a single molecule interaction dependent on the loading rate. Our group recently studied single molecule interactions of cyclodextrin heptathioether monolayers[4,5] on gold with a ferrocene-modified AFM tip, thus providing the first example of a single molecule interaction of small molecules with fast unbinding kinetics.[6] This system showed no dependence on the loading rate.

In Chapter 6, the complexation behavior of monolayers of cyclodextrin heptathioether **1** on gold with organic guests in aqueous solution was studied in detail by SPR. In this Chapter, the interactions of the monolayers of **1** with guests immobilized on an AFM tip are studied. The study of single molecule binding events with AFM commonly involves the use of force-distance curves. A force-distance curve is a plot of the measured force, assessed by a deflection of the cantilever, as a function of the distance the sample has traveled with respect to a reference point (Δz, Figure 7.1). Usually, the reference point is chosen as the sample position at maximum repulsion. In order to calculate the force from the tip deflection, the spring constant has to be determined, and the force is assumed to be linearly dependent on this (harmonic potential).

NH
=O

S   7

1
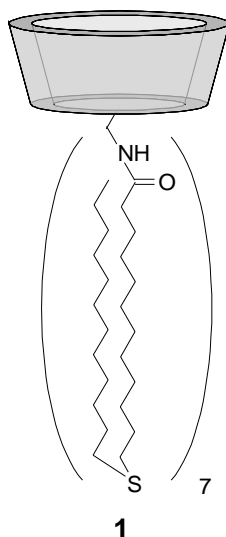
A force-distance curve is acquired by fixing the piezo in the *x-y* direction and moving it in the *z* direction, as depicted in Figure 7.1. The distance Δz is the distance of piezo travel with respect to the point of maximum repulsion, at which the direction of the movement changes.
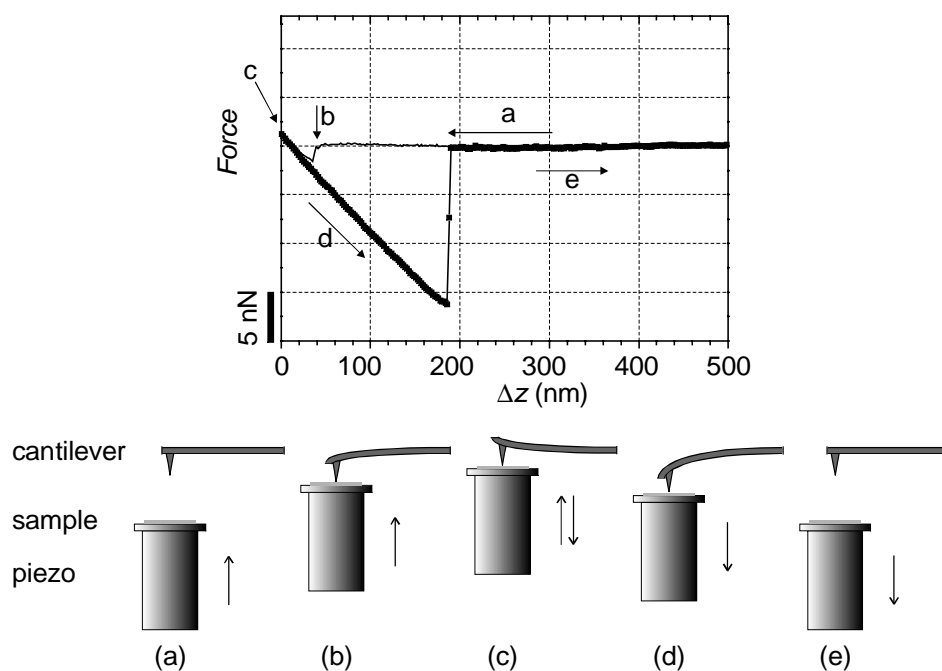
Figure 7.1. *Example of a force-distance curve and schematic representations of important moments during the course of the measurement.*

The features observed in a force-distance diagram are often described using force gradients. If the tip is far away from the surface, there are no interactions and the cantilever is not deflected (a). When the sample approaches the tip, the value of the force gradient for the tip-sample interaction exceeds the force gradient for the cantilever deflection and a snap-on event (b) can occur. Approaching the sample even closer will eventually make the

tip bend upward (c), resulting in repulsive forces. On retraction of the sample, the tip will stay in contact through adhesive forces (d) until again a sudden jump occurs, *i.e.* the pull-off event. This point represents the maximum attractive force (adhesion force). At still greater separations, again no surface forces are measured (e). In the previous study,[6] a loading rate-independent pull-off force of 56 pN was found for the interaction between tip-immobilized ferrocene and a β-cyclodextrin SAM on gold. In this Chapter, other cyclodextrin-guest interactions will be described and a model will be presented to relate the pull-off force to thermodynamic parameters for the host-guest interaction.

7.2 Synthesis and characterization of guest adsorbates

Modification of AFM tips was performed by depositing gold on a silicon nitride tip by evaporation and subsequently adsorbing a (mixed) self-assembled monolayer of thiol compounds. Complexation of a guest by a cyclodextrin requires enough space around the guest molecule for the cavity to slide over it. Spacing of the guest molecules is achieved by preparing mixed adsorbate layers of a guest-substituted alkylthiol and a shorter inert thiol. So far, only 6-ferrocenyl hexanethiol **2** (Chart 7.1) was used as a guest adsorbate because its surface coverage in mixed monolayers can be accurately determined by cyclic voltammetry.[6] For **2**, a good correlation was found between the ratio **2** : coadsorbate in the solution used to prepare the monolayer and in the resulting monolayer.[6]

Two other thiol-modified guests were synthesized to allow study of the dependence of the pull-off force for a cyclodextrin-guest complex on the binding affinity. The guest motifs chosen were the *tert*-butylphenyl moiety and the adamantyl moiety. Reaction of 4-*tert*-butylaniline or 1-adamantylamine with 5-bromopentanoic acid yielded alkyl-substituted guests for β-cyclodextrin. Substitution of the bromide for thioacetate and subsequent deprotection afforded the desired guest adsorbates 5-mercaptopentanoic acid (4-*tert*-butylphenyl)-amide **3** and 5-mercaptopentanoic acid adamantan-1-ylamide **4**.
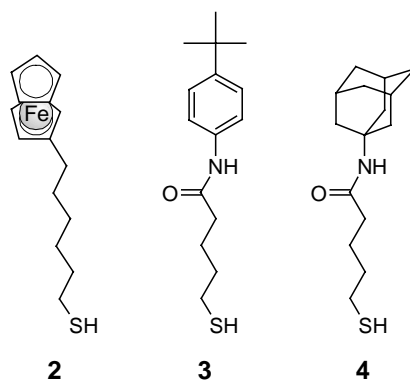

Chart 7.1. *Structures of the guest adsorbates used.*

Unlike ferrocene adsorbate **2**, the guest adsorbates **3** and **4** are not redox active, prohibiting determination of the surface coverage of these adsorbates in mixed monolayers with mercaptoethanol by cyclic voltammetry. Contact angle measurements of mixed monolayers of **4** and mercaptoethanol prepared from solutions containing 1% of adamantane adsorbate **4** indicated these to be more hydrophobic than monolayers prepared from a solution of mercaptoethanol, which is interpreted as incorporation of **4** in the monolayer. The contact angle increased with increasing percentages of **4**. X-ray Photoelectron Spectroscopy (XPS) measurements showed a linear dependence of the atom percentages of carbon, nitrogen, and oxygen on the ratio of the two adsorbates in solution (Figure 7.2). AFM images of mixed monolayers prepared from solutions containing 20 % and 50 % of **4** did not show domain formation. All these results strongly suggest that no surface phase segregation occurs and that the solution and surface ratios of the adsorbates are equal. This is assumed to be the case for **3** as well.
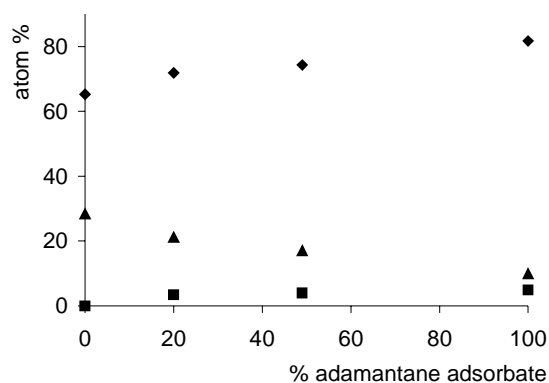

Figure 7.2. *Plot of the content of carbon (♦), nitrogen (■), and oxygen (▲) of mixed monolayers of **4** and mercaptoethanol as a function of the ratio of **4** to mercaptoethanol in solution, determined by XPS.*

7.3   The strength of cyclodextrin complexes

Force-distance curves for the interaction of tips covered with mercaptoundecanol and substrates with monolayers of **1** closely resembled the typical force-distance curve of Figure 7.1. Only a single pull-off was observed, with a value of approximately 800 pN, which is attributed to non-specific interactions between tip and sample. Similar results were obtained for the interaction of tips covered with mixed monolayers containing 1% of guest adsorbate **2**, **3**, or **4** and 99% of mercaptoethanol and substrates with monolayers of mercaptoundecanol.

This picture changed drastically when the interaction between a guest-coated tip and a monolayer of cyclodextrin heptathioether **1** was measured (Figure 7.3). In Figure 7.3, a

typical force-distance curve for the interaction between a tip covered with 1% of adamantane adsorbate **4** and a substrate with a monolayer of **1** is shown. Instead of just one, several pull-off events are observed. Similar curves were obtained for the interaction with ferrocene guest **2** and with 4-*tert*-butylphenyl guest **3**. These curves are similar to the data described before for **2**.[6]
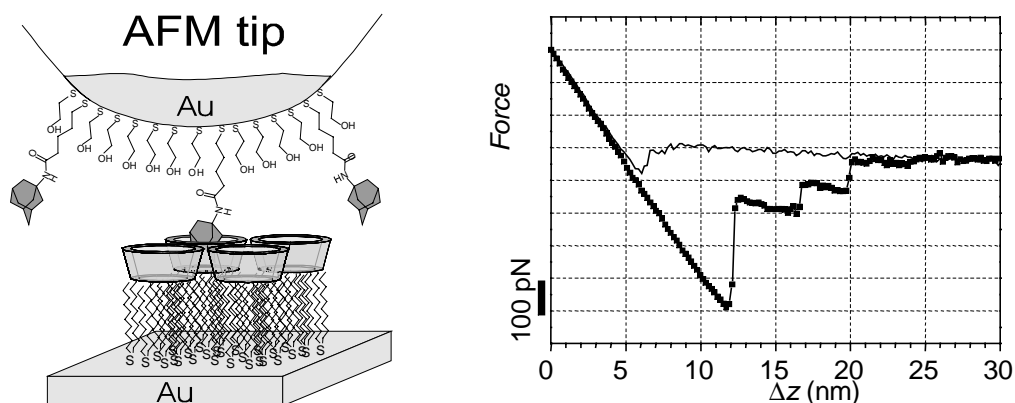

Figure 7.3. *Schematic representation and representative force-distance curve for the interaction between a tip covered with 1% of adamantane derivative **4** and a monolayer of cyclodextrin **1**.*

The occurrence of multiple pull-off events during retraction of the sample is attributed to the rupture of individual host-guest complexes in the contact area between the tip and the sample. Additional proof for this comes from experiments performed in the presence of the external guest 1-anilinonaphthalene-8-sulfonic acid (1,8-ANS).[6,7] After the addition of 1,8-ANS the number of interactions between **4** and the monolayer of **1** decreased markedly. In the case of **2**, which contains a guest motif that has a lower association constant with monolayers of **1**, the number of pull-off events was reduced more drastically. In 50 % of the curves, only a single pull-off was observed, the others showed up to three events. After washing away the 1,8-ANS with water, the multiple pull-offs were observed again. These observations are in agreement with a reversible blocking of a large portion of the available cavities in the monolayer of **1** by the external guest.

All deflection changes associated with the corresponding pull-off events were measured, translated into forces, and histograms with bin sizes determined by the experimental error were constructed. The histograms of the interactions between functionalized tips and monolayers of **1** showed several maxima at apparently equidistant forces in all three cases (Figure 7.4).
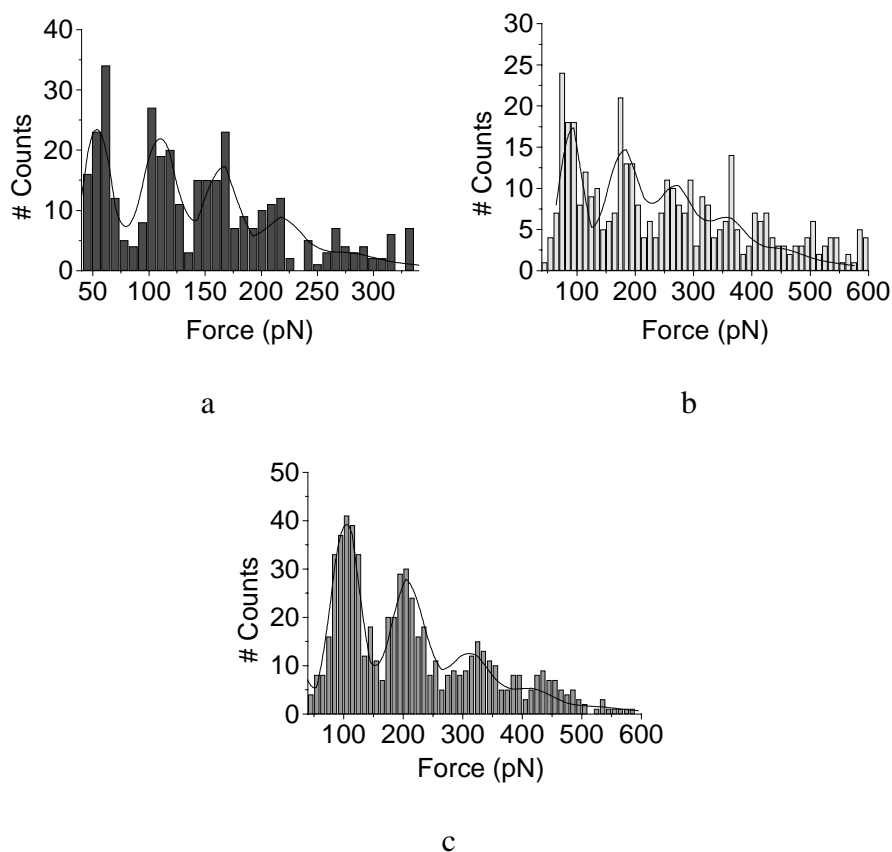
a

b

c

Figure 7.4. *Histograms for the interaction of tips coated with 1% of **2** (a), 1% of **3** (b), and 1% of **4** (c) with substrates with monolayers of **1**. The bars represent the number of observations, the curve the fit to the data, using a set of Gaussians (see Appendix A).*

The first maximum is assumed to originate from the rupture of a single host-guest complex with a quantized force F_q,[6] the subsequent ones from the simultaneous rupture of multiple complexes with force values at integer multiples nF_q. The area of the peaks is assumed to follow Poisson statistics.[8] The peaks themselves are supposed to follow a Gaussian distribution centered at nF_q. Using these assumptions, a least-squares curve-fitting procedure was developed to describe the histogram as a number of Gaussian peaks with surface areas determined by a Poisson distribution (For details: see Appendix A). The additional parameters that are obtained through the fitting procedure compared to other methods employed for the determination of quantized forces, such as autocorrelation, may give more insight in the physical background of the pull-off force. Analysis of the histograms using this procedure (solid lines in Figure 7.4) allowed the determination of F_q for the interaction between guest-functionalized tips and monolayers of **1** (Table 7.1). Here, λ is the Poisson parameter, representing the mean number of complexes being broken per pull-off event (see Appendix A) and σ_1 and σ_2 are the Gaussian peak widths of the first and second maxima, and thus the errors in the forces for the rupture of one and two complexes. These errors are larger than the experimental error of the AFM

measurement (10 pN), and nearly always increase with an increasing number of complexes being broken, indicating the presence of an intrinsic variability in F_q, possibly related to the path along which the dissociation of the complex takes place.

Table 7.1. *Unbinding forces and other parameters for the interaction between guest-functionalized tips and cyclodextrin monolayers.*

guest	1% guest				0.2% guest			
	F_q (pN)	σ_1 (pN)	σ_2 (pN)	λ	F_q (pN)	σ_1 (pN)	σ_2 (pN)	λ
2	59	10	10	2.6	56	11	15	2.3
3	89	19	28	2.4	-	-	-	
4	102	25	24	2.0	104	22	31	1.8

The binding constants of models of these guest adsorbates with β-cyclodextrin in solution and to monolayers of **1** have been reported in Chapter 6. The results are summarized in Table 7.2. From the comparison of Table 7.1 with Table 7.2, it can be seen that guests having a higher association constant to the cyclodextrin monolayer give a higher unbinding force. There seems to be no correlation with the binding enthalpy to β-cyclodextrin in solution.

Table 7.2. *Binding parameters of ferrocenemethanol (**5**), 4-*tert*-butylphenylacetanilide (**6**), and 1-acetamidoadamantane (**7**) to monolayers of **1** and β-cyclodextrin in solution.*

guest (model for)	1	solution		
	ΔG^o (kcal mol^{-1})	ΔG^o (kcal mol^{-1})	ΔH^o (kcal mol^{-1})	$T\Delta S^o$ (kcal mol^{-1})
5 (**2**)	-5.4	-5.4	-6.1	-0.7
6 (**3**)	-6.0	-6.1	-5.2	0.9
7 (**4**)	-6.5	-6.6	-5.9	0.7

The quantized pull-off force appears to be independent of the guest concentration on the tip. Dilution of the monolayer on the tip to a guest content of 0.2% resulted in an increase in the number of curves with very large pull-off forces (> 800 pN). The majority of these large forces were the last pull-off event of a curve. They were attributed to non-specific interaction. Discarding these, a decrease in the number of pull-off events per curve was observed. Many curves showed only a single pull-off that corresponded to one, two, or three times the quantized force (Figure 7.5). Quantitative analysis of histograms obtained for these systems afforded identical pull-off forces compared to the ones obtained at 1% guest concentrations.
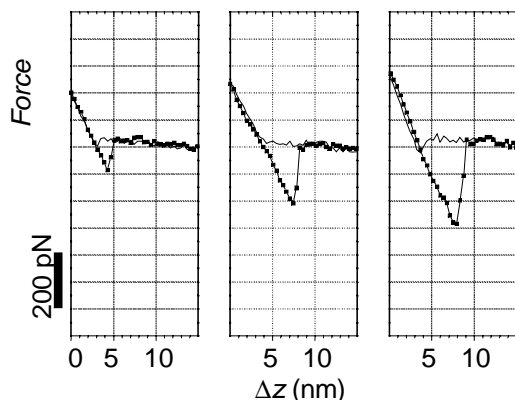
Figure 7.5. *Pull-off curves for the interaction of a tip containing 0.2% of **4** and a substrate with a monolayer of **1** showing the rupture of single, double, and triple host-guest complexes.*

7.4   Loading rate dependence of the pull-off force

The loading rate was varied over several orders of magnitude for tips covered with monolayers with 1% of guest. This had no effect on the magnitude of the quantized force for any of the guests, as shown in Figure 7.6 for guest **4**. For **2**, the loading rate independence has been described before.[6]
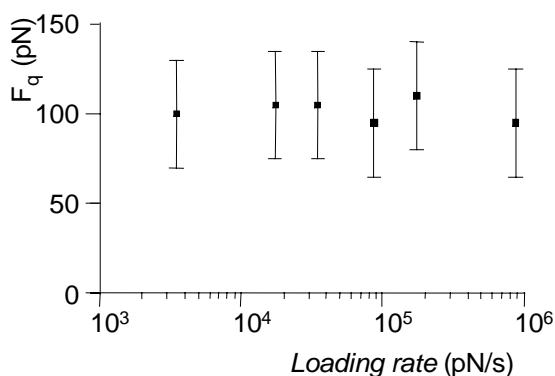
Figure 7.6. *Loading rate dependence of the pull-off force for the interaction between **4** and monolayers of **1**.*

The kinetics of the cyclodextrin-guest system is very fast. Complexation is diffusion controlled ($k_{com} = 10^9$ M^{-1} s^{-1}), K values of $\sim 10^4$ - 10^5 M^{-1} entail a thermal $k_{off} > 10^4$ s^{-1}. At the molecular level, this means many fast complexation and decomplexation events at every point of the force-distance curve while the tip and sample are in contact.

Ritchie and Evans derived a theoretical model for the dependence of the unbinding force for slow, biological sytems on the loading rate.[9] When only dissociation is taken into

account, unbinding is a stochastic process driven by thermal fluctuations, described by a probability $N(t)$ to be in the bound state at time t obeying Equation 7.1, with $N(0) = 1$.

$$dN(t)/dt = -k_{off}(F(t)) \times N(t)$$ *Equation 7.1.*

Where k_{off} is the rate constant of unbinding. For a constant loading rate r, the force increases linearly with time ($F = rt$). The study by Ritchie and Evans[9] predicted the existence of three separate regimes for the unbinding force as a function of the loading rate. For very slow loading, strength appeared at a certain rate or began at zero loading rate, depending on the model used, and then increased as a low power of the loading rate. At higher rates, the off-rate increased exponentially with the force starting from the thermal dissociation rate (k_{off}) of the complex.[10]

$$k_{off}^{*}(F) = k_{off}\, e^{F/F_0}$$ *Equation 7.2.*

From this, it follows that the most probable unbinding force (F^{*}), which corresponds to the measured pull-off force, depends logarithmically on the loading rate r.

$$F^{*} = F_0 \ln \frac{r}{F_0 k_{off}}$$ *Equation 7.3.*

The origin of the quantity F_0 is usually ignored, it only serves as the slope for the loading-rate dependence. At very high rates, the separation is only retarded by viscous drag.

In a later experimental study on the biotin-(strept)avidin system, the pull-off force approached zero at very low loading rates, to progress through a series of regimes of linear dependence on the logarithm of the loading rate with ascending slopes.[11] Each increase in slope signifies suppression of an outer barrier of a complex energy landscape by force, causing an inner barrier to become the dominant kinetic impedance.

The energy landscape a cyclodextrin-guest complex traverses during unbinding is far less complicated than that for the (strept)avidin-biotin complex, probably consisting of only a single large barrier rather than numerous smaller ones. Apparently, this causes the low-loading rate regime to level off at a measurable force rather than at near zero force. In the fast loading regime, the quantity F_0 determining the slope of the loading rate dependence changes when it is overcome by force. It is replaced by a larger force resulting from an inner barrier in the energy landscape of the receptor-ligand interaction. In the system studied here, the quantized pull-off force F_q for each system may well be the only barrier, and consequently be equal to the F_0 to be used when crossover to the fast loading regime

takes place. Solving Equation 7.3 using the values for the cyclodextrin-adamantane system shows that crossover to the fast loading rate regime cannot be expected at the loading rates achievable by AFM (Figure 7.7).
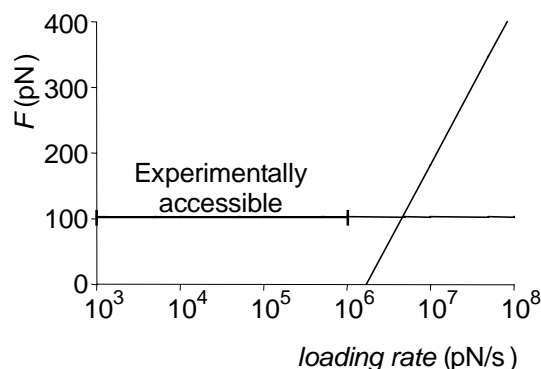

Figure 7.7. *Simulated loading rate dependence of the pull-off force for the adamantane-cyclodextrin system.*

From Equation 7.3, the following can be derived as the minimum requirement to observe a loading-rate dependent pull-off force:

$$\frac{k_{com}}{K} = k_{off} < \frac{r}{F_0 e}$$

Equation 7.4.

Since loading rates up to approximately 10^6 pN/s are accessible by AFM, and F_0 is likely to increase only further with increasing binding constants,[11] Equation 7.4 indicates K values larger than 10^6 M^{-1} are required to observe loading rate dependence in an AFM experiment. No known guests for cyclodextrins incorporated into monolayers meeting this requirement exist. Probing the strength of metal coordination complexes, for which examples with higher binding constants and diffusion-controlled complexation exist, may close the gap between loading rate-independent and loading rate-dependent pull-off forces.

7.5   Modeling the tip-surface interaction

A recent study of the Brownian motion of an AFM tip near a surface revealed that the movement is governed by the sum of the harmonic cantilever potential and the tip-surface interaction potential.[12] From the probability distribution of the tip position, the tip surface potential could be reconstructed. The interaction of a cyclodextrin cavity with a guest can be described as an energy well, the shape of which is approximated by a Lennard-Jones potential (LJP):

$$U_{LJP} = 4\varepsilon \left(\left(\frac{s}{z+z_0} \right)^{12} - \left(\frac{s}{z+z_0} \right)^6 \right)$$

Equation 7.5.

Here, z is the distance from the LJP minimum, z_0 is an offset parameter with a value of $\sqrt[6]{2}s$, ε is the well depth (for $z = 0$, $U_{LJP} = -\varepsilon$ and $\frac{dU_{LJP}}{dz} = 0$), and s determines the width of the well. The shape of the well, which corresponds to the depth of the cyclodextrin cavity, has been obtained from a molecular dynamics simulation ($s = 7.78$ Å).[13,14] The depth of the well is related to the ΔG^0 of the host-guest interaction. The tip is described by a harmonic potential:

$$U_{tip} = \frac{1}{2} k (z - z_0)^2$$

Equation 7.6.

Where k is the spring constant of the AFM cantilever and $z - z_0$ is the difference between the minima of the LJP curve and the tip harmonic which is determined by the piezo movement.[15] The overall potential is the sum of the Lennard-Jones and harmonic potentials (Figure 7.8). Initially, when the tip rests on the surface and no deflection is observed, the two potential minima coincide. Here, Δz is chosen to be 0. Retraction of the tip means that the potential minimum of the tip shifts to the right ($\Delta z > 0$), thus raising the minimum observed at $\Delta z = 0$ (the original LJP well). The minimum Δz change between data points that can be achieved with the equipment used, is 2 Å. Up to a certain point, only one minimum ($U_{in} = U_{LJP} + U_{tip}$ at about $z = 0$), governed by the interaction potential, exists (Figure 7.8a). Near the point where a pull-off event takes place, a second minimum ($U_{out} = U_{LJP} + U_{tip}$ at about $z = \Delta z$), governed by the tip appears (Figure 7.8b), and quickly becomes the predominant one (Figure 7.8c).

The chance p of the system to be "in" (tip in contact with the surface allowing rapid complexation and decomplexation) or "out" (tip not in contact with the substrate) is governed by a Boltzmann distribution:

$$\frac{p_{in}}{p_{out}} = \frac{w_{in}}{w_{out}} e^{-(U_{in} - U_{out})/RT}$$

Equation 7.7.

Where w_{in} and w_{out} are the widths of the minima, which are inversely related to the stifnesses, *i.e.* the spring constants of the complex and the cantilever (see Appendix B). The calculated chances to be in the "in" state (Figure 7.8) clearly show that within two data

points, the system goes from "in" to "out", explaining the abruptly observed pull-off events. Only when multiple datapoints are obtained at a constant or slowly changing Δz, recurrent switching of the tip position between "in" and "out" as observed for a non-derivatized tip and a flat sample can be expected.[12] The measured pull-off force corresponds to the tip deflection in the last point where the system is still in the "in" state. This force is therefore correlated to the Boltzmann distribution and has an intrinsic variability.
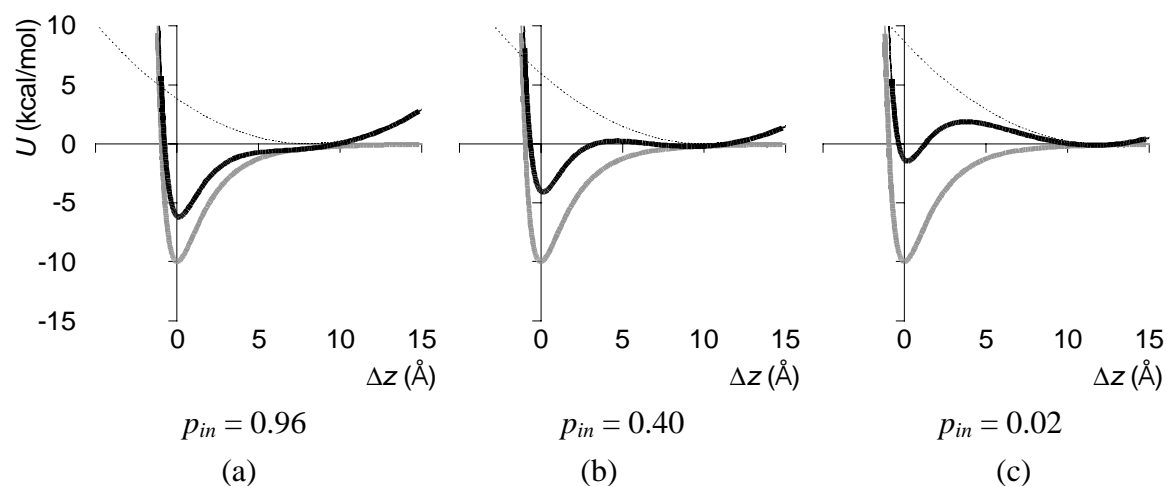

$p_{in} = 0.96$ $p_{in} = 0.40$ $p_{in} = 0.02$

(a)   (b)   (c)

Figure 7.8. *Lennard-Jones (—), harmonic (···) and sum (—) potential at tip-sample distances Δz of 8 Å (a), 10 Å (b), and 12 Å (c). These distances correspond to consecutive points in the experimental force-distance curves.*

A detailed description of this model is given in Appendix B. The model predicts roughly a square-root dependence of the pull-off force F_q on ΔG^0. Using the binding constants given in Table 7.1, a plot of the free energy versus the unbinding force was constructed (Figure 7.9). From the limited range of binding energies sampled it is unclear whether this square root dependence exists.
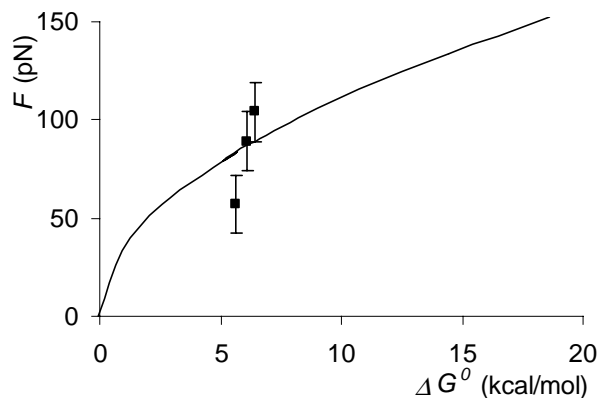

Figure 7.9. *Plot of the unbinding force versus the binding energy. Squares: experimental points; line: simulated square root curve (See Appendix B).*

7.6 Conclusions

This Chapter represents the first detailed study of single molecule interactions of small, synthetic molecules. The relatively simple unbinding pathway and extremely fast kinetics compared to the biological systems usually studied, renders the cyclodextrin guest-system an excellent model for studying the low loading rate regime with AFM. The data presented here suggests that in the low loading rate regime, the pull-off force measured by AFM for a given host-guest system depends on the association constant for this system.

Appendix A: Fitting procedure for histograms

The histograms are obtained by measuring all pull-off forces and dividing them in bins with a bin size determined by the thermal noise of the AFM apparatus, which is 10 pN. Thus, histograms are obtained that are assumed to be described by a Poisson distribution of Gaussian peaks. The Poisson distribution is a discrete distribution that is often used as a model for the number of events in a specific timeframe. It is given by:

$$p_n = e^{-\lambda}\frac{\lambda^n}{n!}$$

Equation 7.8.

Where p_n is the probability of observing n events. This probability is only determined by λ, the mean number of events observed.

The Gaussian peaks for the individual maxima are defined by:

$$D_n = \frac{1}{\sigma_n\sqrt{2\pi}}e^{-(F-nF_q)^2/2\sigma_n^2}$$

Equation 7.9.

Where D_n is the distribution around the nth maximum, σ_n is the standard deviation of this maximum, and F_q is the quantized force.

The total area of the histogram is given by:

$$(\sum_n \int D_n dF \times p_n) \times N_{tot}$$

Equation 7.10.

With N_{tot} being the total amount of observations. To allow the experimentally observed number of observations to be fitted to this equation, the number of observations for bin i (N_i) containing forces from $(i-1){\times}f$ to $i{\times}f$ is calculated according to:

$$N_i = (\sum_{n} \int_{(i-1)f}^{if} D_n dF \times p_n) \times N_{tot}$$

Equation 7.11.

The error

$$\sum (N_i^{calc} - N_i^{exp})^2$$

Equation 7.12.

is then minimized by variation of λ, F_q, σ_n, and N_{tot}.

Appendix B: A model for the tip-surface interaction

The interaction potential is given by Equation 7.5. The stiffness of the complex is needed in the calculation of the Boltzmann distribution and is given by:

$$k_{LJP} = -\frac{d^2 U_{LJP}}{dz^2}, \text{ for } z = 0.$$

Equation 7.13.

Therefore, using $s = 7.78$ Å, $k_{LJP} = 0.994\varepsilon$ kcal mol^{-1} Å^{-1} = 62.94ε pN Å^{-1}, with ε in kcal mol^{-1}. For the complexes studied here, with $\Delta G \approx 6$ kcal mol^{-1}, $\varepsilon \approx 10$ kcal mol^{-1} and $k_{LJP} \approx$ 380 pN Å^{-1}.[16,17] The tip potential is given by Equation 7.6, where $k_{tip} = 8$ pN/Å = 0.12 kcal mol^{-1} Å^{-2}. The total interaction is given by:

$$U_{tot} = U_{LJP} + U_{tip}$$

Equation 7.14.

In the situation where two minima are present, the chance of being in either minimum is given by Boltzmann statistics (Equation 7.7), where:

$$w_{in} = \frac{1}{k_{LJP}} \text{ and } w_{out} = \frac{1}{k_{tip}}$$

Equation 7.15.

$$U_{in} \approx U_{tot,z=0} = -\varepsilon + \frac{1}{2} k_{tip} (\Delta z)^2 \qquad \text{\textit{Equation 7.16.}}$$

$$U_{out} \approx U_{tot,z=\Delta z} = 4\varepsilon \left(\left(\frac{s}{\Delta z + z_0} \right)^{12} - \left(\frac{s}{\Delta z + z_0} \right)^6 \right) \qquad \text{\textit{Equation 7.17.}}$$

Thus $p_{in} = 1 - p_{out}$ can be approximated using these equations, as a function of Δz and ε. For $\varepsilon = 10$, p_{in} as a function of Δz is shown in Figure 7.10.
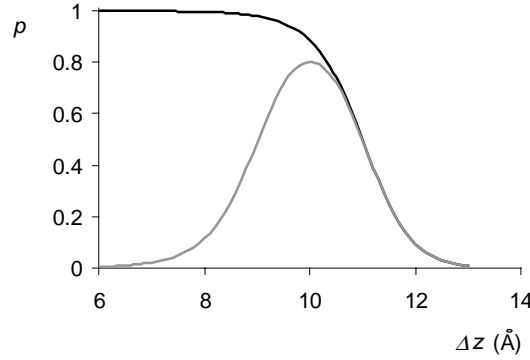
Figure 7.10. *Plot of* p_{in} *(—) and* $p_{pull\text{-}off}$ *(—) as a function of the tip-sample distance* Δz.

For higher ε, $p_{in}(\Delta z)$ shows a sharper transition from 1 to 0. A pull-off event for a single host-guest complex is observed when for one datapoint 'in' is observed, while for the next 'out' is observed. The chance that this occurs is given by:

$$p_{pull-off} = p_{in}(\Delta z) \times (1 - p_{in}(z + \Delta z)) \qquad \text{\textit{Equation 7.18.}}$$

This curve is also shown in Figure 7.10. It has a Gaussian shape with maximum at Δz_{max}, which gives the pull-off force according to $F_q = k_{tip} \times \Delta z_{max}$. The distribution has a width corresponding to $\Delta z_{max} \pm 1$ Å, almost irrespective of ε; only for small ε (<5) the measurement uncertainty becomes larger. This means that with the AFM cantilevers used here measured forces F_q should always show a distribution with $\sigma \approx 10$ pN. This is about equal to the experimental error. The quantized force as a function of ε using this model is shown in Figure 7.11. It has a square root-dependence with $F_q = 31\sqrt{\varepsilon - \varepsilon_0}$. The start at ε_0 = 3.1 kcal mol^{-1} means that forces can only be observed for $\varepsilon > \varepsilon_0$. This can also be qualitatively understood, since for lower values the chance of spontaneous dissociation becomes significantly larger than 0. The relationship between ε and ΔG^0 is linear.[17] Its offset negates ε_0, resulting in the simulated curve of Figure 7.9.
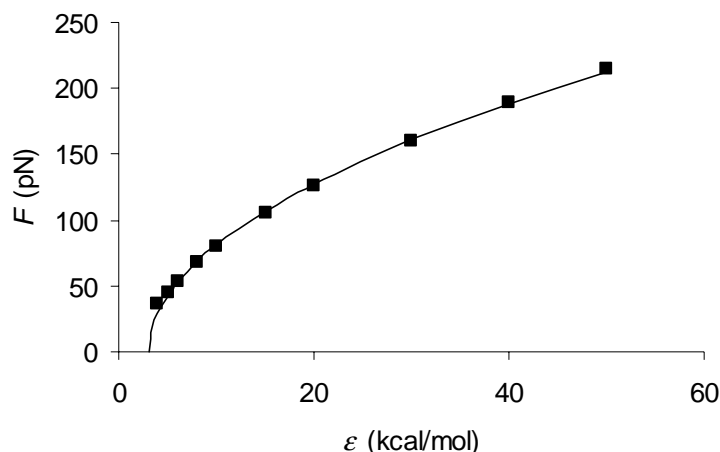
Figure 7.11. *Pull-off forces as a function of ε, calculated using Equation 7.15 (squares) and fit to a square root function with an offset ε_0 (solid line).*

Appendix C: The rupture of multiple parallel bonds

For the rupture of multiple equivalent bonds under a continuous loading rate, two limiting cases can be distinguished. If one bond at a time is broken and relaxation occurs between the breaking of consecutive bonds, a sawtooth-like force-distance curve is observed. This type of behavior is encountered for the unfolding of proteins with several identical domains, such as titin.[18] The observation of force distance curves with more than one pull-off event for the system studied here is consistent with this type of behavior.

The observation of pull-off events corresponding to integer multiples of the quantized force probably originates from the simultaneous rupture of several bonds. The geometry of the experiment renders these bonds *parallel*. Previously, Gaub observed integer multiples of a quantized force for the breaking of *parallel* biotin-streptavidin bonds. These experimental data contradict a recent theoretical study on the rupture of multiple bonds *in parallel*, which predicts a logarithmic dependence of the force on the number of bonds for irreversible bonds, and a square-root dependence for reversible bonds.[19] A tentative solution to this discrepancy is offered by looking at the work required of each individual bond of a number of parallel bonds to counterbalance the work done by the tip.

Figure 7.12 shows a system with N springs in parallel. The distances x and y are the cantilever deflection and the displacement of the complex from its equilibrium position respectively. The values k_1 and k_0 are the corresponding Hookean spring constants.
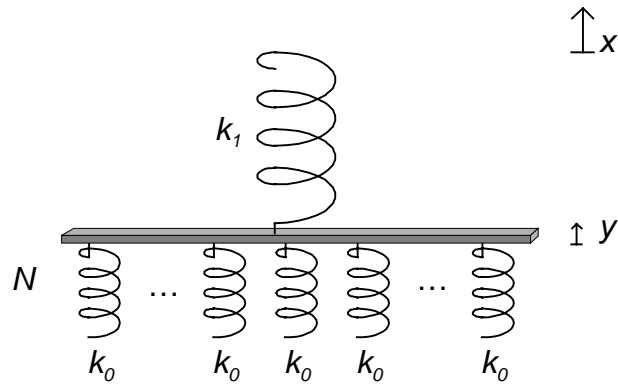
Figure 7.12. *Schematic representation of a system consisting of a cantilever with a spring constant k_1 and N parallel complexes with a spring constant k_0.*

At equilibrium, it is required that:

$$F = k'x = k_1(x-y) = Nk_0y \text{, where } k' = \frac{Nk_0k_1}{Nk_0 + k_1}$$

Equation 7.19.

From this equation, it follows that:

$$y = \frac{k_1}{Nk_0 + k_1}x$$

Equation 7.20.

The total work exerted on the system is:

$$W = \int_0^x F(x)dx = \int_0^x k'xdx = \frac{1}{2}k'x^2 = \frac{1}{2}\frac{Nk_0k_1}{Nk_0 + k_1}x^2$$

Equation 7.21.

The total work consists of work exerted on the cantilever and work exerted on the complex:

$$W = W_1 + NW_0$$

Equation 7.22.

The work exerted on the cantilever is:

$$W_1 = \int_0^{x-y} k_1(x-y)d(x-y) = \frac{1}{2}k_1(x-y)^2 = \frac{1}{2}\frac{N^2k_0^2k_1}{(Nk_0 + k_1)^2}x^2$$

Equation 7.23.

121

And that exerted on a complex is:

$$W_0 = \int_0^y k_0 y\, dy = \tfrac{1}{2} k_0 y^2 = \frac{1}{2} \frac{k_0 k_1^2}{(Nk_0 + k_1)^2} x^2 \qquad \textit{Equation 7.24.}$$

Because the complex is much stiffer than the cantilever, $k_0 \gg k_1$ (see above: $k_0 = 380$ pN/Å and $k_1 = 8$ pN/Å). Using this, equation is simplified to:

$$W_{0,N} = \frac{1}{2} \frac{k_1^2}{N^2 k_0} x^2 = \frac{1}{N^2} W_{0,1} \qquad \textit{Equation 7.25.}$$

Thus, in order to exert the same work on a spring in a parallel array of N springs $x_N = Nx_1$ which means that the deflection of the cantilever scales linearly with the number of complexes.

7.7   Experimental section

For a general introduction on synthetic procedures, see Chapter 3.7. Monolayers were prepared and characterized as reported in Chapter 6.6.

5-Bromopentanoic acid (4-*tert*-butyl-phenyl)-amide. A solution of bromovaleric acid (5 g, 27.6 mmol) in oxalyl chloride (20 mL) was stirred at 40 ℃ for 1.5 h. After evaporation of the oxalyl chloride by vacuum distillation, a solution of 4-*tert*-butylaniline (4.1 g, 27.5 mmol) and triethylamine (3.1 g, 31 mmol) in CH_2Cl_2 (20 mL) was added dropwise and the resulting solution was stirred at ambient temperature for 4 h. CH_2Cl_2 was added and the organic layer was washed with HCl (1 M), water, aqueous NaOH (1 M), and brine, and dried ($MgSO_4$). Evaporation of the solvent and recrystallization from HCl (0.2 M) afforded the product as small white crystals in 70% yield. ^{1}H NMR ($CDCl_3$) δ 7.45 (d, $J = 8.7$ Hz, 2 H), 7.37 (d, $J = 8.7$ Hz, 2 H), 7.19 (s, 1 H) 3.47 (t, $J = 6.3$ Hz, 2 H), 2.42 (t, $J = 6.6$ Hz, 2 H), 2.01-1.89 (m, 4 H), 1.33 (s, 9 H); ^{13}C NMR ($CDCl_3$) δ ; MS (FAB) m/z calcd. for $C_{15}H_{22}BrNO$ 311.1 found 312.3[$M + H$]$^+$).

5-Mercaptopentanoic acid (4-*tert*-butyl-phenyl)-amide 3. Potassium carbonate (0.49 g, 3.5 mmol) was added to a solution of thioacetic acid (0.27 g, 3.5 mmol) in DMF (20 mL). After dropwise addition of a solution of 5-bromo-pentanoic acid (4-*tert*-butyl-phenyl)-amide (1.0 g, 3.2 mmol) in DMF (10 mL) the solution was stirred at ambient temperature

in the dark for 16 h. CH_2Cl_2 and HCl (0.5 M) were added and the organic layer was washed with HCl (three times, 0.5 M), water, and brine. After evaporation of the solvent a degassed 1:2 mixture of aqueous K_2CO_3 (1 M) and MeOH was added and the resulting solution was refluxed for 45 min, poured into HCl (1 M), and extracted three times with CH_2Cl_2. The organic layer was washed with HCl (1 M) and brine, dried ($MgSO_4$), and the solvent was evaporated to afford the product as a white waxy solid in 65% yield. ^{1}H NMR ($CDCl_3$) δ 7.46 (d, J = 8.7 Hz, 2 H), 7.37 (d, J = 8.7 Hz, 2 H), 7.13 (s, 1 H) 2.60 (q, J = 7.8 Hz, 2 H), 2.40 (t, J = 7.2 Hz, 2 H), 1.92-1.71 (m, 4 H), 1.41 (t, J = 7.8 Hz, 1 H), 1.33 (s, 9 H); ^{13}C NMR ($CDCl_3$) δ 170.0, 146.8, 134.6, 125.3, 119.1, 36.5, 33.8, 32.9, 30.8, 23.8, 23.7; MS (FAB) *m/z* calcd. for $C_{15}H_{23}NOS$ 265.2, found 266.2 ($[M + H]^+$).

5-Bromopentanoic acid adamantan-1-ylamide. A solution of bromovaleric acid (3 g, 17 mmol) and oxalyl chloride (20 mL) in CH_2Cl_2 (50 ml) was refluxed for 5 h. After evaporation of the oxalyl chloride by vacuum distillation, a solution of 1-adamantylamine (2.5 g, 17 mmol) and triethylamine (3.5 g, 35 mmol) in CH_2Cl_2 (50 mL) was added dropwise and the resulting solution was stirred at ambient temperature for 16 h. The organic layer was washed with HCl (1 M), water, aqueous NaOH (1 M), and brine, and dried ($MgSO_4$). After evaporation of the solvent purification by column chromatography (SiO_2, eluent CH_2Cl_2) the product was obtained as a waxy colorless solid in 10% yield. ^{1}H NMR ($CDCl_3$) δ 5.10 (s, 1 H) 3.41 (t, J = 6.6 Hz, 2 H), 2.14-2.04 (m, 5 H), 1.98 (br s, 6 H), 1.93-1.77 (m, 4 H), 1.67 (br s, 6 H); ^{13}C NMR ($CDCl_3$) δ; MS (FAB) *m/z* calcd. for $C_{15}H_{24}BrNO$ 313.1, found 314.0 ($[M + H]^+$).

5-Mercaptopentanoic acid adamantan-1-ylamide 4. Potassium carbonate (0.10 g, 0.72 mmol) was added to a solution of thioacetic acid (0.06 g, 0.72 mmol) in DMF (10 mL). After dropwise addition of a solution of 5-bromo-pentanoic acid adamantan-1-ylamide (0.21 g, 0.67 mmol) in DMF (5 mL) the solution was stirred at ambient temperature in the dark for 16 h. CH_2Cl_2 and HCl (0.5 M) were added and the organic layer was washed with HCl (three times, 0.5 M), water, and brine. After evaporation of the solvent a degassed 1:2 mixture of aqueous K_2CO_3 (1 M) and MeOH was added and the resulting solution was refluxed for 45 min, poured into HCl (1 M), and extracted three times with CH_2Cl_2. The organic layer was washed with HCl (1 M) and brine, dried ($MgSO_4$), and the solvent was evaporated. Purification by column chromatography (SiO_2, eluent ethyl acetate/hexanes 1:7) afforded the product as a colorless waxy solid in 50 % yield. . ^{1}H NMR ($CDCl_3$) δ 5.09 (s, 1 H) 2.51 (q, J = 7.2 Hz, 2 H), 2.09-2.04 (m, 5 H), 1.96 (br s, 6 H), 1.73-1.57 (m, 10 H), 1.33 (t, J = 7.8 Hz, 1 H); ^{13}C NMR ($CDCl_3$) δ 171.1, 51.3, 41.2, 36.5, 35.8, 32.9, 28.9, 23.9; MS (FAB) *m/z* calcd. for $C_{15}H_{25}NOS$ 267.2, found 268.2 ($[M + H]^+$).

AFM and Tip Modification. Triangular shaped silicon nitride cantilevers and silicon nitride tips (Digital Instruments (DI), Santa Barbara, CA) were coated with with ca. 2 nm

Ti and ca. 75 nm Au in a Balzers SCD040 sputtering machine in high vacuum. The tips were functionalized as described previously[20] in 1mM solutions of a mixture of 2-hydroxy-ethanethiol and a guest adsorbate or 2-hydroxy-ethanethiol in ethanol. The AFM measurements were carried out with a NanoScope III multimode AFM (DI) utilizing a liquid cell (DI). The piezo positioner was calibrated in the z-direction by measuring step heights of Au(111). The cantilever spring constants were calibrated as described by Tortonese and Kirk.[21] Force-distance curves were recorded in pure water and 100 μM aqueous 1,8-ANS at different positions on the sample surface with a maximum external load of <1.0 nN. The unloading rate was varied between 10^3 pN/s and 10^6 pN/s. The corresponding reference measurements were carried out in pure water. The quantitative analysis of the observed individual pull-off events was performed for several hundred force curves of a given set. Each individually resolved pull-off event with a rupture force of >10 pN was included in the analysis.

7.8 References

[1]   Florin, E.-L.; Moy, V.T.; Gaub, H.E. *Science* **1994**, *264*, 415-417.

[2]   Lee, G.U.; Kidwell, D.A.; Colton, R.J. *Langmuir* **1994**, *10*, 354-357.

[3]   Lee, G.U.; Chrisey, L.A.; Colton, R.J. *Science* **1994**, *266*, 771-773.

[4]   Beulen, M.W.J.; Bügler, J.; Lammerink, B.; Geurts, F.A.J.; Biemond, E.M.E. F.; Van Leerdam, K.G.C.; Van Veggel, F.C.J.M.; Engbersen, J.F.J.; Reinhoudt, D.N. *Langmuir* **1998**, *14*, 6424-6429.

[5]   Beulen, M.W.J.; Bügler, J.; De Jong, M.R.; Lammerink, B.; Huskens, J.; Schönherr, H.; Vancso, G.J.; Boukamp, B.A.; Wieder, H.; Offenhäuser, A.; Knoll, W.; Van Veggel, F.C.J.M.; Reinhoudt, D.N. *Chem. Eur. J.* **2000**, *6*, 1176-1183.

[6]   Schönherr, H.; Beulen, M.W.J.; Bügler, J.; Huskens, J.; Van Veggel, F.C.J.M.; Reinhoudt, D.N.; Vancso, G.J. *J. Am. Chem. Soc.* **2000**, *122*, 4963-4967.

[7]   The binding constant of 1,8-ANS to monolayers of **1** was determined as described in ref 5: $K = 2.6 \times 10^4 \ M^{-1}$.

[8]   Although Poisson distributions are commonly used to describe events with a low probability, this approximation gives better results than a random distribution with a fixed total number of events.

[9]   Evans, E.; Ritchie, K. *Biophys. J.* **1997**, *72*, 1541-1555.

[10]   Bell, G.I.; *Science*, **1978**, *200*, 618-627.

[11]   Merkel, R.; Nassoy, P.; Leung, A.; Ritchie, K.; Evans, E. *Nature* **1999**, *397*, 50-53.

[12]   Willemsen, O.H.; Kuipers, L.; Van der Werf, K.O.; De Grooth, B.; Greve, J. *Langmuir* **2000**, *16*, 4339-4347.

[13]   MD calculations were carried out in a cubic box of 31 Å dimensions using Quanta97. The water was modeled as the TIP3Pmodel,[14] as implemented in

CHARMM. A non-bonded cutoff of 11 Å and a dielectric constant ε of 1 were used.

[14] Jorgensen, W.L.; Chandrasekhar, J.; Madura, J.D.; Impey, R.W.; Klein, M.L. *J. Chem. Phys.* **1983**, *79*, 926-935.

[15] Using the method described before,[6] spring constants were determined to be 8 pN/Å.

[16] (a) Van Veggel, F.C.J.M.; Oude Wolbers, M.P.; Reinhoudt, D.N. *J. Phys. Chem. A* **1998**, *102*, 3060-3066; (b) Jorgensen, W.L. *Acc. Chem. Res.* **1989**, *22*, 184-189.

[17] The method to compute the free energy of binding of two Lennard-Jones particles from their potential of mean force described in ref. 16 involves a sphere integral. In the system studied here, with a surface confined host *in* which the guest is included, the volume over which must be integrated is smaller. As an approximation, a cylinder with a radius of 1 Å was used.

[18] Rief, M.; Fernandez, J.M.; Gaub, H.E. *Phys. Rev. Lett.* **1998**, *81*, 4764-4767.

[19] Seifert, U *Phys. Rev. Lett.* **2000**, *84*, 2750-2752.

[20] Schönherr, H.; Hruska, Z.; Vancso, G. J. *Macromolecules* **199**8, *31*, 3679 3685.

[21] Tortonese, M.; Kirk, M. *Proc. SPIE* **1997**, *3009*, 53-60.

Summary

This thesis deals with potential ways to use cyclodextrin derivatives in sensing systems for organic molecules. With this objective in mind, the interactions of cyclodextrin derivatives with guests were studied on various levels. Detailed complexation studies were performed in solution. Cyclodextrin dimers were shown to be excellent receptor molecules for the recognition of steroids. Their ability to form complexes with ditopic guests was used to solubilize and to template the formation of metal complexes for radiopharmaceutical applications. The knowledge obtained from the binding studies in solution was used to explain the binding phenomena observed at cyclodextrin-modified surfaces. Finally, interactions between single hosts and guests were studied using Atomic Force Microscopy (AFM).

In Chapter 2, an introduction to various aspects of the sensing of organic molecules is given. After a brief overview of the available mechanisms for the transduction of a binding event into a sensor signal, different molecules capable of sensing organic analytes are discussed, with the focus on cyclodextrin-based receptor molecules. Furthermore, the detection of organic molecules at interfaces is discussed. Finally, the state of the art in the detection of single molecules is reviewed.

The syntheses of a cyclodextrin dimer with a flexible dipropylamine spacer and of a dansyl-appended fluorescent analogue are described in Chapter 3. Using molecular docking, a computational procedure commonly applied in medicinal chemistry for lead identification, several potential guests for the dipropylamine-spaced dimer were suggested. Competition fluorescence experiments confirmed the binding of a large percentage of the suggested guests to the dimer. Steroids were identified as the main class of molecules that bind to the dimer, but some other classes were discovered as well. From the large fraction of calculated guests that were shown to bind to the dimer it was concluded that docking is a promising method to predict the binding behavior of synthetic host molecules. Finally, binding of steroids to a dansyl-appended cyclodextrin dimer was shown to lead to a fluorescence response.

In Chapter 4, a detailed investigation of the binding and sensing behavior with bile salts of receptor molecules based on cyclodextrins is described. The thermodynamics of the interactions were studied using microcalorimetry. The stabilities of the β-cyclodextrin complexes of these guests vary depending on the substitution pattern of the steroid. The binding behavior to native β-cyclodextrin is reflected in the dimers. Steroids that bind weakly to one cyclodextrin cavity are complexed in a 1:1 fashion by the dimers, whereas guests that bind strongly in one cavity form 1:2 complexes. Fluorescence titrations showed that steroids that bind weakly to native cyclodextrin are not detected by a monomeric

Summary

dansyl-appended cyclodextrin derivative, but do give a fluorescence response when added to the dimeric sensor molecule. Thus, cyclodextrin dimers are promising receptor molecules for sensing applications.

Chapter 5 describes the use of the beneficial properties of cyclodextrin dimers in radiopharmaceutical apllications. Several small, lipophilic rhenium complexes form inclusion complexes with native β-cyclodextrin (β-CD) and β-CD dimers. With dimers very high association constants were obtained. The use of β-CD also enabled the synthesis of these rhenium complexes in water, in excellent yields, via complexation of the otherwise insoluble corresponding ligands. The influence of the reaction time and temperature on the configuration of the reaction products have been investigated in depth for one of these complexes. Using a β-CD dimer, it is possible to specifically template the formation of one configuration. The Chapter ends with a description of the first steps towards a supramolecular approach to the radiolabeling of biomolecules.

In an actual sensing system, the receptor molecules need to be immobilized. Chapter 6 describes the preparation of self-assembled monolayers (SAMs) of cyclodextrin derivatives modified with seven thioether moieties or with one thiol moiety on gold employing the well-known sulfur-gold interaction to achieve this immobilization. The monolayers were characterized using electrochemistry, wettability, and AFM. β-Cyclodextrin heptathioether monolayers and mixed monolayers of the cyclodextrin monoalkylthiol and varying amounts of mercaptoundecanol were shown to be well packed. Guest recognition at these monolayers in water was studied by surface plasmon resonance (SPR) spectroscopy. For simple organic guests, monolayers of the cyclodextrin derivative modified with seven thioethers showed the same selectivity and binding strength as β-cyclodextrin in solution; the selectivity towards bile salts differed from solution. The mixed monolayers of the cyclodextrin monoalkylthiol, in which the cyclodextrin is less substituted and has more mobility, binds steroidal guests with the same selectivity as β-cyclodextrin in solution. Furthermore cooperative binding of the bile salts by two cyclodextrin moieties occurred at these layers.

Chapter 7 describes how single molecular interactions between β-cyclodextrin heptathioethers immobilized on a gold surface and guests immobilized on an AFM tip were investigated. Quantized unbinding forces were observed for the interaction between a cyclodextrin surface and an AFM tip coated with guests. The magnitude of a single decomplexation force is dependent on the type of guest, being 57 pN, 89 pN, and 103 pN for the interaction with a ferrocene, *tert*-butylphenyl, or adamantane coated tip, respectively. A model is proposed to correlate these forces with the binding strengths of the complexes of these guests with β-cyclodextrin in solution. In contrast to the biological systems usually studied, the kinetics of these host-guest systems is fast, causing the host-guest complexes to form and dissociate many times during each experimental datapoint. This fast kinetics is proven by the loading-rate independence of the forces

Samenvatting

Dit proefschrift beschrijft een aantal manieren om cyclodextrines te gebruiken in detectiesystemen voor organische moleculen. Hiertoe werd de interactie van cyclodextrines met gasten op verschillende niveaus bestudeerd. Middels complexeringsstudies in oplossing werd aangetoond dat cyclodextrinedimeren uitstekende receptormoleculen voor de herkenning van steroïden zijn. Verder werd vorming van sterke complexen met ditope gasten aangewend ter verbetering van de wateroplosbaarheid en de vorming in waterig milieu van lipofiele metaalcomplexen. De kennis verkregen uit de studies in oplossing werd gebruikt ter verklaring van het complexeringsgedrag van steroïden met cyclodextrines in zelf-organiserende monolagen. De interactie tussen individuele gast- en gastheermoleculen werd bestudeerd met behulp van atomaire krachtmicroscopie (AFM).

Hoofdstuk 2 geeft een inleiding in verschillende aspecten van de detectie van organische moleculen. Na een kort overzicht van de beschikbare mechanismen die een interactie vertalen naar een sensorsignaal, worden verschillende receptormoleculen voor organische substraten besproken. De nadruk ligt hierbij op receptoren gebaseed op cyclodextrines. Vervolgens wordt een overzicht gegeven van receptormoleculen in zelf-organiserende monolagen voor sensordoeleinden, waarna het hoofdstuk eindigt met een bespreking van de stand van zaken op het gebied van de detectie van individuele moleculen.

In Hoofdstuk 3 worden de syntheses van twee cyclodextrinedimeren met een dipropylamine brug besproken. Met behulp van moleculaire docking, een computationele screeningstechniek bekend uit het onderzoek naar nieuwe medicijnen, werd gezocht naar potentiële gasten voor dit type dimeer. Met competitiefluorescentie werd vervolgens vastgesteld dat een groot gedeelte van de gevonden mogelijke gasten daadwerkelijk sterk bond in het dimeer. Steroïden zijn de voornaamste klasse van moleculen die worden gebonden, daarnaast werd nog een aantal andere gasten gevonden. De gebruikte methode lijkt een veelbelovende techniek voor de identificatie van potentiële gasten voor synthetische gastheren. Een dimeer is gefunctionaliseerd met een fluorescente dansylgroep op het centrale stikstofatoom van de brug. Aangetoond werd dat de binding van steroïden in het dansylgefunctionaliseerde dimeer een verandering in de fluorescentieintensiteit tot gevolg heeft.

Het complexerings- en sensorgedrag van op cyclodextrine gebaseerde receptoren met de steroïdale galzouten wordt verder uitgewerkt in Hoofdstuk 4. De thermodynamische parameters voor de verschillende interacties werden bepaald met behulp van microcalorimetrie. De stabiliteit van de complexen met niet-gemodificeerd β-cyclodextrine is afhankelijk van het substitutiepatroon van de steroïden. Dit gedrag wordt weerspiegeld in het bindingsgedrag van de dimeren, de vorming van 1:1 of 1:2 complexen van de

dimeren met de steroïden valt samen met zwakke respectievelijk sterke binding van het steroïde in β-cyclodextrine. De zwak in β-cyclodextrine bindende steroïden konden niet worden gedetecteerd door middel van veranderingen in fluorescentie als ze aan een monomeer dansylgefunctionaliseerd cyclodextrinederivaat worden toegevoegd, maar wel door een fluorescent dimeer. Hieruit blijkt dat cyclodextrinedimeren veelbelovende receptoren voor sensortoepassingen zijn.

In Hoofdstuk 5 wordt mogelijkheid beschreven om cyclodextrinedimeren toe te passen in radiofarmaceutica. Een aantal lipofiele rheniumcomplexen vormt in water complexen met β-cyclodextrine en derivaten, waarbij vooral de complexen met cyclodextrinedimeren zeer stabiel blijken te zijn. Complexering van de in water onoplosbare vrije liganden met β-cyclodextrine maakte de vorming van de metaalcomplexen in water mogelijk. Afhankelijk van de reactietijd en reactietemperatuur kunnen meerdere configuraties van de metaalcomplexen gevormd worden. Dimeren functioneerden als een mal die ervoor zorgt dat maar een van de mogelijke configuraties wordt gevormd. Het hoofdstuk eindigt met een beschrijving van de eerste stappen voor een nieuwe, supramoleculaire methode om biomoleculen radioactief te labelen, waarbij gebruik gemaakt wordt van de sterke binding van bepaalde rheniumverbindingen in cyclodextrindedimeren.

Toepassing van receptormoleculen in een sensorsysteem vereist dat ze op enigerlei wijze geïmmobiliseerd kunnen worden. Hoofdstuk 6 beschrijft de bereiding van zelf-organiserende monolagen van cyclodextrines gemodificeerd met zeven lange thioethersubstituenten en van cyclodextrinederivaten met een lange thiolsubstituent, gebruikmakend van de zwavel-goud interactie. De monolagen werden gekarakteriseerd met behulp van electrochemie, randhoekmetingen en AFM. Hieruit bleek dat β-cyclodextrine heptathioether monolagen en gemengde monolagen van het cyclodextrine monoalkylthiol met verschillende hoeveelheden mercaptoundecanol goed gepakt waren. De herkenning van gasten aan het grensvlak van deze monolagen met water werd bestudeerd met behulp van oppervlakteplasmonresonantie (SPR) spectroscopie. De monolagen van cyclodextrine gemodificeerd met zeven thioethers binden eenvoudige organische verbindingen met vergelijkbare selectiviteit en affiniteit als β-cyclodextrine in oplossing, de herkenning van galzouten is sterk gewijzigd ten opzichte van de binding in β-cyclodextrine in oplossing. De herkenning van deze steroïden door cyclodextrine in de gemengde monolagen heeft wel dezelfde selectiviteit als in oplossing. Dit wordt toegeschreven aan de grotere bewegingsvrijheid van dit minder gesubstitueerde cyclodextrine. Aangetoond werd dat in deze monolagen twee cyclodextrines bijdragen aan de binding van een gast.

Hoofdstuk 7 beschrijft een studie naar de interacties tussen op een goudoppervlak geïmmobiliseerde β-cyclodextrine heptathioethers en op een AFM-tip geïmmobiliseerde gasten. Er werden gequantiseerde krachten waargenomen voor de interactie tussen de gasten op de tip en de cyclodextrinemonolaag. Dit wordt toegeschreven aan de decomplexering van individuele complexen. De grootte van de kracht is afhankelijk van

het type gast, krachten van 57 pN, 89 pN en 103 pN werden gevonden voor de interactie met respectievelijk ferroceen, *tert*-butylphenyl en adamantaan. Er is een model voorgesteld om deze krachten te correleren met de thermodynamische parameters voor deze interacties. Omdat, in tegenstelling tot biologische systemen, de kinetiek van vorming en verbreking van cyclodextrinecomplexen snel is, vormen en dissociëren de complexen meerdere keren tijdens één experimenteel datapunt. Dit heeft tot gevolg dat de gemeten krachten *onafhankelijk* zijn van de snelheid waarmee het experiment wordt uitgevoerd.

Dankwoord

Na ruim vier jaar dreigt er nu een einde te komen aan mijn twentse periode. Een groot aantal mensen heeft er toe bijgedragen dat ik in die tijd veel heb geleerd en het nog naar mijn zin heb gehad ook. Dit is de plek bij uitstek om iedereen te bedanken die bij het een en/of het ander een rol heeft gespeeld.

Allereerst bedank ik mijn promotor David Reinhoudt. David, ik heb de vele onderzoeksmogelijkheden in je vakgroep en de vrijheid die je me gaf zeer gewaardeerd. Mijn dagelijkse begeleider en assistent-promotor Jurriaan Huskens bedank ik voor de aangename en leerzame samenwerking. Jurriaan, jouw talent om aan vrijwel elk probleem een mouw te fitten heeft een grote invloed gehad op de inhoud van dit proefschrift. Ik bedank ook Johan Engbersen voor de begeleiding in mijn eerste jaar. Gelukkig stond ik niet alleen in mijn worstelingen met de cyclodextrines. Jürgen Bügler en Jasper Michels waren net bezig aan hun cyclodextrine-onderzoek toen ik begon. Ik heb prettig en gezellig met jullie samengewerkt (natuurlijk was dat wederzijds Jasper). Nieuweling Alart Mulder zal na mijn vertrek de vaandeldrager van het cyclodextrine-onderzoek in Twente zijn. Ik wens je veel succes met de cyclodextrientjes nu je er alleen voor staat.

Het in dit proefschrift beschreven onderzoek was onderdeel van een gezamenlijk project met de vakgroep Organische Chemie van de Katholieke Universiteit Nijmegen. Professor Roeland Nolte, Martin Feiters en Bart Nelissen ben ik dankbaar voor de prettige samenwerking. De mogelijkheid om contact te houden met mijn oude universiteit heb ik zeer gewaardeerd. Het onderzoek is uitgevoerd met geldelijke steun van CW/STW. De leden van de gebruikerscommissie bedank ik voor hun inbreng in het project.

Tijdens mijn promotie heb ik gebruik gemaakt van de kennis van een aantal mensen van buiten de Universiteit Twente. Ronald Knegtel (Vertex Pharmaceuticals) en Peter Grootenhuis (Combichem) ben ik dankbaar voor de plezierige samenwerking aan de in Hoofdstuk 3 beschreven dockingstudie. I would like to thank Patrick Berthault (CEA/Saclay) for his NMR-contribution, which is described in Chapter 4. De in Hoofdstuk 4 beschreven levensduur metingen zijn uitgevoerd bij Ton Visser en Arie van Hoek (Wageningen Universiteit), waarvoor dank.

Het in Hoofdstuk 5 beschreven onderzoek naar het gebruik van cyclodextrines in combinatie met radiofarmaceutica is het resultaat van een uiterst aangename en vruchtbare samenwerking met Kjeld van Bommel. In vier jaar evolueerde mijn onderzoek van oplossingen naar oppervlakken. Marcel Beulen en Arianna Friggeri hebben mij geholpen

bij mijn eerste stappen op een vaste ondergrond, hetgeen een woord van dank zeker waard is. The AFM-measurements described in Chapter 7 were performed by Szczepan Zapotoczny from the group of Professor Julius Vancso. Ook Tommaso Auletta, Frank van Veggel en Kobus Kuipers waren betrokken bij dit project. Hen allen dank ik voor hun bijdrage, de plezierige samenwerking en de lange, krachtige, doch stimulerende discussies.

Joop Toevank, Irene Wolbers, Marc Brouwer en Marcel de Bruine zorgden ervoor dat chemicaliën en materialen altijd op tijd aanwezig waren. Voor het uitvoeren van analyses aan de gesynthetiseerde verbindingen wil ik Hanny Visser, Ron Hulst, Tieme Stevens en Roel Fokkens bedanken. Tieme, de manier waarop je (bijna) elk cyclodextrinederivaat in no-time aan het vliegen kreeg bleef me verbazen. Carla Weber-van der Ploeg en Rita de Wilde ben ik dankbaar voor hun hulp bij het afhandelen van de vele administratieve uitdagingen waarvoor een mens zich gedurende zijn promotie geplaatst ziet.

Dat ik in Enschede een leuke tijd heb gehad is voor een groot deel te danken aan de goede sfeer in de vakgroep. Hoewel iedereen in de vakgroep speciaal is, zijn Jasper Michels, Leonard Prins, Steve Klink, Kjeld van Bommel, Arianna Friggeri, Henk-Jan van Manen, Niels van der Veen, Mercedes Crego Calama, Gerald Hebbink, Lennart Grave, Xue-Mei Li, Maria Arduini, Francesca Corbellini, Marta Reinoso en Stefano Levi extra speciaal. Zoals Jessica Kerckhoffs, tenslotte, is er maar een.

Jasper Michels en Mercedes Crego Calama ben ik dankbaar voor het kritisch doorlezen van het concept van mijn proefschrift en voor het geven van tips en aanwijzingen ter verbetering ervan. De eventueel nog resterende fouten zijn natuurlijk mijn schuld. Het paranimfschap zal worden vervuld door Bart Nelissen en Leonard Prins, waarvoor alvast hartelijk bedankt.

Tenslotte wil ik mijn ouders bedanken, die me altijd gestimuleerd hebben om me te ontwikkelen en me daarvoor de mogelijkheden hebben aangereikt.

<div align="right">Menno</div>

Curriculum Vitae

Menno de Jong werd geboren in Ede op 20 april 1973. In 1991 behaalde hij het VWO-diploma aan het Elzendaalcollege in Boxmeer, waarna hij Scheikunde ging studeren aan de Katholieke Universiteit Nijmegen. In het kader van een bijvakstage heeft hij in de vakgroep Biochemie onder leiding van dr. G. Pruijn en Prof. dr. W. J. van Venrooij onderzoek gedaan naar structuur en functie van antigene cellulaire componenten die betrokken zijn bij auto-immuunziekten. De hoofdvakstage werd verricht in de vakgroep Organische Chemie onder leiding van dr. F. Venema, dr. M. C. Feiters en Prof. dr. R. J. M. Nolte. Tijdens deze periode werkte hij aan cyclodextrinederivaten voor gebruik als coatings in dampsensoren. In 1996 werd het doctoraal examen afgelegd.

Van februari 1997 tot mei 2001 was hij werkzaam als onderzoeker in opleiding in de vakgroep Supramoleculaire Chemie en Technologie aan de Universiteit Twente onder supervisie van Prof. dr. ir. D. N. Reinhoudt, dr. ir. J. Huskens en dr. J. F. J. Engbersen (tot januari 1998). De resultaten van het gedurende deze periode verrichte onderzoek zijn beschreven in dit proefschrift.

Vanaf oktober 2001 zal hij werkzaam zijn als post-doctoral fellow in de groep van Prof. dr. M. A. Reed, Yale University, New Haven, USA. Hiervoor werd hem het Reimar-Lüst-Stipendium van de Körber-Stiftung toegekend.